X-ray Emissions from Progenitors of Type Ia Supernovae

Proefschrift

ter verkrijging van de graad van doctor
aan de Radboud Universiteit Nijmegen
op gezag van de rector magnificus prof. mr. S.C.J.J. Kortmann,
volgens besluit van het college van decanen
in het openbaar te verdedigen op 15 November, 2013
om 10:30 uur precies

door

Mikkel Thomas Bøje Nielsen

Promotores:	Prof. Dr. G. Nelemans & Prof. Dr. C. Dominik
Copromotor:	Dr. R. Voss
Manuscriptcommissie:	Prof. Dr. E. Cator, Radboud University Nijmegen Prof. Dr. P.J. Groot, Radboud University Nijmegen Prof. Dr. E.P.J. van den Heuvel, Universiteit van Amsterdam (UvA) Prof. Dr. J. Kuijpers , Radboud University Nijmegen Dr. J. Vink, Universiteit van Amsterdam (UvA)

X-ray Emissions from Progenitors of Type Ia Supernovae
Thesis, Radboud University Nijmegen
Illustrated; with bibliographic information and Dutch summary
Cover illustration: Artist's impression of the Chandra X-ray Observatory
(credit: http://www.nasa.gov/chandra)

ISBN-13: 978-94-6191-930-4

Contents

Introduction

The modern scientific method begins with a supernova.

The bright, so-called 'Nova Stella' observed by the Danish astronomer Tycho Brahe in 1572 was not, despite the name given to it by Brahe, a new star. It was the cataclysmic death of an old star, a supernova explosion. The observation of this object was a fundamental discovery, as it unequivocally contradicted the prevailing notion, propagated and violently enforced for centuries by the Christian Church, that the celestial sphere was an eternal, unchanging realm, in which the Earth rested at the center of all of Creation, while the Sun, the planets and the stars orbited it. The observation of Tycho's supernova clearly demonstrated the incorrectness of this notion, and started a process of scientific discovery which culminated with Newton's 'De Principia Naturalis', along with the adoption of the heliocentric worldview, as described by Nicolaus Copernicus.

Type Ia Supernovae

Supernovae are extraordinarily bright cosmic explosions which for a period of a few weeks to a month may outshine the integrated luminosity of the entire galaxy in which they take place, see e.g. Figure 1. For type Ia supernovae, the explosion energies are estimated to be around $\sim 10^{51}$ erg (Wapstra & Gove 1971; Iben & Tutukov 1984), making them some of the most energetic astrophysical events in the Universe. The inherent brightness of type Ia supernovae means that they can be detected in very distant galaxies (Rubin et al. 2013).

Observationally, supernovae are divided into two main types, based on spectral characteristics; those whose spectra lack hydrogen are characterised as Type I, while those with hydrogen in their spectra are characterised as type II. Further observationally-based sub-divisions of both type I and type II exist; for type I supernovae, helium-depleted events displaying a strong, singly-ionised silicon line in their early and peak-brightness spectra are characterised as type Ia.

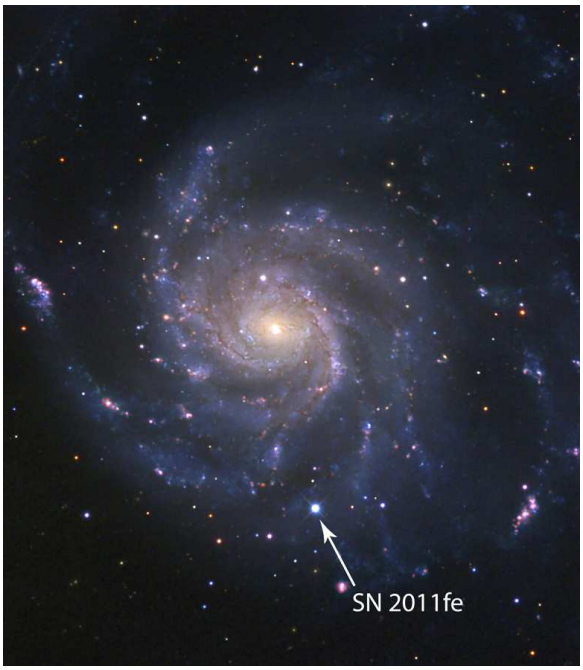

Figure 1: Optical image of SN2011fe in M101. Credit: PTF/LCOGT.

At first glance, one might expect the observational division between type I and II supernovae to correspond to two distinct physical progenitor system types. As it turns out, this is not the case. The current understanding is that supernovae of type Ib, Ic and II are the results of gravitational collapse of iron-cores in short-lived, massive stars (above $\gtrsim 8$ $M_\odot$, e.g. Smartt 2009), while type Ia supernovae are believed to be thermonuclear run-aways of electron-degenerate cores of carbon-oxygen white dwarfs, i.e remnants of medium to low mass ($\lesssim 8$ $M_\odot$) stars.

Type Ia supernovae stand apart from core-collapse supernovae in a number of ways. Firstly, core-collapse supernovae leave behind a compact remnant, i.e. a neutron star or a black hole, while type Ia supernovae do not; type Ia supernova explosions are believed to completely disrupt their progenitor stars, leaving behind only a rapidly expanding shell of material that has been partially processed by thermonuclear reactions during the explosion. Secondly, core-collapse supernovae are a heterogeneous group of events with significant inherent differences in explosion morphologies, light-curves, brightness and spectral behaviour. Type Ia supernovae, on the other hand, are remarkably homogeneous. The explosions themselves are morphologically more symmetric than core-collapse supernovae (Lopez et al. 2009) (see e.g. Figures 2 & 3). Although there is evidence of some variation, the majority of type Ia supernova have quite similar spectral behaviour, and obey a characteristic correlation between absolute brightness at maximum light and light-curve fall-off time, with the brighter events falling off more slowly (see Figure 4). This correlation is known as the Phillips relation (Phillips 1993), and coupled

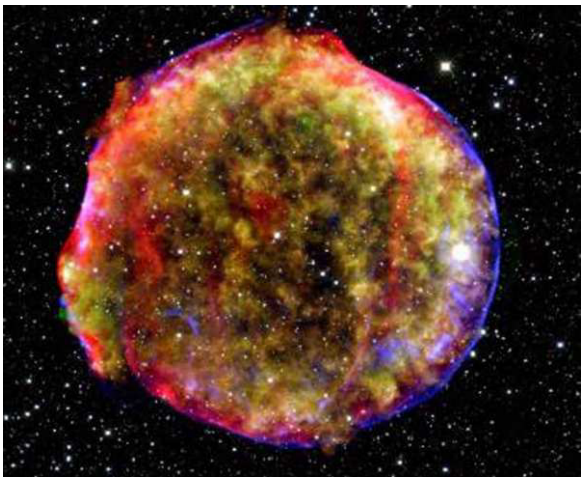

Figure 2: Tycho's supernova remnant (SN1572). Image is a combination of infrared and X-ray images from the Spitzer and Chandra space observatories, and Calar Alto Observatory. Credit: Hughes, Rho & Krause.

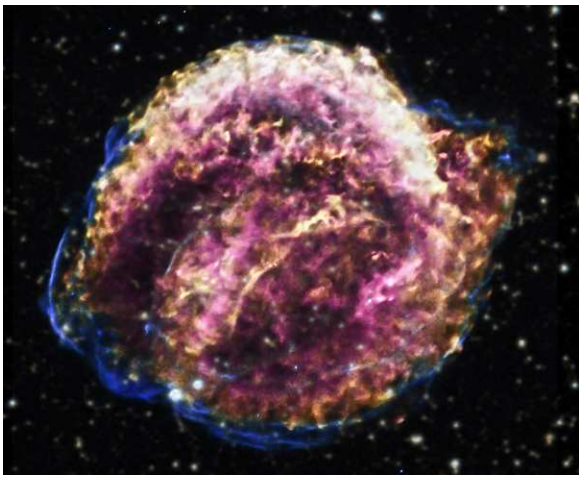

Figure 3: Kepler's supernova remnant (SN1604). Image is a combination of X-ray images from the Chandra space observatory and optical images from the Digitized Space Survey. Credit: X-ray: NASA/CXC/SAO/D.Patnaude, Optical: Digitized Space Survey (DSS)

with the inherent brightness of a supernova explosion enables the use of type Ia supernovae as standardisable cosmic candles, by which it is possible to measure the expansion history of the Universe beyond the range where other distance-measuring methods such as Cepheids can be employed. Before systematic analyses of distant type Ia supernovae were carried out in the late 1990s, the expansion of the Universe was expected to be slowing down, due to graviational

interaction between the matter in the Cosmos. However, observations of distant type Ia supernovae showed them to be more redshifted than they would have been had the expansion of the Universe been slowing down. The conclusion was that the expansion of the Universe is in fact accelerating (Riess et al. 1998; Perlmutter et al. 1999). This, in turn, has given rise to the cosmological paradigm of 'Dark Energy', a so far mysterious component of the Universe which drives the expansion. For their discovery, Riess, Perlmutter and Schmidt were awarded the 2011 Nobel Prize in Physics.

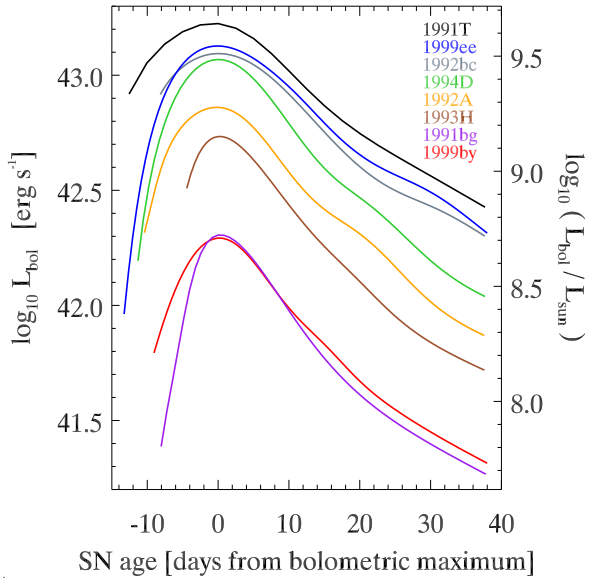

Figure 4: Bolometric light-curves of a selection of type Ia supernovae, illustrating the brightness-width correlation (brighter supernovae have wider light-curves). SN1994D is a Branch-normal supernova, while SN1991T is over-luminous, and 1991bg and 1999by are under-luminous events. Credit: Stritzinger.

In addition to this, type Ia supernovae are of importance to galactical evolution. While the progenitor stars of core-collapse supernovae produce large amounts of iron, most of this is consumed when the iron-core collapses to form either a neutron star or a black hole, and while core-collapse supernovae distribute significant amounts of intermediate-mass elements into the surrounding interstellar medium, little iron survives the explosions. In type Ia supernovae, on the other hand, a large part of the exploding carbon-oxygen object is processed into primarily radioactive nickel which then decays into iron-group elements (iron, cobalt & nickel). Consequently, most of the iron-group elements in the Universe have been formed in type Ia supernovae (e.g. Scannapieco & Bildsten 2005). Besides chemical enrichment, the expanding ejecta from all types of supernovae inject significant amounts of kinetic energy into their galactic surroundings, and the compression caused by supernova shockwaves may set off star-formation in nearby molecular clouds (e.g. Slyz et al. 2005, however, see also Desai et al. 2010). In addition to this, type Ia supernovae produce some of the largest ejecta velocities in

any supernovae (up to 25,000 km/s, or close to 1/10 of the speed of light), sufficient to eject material from the gravitational wells of their host galaxies (Hillebrandt et al. 2013). Therefore, type Ia supernovae are also of importance to the enrichment of the intergalactic medium.

For a typical spiral galaxy, the type Ia supernova rate is roughly one every 300 years (e.g. Cappellaro et al. 1993; Turatto et al. 1994). Core-collapse supernovae of type II occur somewhat more often, while type Ib and Ic are considerably rarer: the ratio is believed to be around 3 core-collapse supernovae per type Ia supernovae, however, the exact ratio is not yet well-determined.

Progenitors of Type Ia Supernovae

Despite the importance of type Ia supernovae for stellar astrophysics, galactic evolution and cosmology, the nature of the progenitor systems giving rise to these events remains mysterious, and no direct, unambiguous detection of a type Ia supernova progenitor has been made at the time of the writing of this thesis. From observations of the supernova explosions themselves, a number of characteristics of the progenitors can be inferred.

Main-sequence and giant stars consist primarily of hydrogen and helium. The absence of these elements in type Ia supernova spectra indicate that the progenitors are likely evolved objects that have lost most or all of their hydrogen prior to the explosions. Secondly, late-time light-curves of type Ia supernovae have exponential fall-offs, characteristic of a radioactive decay time similar to that of ^{56}Ni. This behaviour, along with the chemical abundances inferred from the spectra of type Ia supernovae, can be reproduced quite well by the thermonuclear processing of a massive (> 1 M$_\odot$) carbon-oxygen white dwarf to primarily radioactive nickel. Lastly, the explosion energy of type Ia supernovae is roughly similar to the binding energy of a massive carbon-oxygen white dwarf (Iben 1982; Iben & Tutukov 1984). The Chandrasekhar mass (~ 1.38M$_\odot$) is the largest mass for which degenerate electron-pressure in a white dwarf is able to balance gravity and hence prevent gravitational collapse. Close to the Chandrasekhar mass, the pressure and density in the core of the white dwarf will rise to the point where thermonuclear processing of the carbon-oxygen can take place, leading to a further temperature rise, which again leads to an increase in thermonuclear reaction rates. The result is a runaway process that completely disrupts the progenitor white dwarf in a cataclysmic explosion, a type Ia supernova. The thermonuclear processing of carbon and oxygen is expected to produce large amounts of radioactive ^{56}Ni, and it is the decay of this into cobalt and iron that is believed to power the exponential tail of the type Ia supernova light-curve.

It should be noted that despite the general homogeneity of type Ia supernova explosions, there is growing observational evidence of a number of distinctive sub-groups (e.g. several sub-classes of sub- and super-luminous events) which exhibit small, yet noticeable and systematic spectroscopic and photometric deviations from the larger and more homogeneous group of 'normal', non-peculiar type Ia supernovae (Branch et al. 1993). Peculiar type Ia supernovae may constitute as much as $\sim 30\%$ of the total number of type Ia supernova events (Li et al. 2011a), and the remaining homogeneous group of events is referred to as 'Branch-normal' type Ia supernovae. It is currently an open question whether the observational inhomogeneities

in spectra and photometry stem from minor differences in explosions of conceptually similar progenitors (e.g. slight deviations from perfectly symmetry in the explosions, coupled with viewing-angle effects, as suggested by Maeda et al. 2010), or are the result of distinct types of progenitor systems.

Clues may also be obtained by considering the host populations of type Ia supernovae; old stellar populations such as ellipticals produce type Ia supernovae that are systematically redder and dimmer and have slower ejecta velocities than those taking place in star-burst galaxies. Similarly, arms of spiral galaxies appear to host more and brighter type Ia supernovae than galactic bulges, while the outer regions of spirals give rise to dim supernovae similar to those taking place in old populations (Hillebrandt et al. 2013).

When referring to type Ia supernovae as a general group in the scientific literature, it is normally implicitly understood that this means the Branch-normal events. In the remainder of this thesis, we adopt a similar convention, and the reader should therefore assume that unless noted otherwise, our considerations deal with Branch-normal events.

Progenitor scenarios

Single carbon-oxygen white dwarfs are not formed at masses larger than $1.2M_\odot$, and the majority are born at masses considerably lower than that, typically around $\sim 0.6M_\odot$ (Homeier et al. 1998). However, type Ia supernovae likely originate from carbon-oxygen white dwarfs at or close to the Chandrasekhar mass, as discussed above. This means that progenitors of type Ia supernovae must grow significantly in mass (at least $0.2M_\odot$, and most often more) before they can explode. However, there is no known way in which an isolated white dwarf might be able to grow significantly in mass, and therefore it is usually assumed that type Ia supernovae take place in binary systems, where mass-transfer between the binary components causes the white dwarf to grow sufficiently to explode. This mass-transfer is the fundamental problem concerning type Ia supernovae, and one that is yet to be convincingly solved. Two scenarios for how sufficient mass-gain may be accomplished are usually considered: the single-degenerate and double-degenerate scenarios (see Figure 5).

Single-Degenerate Progenitors as Supersoft X-ray Sources

In the single-degenerate scenario, the progenitor system consists of a massive white dwarf and a non-degnerate companion (usually a giant, although main-sequence and helium-star companions are also sometimes considered), and mass growth happens by accretion of hydrogen- or helium-rich material from the non-degenerate donor star onto the white dwarf accretor (Whelan & Iben 1973). The accreted material must then be processed into carbon and oxygen, leading to an increase in the mass of the white dwarf, to the point where a type Ia supernova can take place. However, the stability of the accretion process turns out to depend strongly on the rate of mass-transfer, as illustrated in Figure 6

For low to moderate mass-transfer rates ($\lesssim 10^{-7}M_\odot$/yr, Nomoto et al. 1979), an unburned hydrogen layer will build up and heat up until it eventually ignites unstably in a nova explosion (Starrfield 1971). The energy of the eruption depends on the mass-transfer rate and mass of

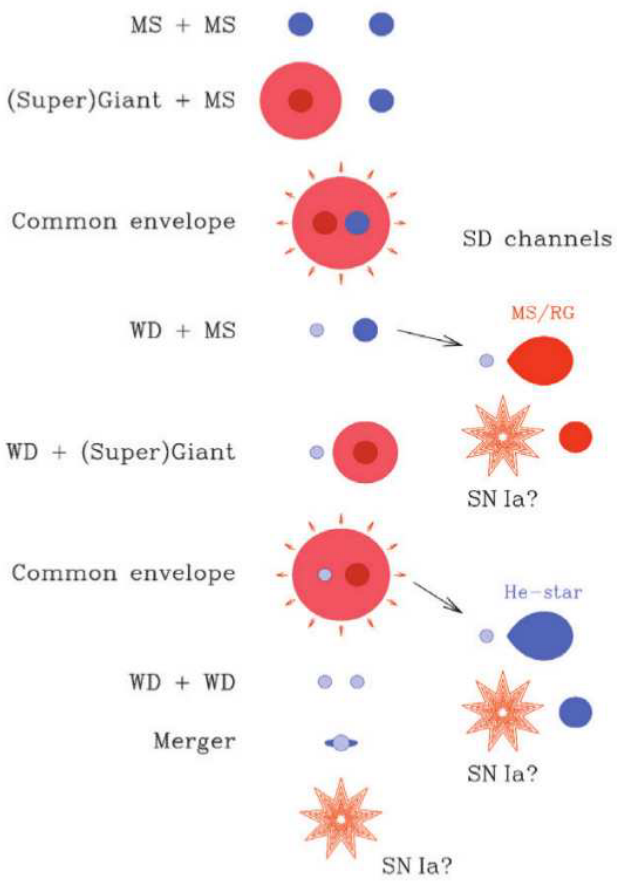

Figure 5: Schematic of the single- and double-degenerate type Ia supernova progenitor scenarios; time progresses from top to bottom. The two scenarios are conceptually similar (binary parameters such as separation and component masses are not similar, obviously) up until the formation of the first white dwarf. After that, the single-degenerate experiences mass transfer from the non-degenerate secondary unto the accreting white dwarf which grows towards the Chandrasekhar mass; in the double-degenerate case, the system goes through another white dwarf formation event, after which the two white dwarfs spiral in and eventually merge (Napiwotzki et al. 2003).

the accretor, and becomes more violent with lower mass-transfer rates and smaller white dwarf masses. For most mass-transfer rates, however, the explosions are likely violent enough to eject most of the accreted material, possibly along with material from the white dwarf itself (Nariai & Nomoto 1979; Sugimoto et al. 1979; Nomoto 1982). The net result is negligible mass growth of the accretor, or possibly even mass loss. Therefore, at these low mass transfer rates, the white dwarf is not expected to be able to grow sufficiently to eventually become a type Ia

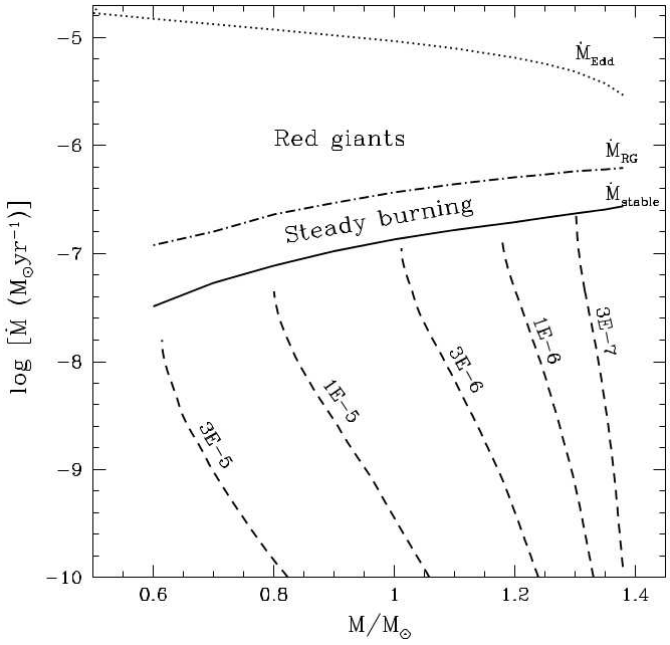

Figure 6: Accretion regimes for massive white dwarfs (Nomoto et al. 2007). The mass of the accreting white dwarf (in terms of Solar masses) is on the x-axis, the mass accretion rate (in terms of Solar masses per year) is on the y-axis.

supernova.

At somewhat higher mass accretion rates ($\sim 10^{-7} - 10^{-6} M_\odot$/yr), the accretion process heats up the material sufficiently for it to ignite and stably burn hydrogen to heavier elements (Nomoto 1982), thereby avoiding the episodic nova behaviour of the lower accretion rates. The result is presumably a steady mass increase of the carbon-oxygen white dwarf, possibly up to the mass needed for a type Ia supernova explosion, if the binary parameters and the mass of the donor permit it. The interval of accretion rates where this takes place is known as the steady-burning regime.

For mass-transfer rates above the steady-burning regime, the white dwarf is not able to process all the material being dumped onto it, and a massive pile-up of unburned material gradually enshrouds the white dwarf. The result is probably that the white dwarf swells up like a red giant star, possibly under the emission of a wind, likely hampering the accretion process (Nomoto et al. 1979; Nomoto 1982; Nomoto et al. 2007). This type of system is likely to be quite complex, as the envelope extends while accretion is going on, then contracts when accretion switches off, then expands again once accretion switches back on, and so on, possibly with shorter periods of more or less steady burning of material on the surface of the white dwarf. Whether the white dwarf will be able to efficiently grow in mass in system such as this is unclear.

For the single-degenerate scenario, therefore, the only way in which a white dwarf can grow

in mass to eventually become a type Ia supernova appears to be by the accretion of material in the fairly narrow interval of accretion rates, corresponding to the steady-burning regime. Because of this constraint and since the amount of material a newly-born carbon-oxygen white dwarf needs to accrete to become a type Ia supernova is at least 0.2 $M_{\odot}$, the accretion and steady burning must take place over an extended period of time, on the order of several times 10^6 years. The steady-burning of hydrogen-rich material to carbon and oxygen should release copious amounts of energy. Steadily accreting white dwarfs should therefore be expected to be highly luminous objects because of the thermonuclear processing of material taking place on their surfaces.

In the early 1990s, a new class of X-ray sources were recognised (Trümper et al. 1991; Greiner et al. 1991), based on earlier observations of the Magellanic Clouds from the Einstein Observatory (Long et al. 1981a). Their spectra were remarkably softer than those of more well-known X-ray sources, with black-body fits giving characteristic temperatures in the 30 - 150 eV range. They were therefore dubbed supersoft X-ray sources. In a subsequent study, van den Heuvel et al. (1992) showed that the spectra and luminosities of several known supersoft X-ray sources can be explained by the steady-burning of hydrogen-rich material on the surface of a white dwarf-sized object, exactly as expected in a single-degenerate type Ia supernova progenitor. For such accreting white dwarfs, the gravitational potentials are significantly shallower than for more compact accretors such as neutron stars and black holes. Consequently, the luminosity from the release of gravitational energy from the infalling material is expected to be at least two orders of magnitude less than the steady-burning luminosity. So the supersoft X-ray emission from the thermonuclear processing of the accreted material would dominate the total luminosity of single-degenerate type Ia supernova progenitors.

If we assume the single-degnerate scenario to be correct, and keep in mind that the steady-burning phase is required to last on the order of several 10^6 years, we should expect a large number of these sources to be present at any one point (hundreds to thousands in a galaxy like the Milky Way, in order to account for the observed rate of type Ia supernovae. After the initial discovery, more supersoft X-ray sources were found with later X-ray instruments such as *ROSAT*, *BeppoSAX*, *XMM-Newton* and *Chandra*. However, the number of supersoft X-ray sources observed to this day appears too low to account for the observed rate of type Ia supernovae, by as much as one or two orders of magnitude (Di Stefano 2010a). Additionally, other studies show the integrated supersoft X-ray luminosity of gas-poor galaxies to be similarly one to two orders of magnitude smaller than what is expected if steady-burning supersoft X-ray sources are type Ia supernova progenitors (Gilfanov & Bogdán 2010). This paucity of supersoft X-ray sources has been seen as a serious problem for the single-degenerate progenitor scenario of type Ia supernovae.

Double-Degenerate Progenitors as Supersoft X-ray Sources

In the double-degenerate scenario, a binary system evolves through two consecutive white dwarf formation events, eventually forming a system consisting of two separate, degenerate, sub-Chandrasekhar mass white dwarfs, but with a combined mass above the Chandrasekhar mass. Through the emission of graviational radiation, the binary orbit slowly decays, until the

two white dwarfs merge, resulting in a single carbon-oxygen white dwarf at or above the mass needed for the supernova (Iben & Tutukov 1984; Webbink 1984).

While it has been assumed for some time that single-degenerate type Ia supernova progenitors are supersoft X-ray sources, it has only recently been suggested that double-degenerate progenitors should exhibit a similar behaviour. In the model by Yoon et al. (2007), the supersoft phase takes place during a part of the merging process, after the break-up of the least massive white dwarf, when material is being accreted unto the surviving component at high accretion rates. However, in that study, the supersoft X-ray luminosity is expected to be an order of magnitude lower and last an order of magnitude shorter than that of the single-degenerate scenario, which would make it possible to distinguish the two scenarios, even if both emit supersoft X-rays.

In a different study, Di Stefano (2010b) suggested that double-degenerate progenitor systems may go through a prolonged supersoft X-ray emitting phase after the formation of the first white dwarf. In this stage, the progenitor system consists of a single white dwarf and an as yet non-degenerate companion (the second white dwarf has not yet formed). This is conceptually similar to a single-degenerate progenitor system, which we expect to emit supersoft X-rays, so it seems tempting to suggest that these proto-double-degenerate systems may also be supersoft X-ray sources, provided the system parameters were right. The constraints on mass accretion rate that governed the supersoft behaviour of the single-degenerate progenitors would also apply to the proto-double-degenerate progenitor systems. The study found, based on a simulated population of binaries, that a significant population of these systems accreting at the prerequisite rate should be expected to exist. If this were true, it would be a problem for the ongoing attempts at solving the type Ia supernova progenitor question, at least in the X-ray part of the spectrum, as it would make it hard to observationally distinguish between single- and double-degenerate progenitors.

Supernova rates

With the advent of wide-field transient surveys such as the Lick Observatory Supernova Search (LOSS, Li et al. 2000) or the SuperNova Legacy Survey (SNLS, e.g. Astier et al. 2006), the number of supernova detections has risen sharply; from a yearly discovery rate of around a handful of SNe of all types in the 1930s and 1940s, over ~ 30 SNe in the early 1990s, to ~ 250 in 2012 (at the time of writing of this thesis, the number of SNe discovered in 2013 is just over 100, indicating that it will be at least as 'rich' a year as 2012 in terms of SN discoveries). The number of known type Ia supernovae is currently large enough to allow stringent analyses to be made concerning the supernova rate and statistical characteristics of the host populations.

The delay-time distribution is the theoretical distribution of delays from the formation of progenitor binaries until the associated supernova explosions for a given stellar population (Yungelson & Livio 2000). Statistical information concerning the progenitor systems can then be obtained by correlating the delay-time distribution with host properties such as e.g. morphological type, total mass or star formation rate. Currently, the inferred delay-time distributions of galaxies at intermediate distances ($\gtrsim 100$ Mpc) can be fitted to a two-component model:

a significant fraction belong to a population of systems with relatively short delay-times ($\lesssim 1$ Gyr, consequently dubbed the "prompt" component), while another component falls off slowly with time (roughly as $\sim t^{-1}$), generating type Ia supernovae out to, and possibly beyond 10 Gyr (the "tardy" component) (Maoz et al. 2011). It has been suggested that the prompt and tardy components correspond to the single- and double-degenerate progenitor channels, but it is currently unclear how warranted such a suggestion is. In any case, the supernova rates and delay-time distributions are based on the statistically significant sample of intermediate distance type Ia supernovae. It is not clear whether the type Ia supernova rate in the local Universe is similar to that of intermediate and cosmological distances.

This thesis

The purpose of the present PhD project has been to explore the X-ray characteristics of the progenitors of type Ia supernovae. The structure of the remainder of this thesis is the following:

If type Ia supernova progenitors are single-degenerate systems in which the accreting white dwarfs are supersoft X-ray sources immediately before they explode as supernove, then these objects should be observable with current X-ray telescopes in the nearby Universe. We conducted the first systematic search for imprints of supersoft X-ray sources in archival Chandra data. The aim was to either make a direct detection, or alternatively, to calculate stringent upper limits on the bolometric luminosities of such sources. At the time of the writing of this thesis, there have been a total of 14 type Ia supernova with pre-explosion observations in the Chandra archive. One of them, SN2007on, may already have yielded a direct detection, see Voss & Nelemans (2008). However, the detection is ambiguous, as explained in Roelofs et al. (2008), and without further follow-up observations with Chandra the ambiguity is unlikely to be solved. Our analysis of the remaining 13 type Ia supernovae is presented in Chapter 2 and 3. We find no unambiguous direct detections of supersoft X-ray sources on the pre-explosion positions of type Ia supernovae.

The absence of supersoft X-ray sources at the pre-explosion positions of type Ia supernovae may mean either that they are simply not there, or that they are there, but are not recognisable as supersoft X-ray sources for one reason or another. This could be the case, for example, if the source was obscured by intervening material. In Chapter 4, we present a model of a single-degenerate type Ia supernova progenitor supersoft X-ray source enshrouded in a local shell of material that has been lost from the system. The object has been to determine if it is possible to hide or significantly obscure a supersoft X-ray source in such local, circumbinary material. We find that our simple model appear to indicate that it is possible, and that this may at least partially explain the conspicious absence of supersoft X-ray sources in pre-explosion Chandra images of the positions of type Ia supernovae.

In Chapter 5, we turn to the double-degenerate progenitor systems of type Ia supernovae. We examine the claim that double-degenerate progenitor systems should be supersoft X-ray sources during certain periods of their evolution. To this effect, we analyse results from a population synthesis code (SeBa). We find no support for the proposed supersoft X-ray behaviour of double-degenerate progenitors of type Ia supernovae, even under very optimistic

assumptions.

In Chapter 6, we examine the rate of local (≤ 50 Mpc) type Ia supernovae to determine how well they agree with the rates at intermediate ranges. We compare this with similar studies of core-collapse supernovae to the extent that such studies are available.

Upper limits on bolometric luminosities of ten type Ia supernova progenitors from Chandra observations

M.T.B. Nielsen, R. Voss, G. Nelemans

Monthly Notices of the Royal Astronomical Society 426, 2668 (2012)

Abstract

We present an analysis of *Chandra* observations of the position of ten nearby (< 25 Mpc) type Ia supernovae, taken before the explosions. No sources corresponding to progenitors were found in any of the observations. We calculated upper limits on the bolometric luminosities of the progenitors assuming black-body X-ray spectra with temperatures of 30-150 eV. This is inspired by the fact that luminous super-soft X-ray sources have been suggested as the direct progenitors of type Ia supernovae. The upper limits of two supernovae in our sample are comparable to the luminosities of the brightest observed super-soft sources, ruling out such sources as the progenitors of these supernovae. In contrast to Liu et al. (2012), we find that for SN2011fe we can rule out Eddington luminosity systems for black body temperatures as low as 40 eV. Our findings are consistent with statistical studies comparing the observed type Ia supernova rate to the number of super-soft sources or the integrated X-ray luminosity in external galaxies. This suggest that either the progenitors of type Ia supernovae are not accreting, nuclear burning white dwarfs, or that they do not look like the classical super-soft sources, e.g. because they are obscured.

Introduction

Type Ia supernovae (SNe) are important astrophysical phenomena, both in relation to cosmology (Riess et al. 1998; Perlmutter et al. 1999) and galactic chemical and dynamical evolution. Despite some fourty years of research on the subject the exact nature of the progenitor systems of SNe Ia remain undetermined. Two scenarios are usually considered by the community (e.g. Hillebrandt & Niemeyer 2000): the single degenerate (SD) and double degenerate (DD) scenarios. In the former, a single carbon-oxygen white dwarf (WD) star accretes matter from a non-degenerate companion star (Whelan & Iben 1973; Nomoto 1982), thereby growing in mass until it reaches a critical mass (~ 1.37 M$_\odot$), at which point the temperature and density in its interior are high enough for carbon and oxygen to fuse explosively into radioactive iron-group elements. In the DD scenario, two WDs with individual masses less than the Chandrasekhar mass merge to form a single carbon-oxygen WD at or above the critical mass needed for thermonuclear runaway (Tutukov & Yungelson 1981; Webbink 1984; Iben & Tutukov 1984). In both cases, the resulting SN explosion completely unbinds the WD, and the subsequent decay of radioactive nickel powers a light curve that can be used as standardizable cosmology candles (Phillips 1993).

It has been suggested that the steady accretion and nuclear burning of material on the surface of the WD in the SD scenario will emit super-soft X-rays (van den Heuvel et al. 1992; Kahabka & van den Heuvel 1997). The spectrum of this type of emission is expected to resemble a black-body with kT_{BB}= 30-100 eV and luminosities between $10^{37} - 10^{38}$ erg s^{-1}. For SNe closer than $\sim$ 25 Mpc such emissions should theoretically be observable with the *Chandra* X-ray Observatory. For this reason, a search of archival *Chandra* images taken before the SN explosions was conducted by Voss & Nelemans (2008), and the results were one possible detection (SN2007on, however, see also Roelofs et al. 2008) and four upper limits (SN2002cv, SN2004W, SN2006mr and SN2007sr, see Nelemans et al. 2008). Upper limits for the progenitor of SN2011fe based on archival *Chandra* images were reported by Butler et al. (2011) and later Li et al. (2011a), both studies using a black-body temperature of $kT_{BB} = 67$ eV. Upper limits for SN2011fe were also reported by Liu et al. (2012), however, below we show that we do not find the same upper limits to the bolometric luminosities as reported in that study.

The search for progenitors in archival X-ray images was inspired by the analoguous search for the progenitors of core-collapse SNe in *HST* archive, see review by Smartt (2009). A similar search for SN type Ia progenitors in *HST* archival images was performed by Maoz & Mannucci (2008) for SN2006dd and SN2006mr in NGC 1316, but no optical counterparts of these SNe were observed. Additionally, *HST* archival images were used to put upper limits on the optical luminosity of the progenitor of SN2007on (Voss & Nelemans 2008) and SN2007sr (Nelemans et al. 2008). Limits on the optical magnitude and bolometric luminosity of the progenitor of SN2011fe were reported by Li et al. (2011a).

In this paper we present a homogenous analysis of ten recent, nearby ($\leq$ 25 Mpc) type Ia SNe for which pre-explosion Chandra images are available: SN2002cv (Larionov et al. (IAUC 7901, IAUC 7903), classified by Meikle & Matilla (IAUC 7911)), SN2003cg (Itagaki et al.; Arbour (IAUC 8097), classified by Kotak et al. (IAUC 8099)), SN2004W (Moore & Li, classified by Fillipenko et al. (IAUC 8286)), SN2006X (Suzuki; Migliardi (IAUC 8667), classified by

Quimby et al. (CBET 393)), SN2006dd (Monard (CBET 533), classified by Salvo et al. (CBET 557)), SN2006mr (Monard (CBET 723), classified by Phillips et al. (CBET 729)), SN2007gi (Itagaki (CBET 1017), classified by Harutyunya et al. (CBET 1021)), SN2007sr (Drake et al. (CBET 1172), classified by Naito et al. (CBET 1173)), SN2008fp (Pignata et al. (CBET 1506), classified by Wang et al. (CBET 1509)) and SN2011fe (discovered and classified by Nugent et al. (CBET 2792)). We derive upper limits on the bolometric luminosities of the progenitors assuming black-body spectra with effective temperatures between 30 and 150 eV. The luminosities found in this study are compared to those of known super-soft X-ray sources (SSS) in nearby galaxies.

Together with SN2007on the ten SNe examined in this study comprise the complete set of currently-known type Ia SNe that have pre-explosion images in the *Chandra* archive. We note that it is currently unclear if the progenitor of SN2007on has been directly observed or not, see Voss & Nelemans (2008) and Roelofs et al. (2008). Due to this ambiguity we refrain from dealing with SN2007on in this study.

Observations

By searching the *Chandra* Data Archive we found pre-explosion images taken with the Advanced CCD Imaging Spectrometer (ACIS-S) at the positions of ten nearby (<25 Mpc) type Ia SNe. The SNe in question are SN2002cv, SN2003cg, SN2004W, SN2006X, SN2006dd, SN2006mr, SN2007gi, SN2007sr, SN2008fp and SN2011fe. No obvious sources were found on the pre-explosion images for any of these SNe.

For SN2002cv, SN2003cg, SN2004W, SN2006X, SN2006dd, SN2006mr, SN2007gi and SN2008fp, only a single pre-explosion *Chandra* image exists for each of the SNe, and SN2006dd and SN2006mr are on the same image. Several of these images have long (>30 ks) exposure times. For SN2007sr and SN2011fe multiple pre-explosion *Chandra* images exist, and these can be combined to give very long (several 100 ks) exposure times.

The observations analysed in this study are summarised on Table 2.

Data Reduction

We analysed the *Chandra* observations using the CIAO 4.3 software suite. Initially, we examined the images in the entire photon energy range of *Chandra*, i.e. ∼300 eV to ∼10 keV, to determine whether a source was present. Thereafter, we limited our analysis to photon energies between 300 eV and 1 keV. For a SSS any counts above 1 keV will be background anyway, so this approach allows more stringent upper limits to be placed on an assumed super-soft progenitor. No sources were found at or near the positions of any of the SNe analysed in this study in the two energy ranges used (i.e. 300 eV - 10 keV and 300 eV - 1 keV).

For our data model we assumed an absorbed black-body, using the spectral models `xsphabs` and `xsbbody`, which correspond to XSPEC's `phabs` and `bbody`, respectively. We generated spectral-weights files for the appropriate interstellar absorption columns (see below) and four different effective temperatures: kT_{BB} = 30 eV, 50 eV, 100 eV, and 150 eV. The spectral-

weights files were used to generate exposure maps for each of the images for each of the four effective temperatures. For SN2007sr and SN2011fe multiple pre-explosion images exist, and for these SN position we combined the binned images and the exposure maps to obtain deeper observations.

The distances to the progenitors of SN2002cv, SN2003cg, SN2004W, SN2006X, SN2007gi and SN2008fp were assumed identical to the galactocentric distances to their host galaxies[1] as listed in the NED online database[2]. The distance to the progenitor of SN2006dd and SN2006mr is taken from Stritzinger et al. (2010). The distance to the progenitor of SN2007sr is the one given in Schweizer et al. (2008). For SN2011fe we used the recent distance value given in Shappee & Stanek (2011).

The hydrogen columns were either found directly in the literature, or by using the formula (Güver & Özel 2009): $N_H = 2.21 \cdot 10^{21} A_V$ where N_H is the neutral hydrogen column in cm^{-2}, and A_V is the total V-band extinction given in magnitudes. The total V-band extinction is found from the reddening law $R_V = A_V E(B-V)$, where R_V is the reddening, and $E(B-V)$ is the selective optical extinction or color excess ($E(B-V) \equiv A_B - A_V$).

For two SNe (SN2004W and SN2008fp) no explicit values for the hydrogen column, reddening, or extinction could be found in the literature. For the two SNe in NGC1316 the column in the host galaxy was assumed to be negligible, following Stritzinger et al. (2010). For these four cases we used the value for the Galactic column found in Dickey & Lockman (1990), as referenced with CIAO's COLDEN tool. For SN2011fe Chomiuk et al. (2012) estimated a column value about twice that of the Galactic one, while Stritzinger et al. (2010) assumed the column in the host galaxy to be negligible. Since SN2011fe is the closest SN Ia in several decades, and the closest to have pre-explosion archival *Chandra* data, we consider both column values in our analysis. The host galaxies, distances, and columns for the SNe analysed in this study are summarised in Table 1.

For each observation we found a good estimate of the average number of background photons from a suitably-chosen region free of point-sources close to the source. We then used a circular aperture of radius 4.5 pixels (covering more than 90% of the point-spread function of all observations) around the position of the SN and extract the number of photons. This aperture contains a Poissonian realisation of the expected average number of counts from a source plus the background[3]. For this photon count $N_{\rm obs}$ we found the maximum average number of counts μ, for which the probability P of observing $N_{\rm obs}$ photons is within 3σ, assuming Poissonian statistics, see e.g. Gehrels (1986): $P\left(\mu, N \leq N_{\rm obs}\right) \leq 0.0013$. This μ represents the 3σ upper

[1] host galaxies were obtained from IAU Central Bureau for Astronomical Telegrams online list of SNe http://www.cbat.eps.harvard.edu/lists/Supernovae.html

[2] http://ned.ipac.caltech.edu/forms/byname.html

[3] This was unproblematic for all observations except one; for SN2006mr choosing a suitable background region was more difficult, due to the proximity of a large, unresolved and uneven background. To be conservative, for SN2006mr we chose a background region that was less bright than the immediate background of the assumed progenitor position and made our calculations using the resulting background photon count. Since this background is clearly smaller than the actual background our upper limits for the progenitor of SN2006mr should be considered even more solid than the rest of our results. However, it also means that formally our analysis indicates the presence of a source at the position of the progenitor of SN2006mr, even though it is not actually possible to infer the presence of one.

Table 1: Host galaxies, distances and total hydrogen columns for each of the SNe analyzed in this study.

supernova	host galaxy	distance [Mpc]	absorbing column [N_H cm^{-2}]	reference
2002cv	NGC 3190	16.4	$1.93 \cdot 10^{22}$	Elias-Rosa et al. (2008)
2003cg	NGC 3169	15.1	$2.99 \cdot 10^{21}$	Elias-Rosa et al. (2006)
2004W	NGC 4649	14.6	$2.12 \cdot 10^{21}$	Dickey & Lockman (1990)
2006X	NGC 4321	20.9	$2.30 \cdot 10^{21}$	Wang et al. (2008)
2006dd	NGC 1316	17.8	$2.13 \cdot 10^{20}$	Dickey & Lockman (1990)
2006mr	NGC 1316	17.8	$2.13 \cdot 10^{20}$	Dickey & Lockman (1990)
2007gi	NGC 4036	21.2	$6.85 \cdot 10^{20}$	Zhang et al. (2010)
2007sr	NGC 4038/39	22.3	$4.00 \cdot 10^{20}$	Nelemans et al. (2008)
2008fp	ESO 428-G14	20.4	$2.21 \cdot 10^{21}$	Dickey & Lockman (1990)
2011fe	M 101	6.4	$3.02 \cdot 10^{20}/1.14 \cdot 10^{20}$	Chomiuk et al. (2012)/ Dickey & Lockman (1990)

limit of any progenitor including background. We find the upper limit to the luminosity of the source according to the formula,

$$L_{X,UL} = 4\pi \frac{(\mu - b)\,\langle E_\gamma \rangle d^2}{\zeta} \tag{1}$$

where b is the expected background for a circular aperture of radius 4.5 pixels, $\langle E_\gamma \rangle$ is the average energy of the photons found from the absorbed XSPEC model for the assumed spectrum, d is the distance to the SN and ζ is the value of the exposure map for the given spectrum at the position of the SN on the detector.

The luminosities were then corrected for interstellar absorption to yield the unabsorbed luminosities.

Since our data model is limited to photons from 300 eV to 1 keV the luminosities found are scaled to provide bolometric luminosities,

$$L_{bol,UL} = \frac{L_{X,UL}}{C} \tag{2}$$

For the values of kT_{BB} used in our analysis the scaling factors are:

$$\begin{aligned} 30 \text{ eV} &: C = 9.58 \cdot 10^{-3} \\ 50 \text{ eV} &: C = 1.40 \cdot 10^{-1} \\ 100 \text{ eV} &: C = 6.01 \cdot 10^{-1} \\ 150 \text{ eV} &: C = 7.22 \cdot 10^{-1} \end{aligned}$$

The observations analysed in this study, along with the photon counts and exposure map values used to calculate the upper limit luminosities, are listed in Tables 2 and 3. The bolomet-

ric luminosities are shown on Figure 7. The individual *Chandra* images are shown on Figures 8-17. These images show all events from 0.3 to 1 keV.

Our results are summarized in Table 3.

Discussion

Disregarding the ambiguous case of SN2007on, we now have ten pre-explosion *Chandra* X-ray images of the positions of SNe Ia, and none of them show evidence of a progenitor.

Figure 7 shows a comparison between our results and the bolometric luminosities of known persistent close-binary and symbiotic SSSs in the Galaxy, Large Magellanic Cloud and Small Magellanic Cloud from Greiner (2000). Clearly, the bolometric luminosity upper limits of SN2011fe and SN2007sr are probing the luminosity space of 'canonical' SSSs (i.e. kT_{BB} = 30-100 eV, $L_{bol} = 10^{37} - 10^{38}$ erg/s). For both these SNe we can rule out a naked, bright SSS progenitor. However, a SSS progenitor in the lower part of the expected effective temperature space is still permitted by the observations.

Upper limits based on archival *Chandra* observations were reported previously for SN2002cv, SN2004W and SN2006mr by Voss & Nelemans (2008) and later corrected in Nelemans et al. (2008). However, the method used in those earlier studies was rather different from the one used in the present study: the *Chandra* counts were binned into soft, medium and hard photons, and for each energy bin the total luminosity was calculated from an assumption that the spectrum was flat. The upper limits given for SN2002cv, SN2004W and SN2006mr in Voss & Nelemans (2008) were $\leq 7.9 \cdot 10^{37}$erg/s, $\leq 3.5 \cdot 10^{37}$erg/s, and $\leq 1.3 \cdot 10^{38}$erg/s, respectively. However, due to the simplified spectral assumption used in that study, and the fact that only Galactic hydrogen was taken into account in Voss & Nelemans (2008), the upper limits found in the present study should be considered more accurate. Bolometric upper limits for SN2007sr for kT_{BB} = 50, 100, 150 eV were reported in Nelemans et al. (2008) and are consistent with the results of the present study. For SN2011fe X-ray upper limits of $< 10^{36}$ erg/s were reported by Butler et al. (2011) for photons with energies between 300 and 700 eV and a 67 eV black-body spectral model. Subsequently, Li et al. (2011a) reported upper limits of $2.7 \cdot 10^{37}$ erg/s on the bolometric luminosity of the progenitor of SN2011fe, similarly based on a black-body model with kT_{BB} = 67 eV. The results of both of the aforementioned studies are in agreement with the results of this paper. We note that the slightly larger upper limits found by Li et al. (2011a) can be explained by the shorter exposure time of their combined image used in their study.

We note that upper limits for SN2011fe were also reported in Liu et al. (2012), who found a value of $L_{\rm X} < 6.2 \cdot 10^{35}$erg/s for kT_{BB} = 100eV in the same energy band as the one used in our study (0.3 − 1keV). However, for reasons that are unclear to us Liu et al. (2012) subsequently finds different corresponding bolometric luminosities, which could indicate an incorrect conversion factor from X-ray to bolometric luminosity. Additionally, that paper makes an incorrect statement concerning the black-body temperatures and response matrices used to find the upper limits found in our study (last paragraph of Section 3 in that article). As should be clear from our Section we have consistently used the black-body temperature to calculate our X-ray to bolometric luminosity conversion factors. Also, the fact that the

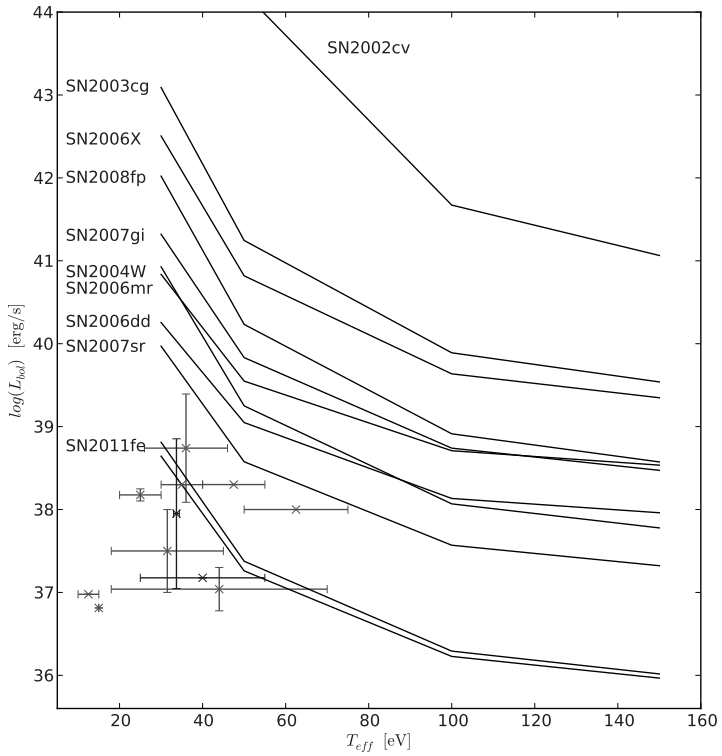

Figure 7: Comparison between the bolometric luminosity upper limits found in this paper with bolometric luminosities of known super-soft X-ray sources in nearby galaxies. The black lines are the upper limits reported in this paper (for SN2011fe the two curves correspond to the two different column values used, see section). The green, blue and red points are known persistent SSS in the Milky Way, SMC and LMC, respectively, taken from the online SSS catalog by Greiner, see Greiner (2000) and references therein. The plot only include sources that are characterized as close-binary super-soft (CBSS) or symbiotic (Sy) systems. We note that many of the fits are based on single observations, and suffer from relatively large systematic uncertainties.

ACIS-S detector is unreliable below 300 eV has no impact on our results, because we only use observed photons with energies above this threshold.

As mentioned in the introduction, Di Stefano (2010a) showed that the number of observed SSSs in nearby galaxies is one to two orders of magnitude too small compared with the estimated number of expected SSSs if these were the progenitors of type Ia SNe. A similar result was found by Gilfanov & Bogdán (2010) who showed that the integrated super-soft X-ray luminosity of elliptical galaxies is roughly two orders of magnitude too low to account for the SN Ia rate. Although our constraints are not as strong as those found in the two above-mentioned studies our results are consistent with them.

The search for archival *Chandra* images was initially undertaken in an attempt to solve the SD vs. DD question, since at least in the naïve picture the SD progenitors were expected to be X-ray bright, while the DD progenitors were not. However, as a number of recent studies show the question of X-ray brightness of Ia progenitors has turned out to be somewhat more complicated than this:

•*Chandra* and other current X-ray satellites are only sensitive at photon energies considerably above the kT_{BB} of SSS, above ~ 300 eV or so. The corrections applied in Eq. (2) illustrate that a small change in kT_{BB} has a drastic effect on the correctional constant C for lower-kT_{BB} sources. The effective temperature of a SD progenitor depends crucially on the extent of the emitting region, and the radius of an actual SD accretor therefore does not have to diverge much from that of the theoretical model to make the system unobservable to *Chandra*. For such lower kT_{BB}-sources, UV observations should be more useful than X-rays. However, UV observations of these sources are problematic for other reasons, such as interstellar extinction.

•As discussed by Hachisu et al. (2010), a significant fraction of the progenitors of SD SNe Ia may spend the final phase of their accretion towards going SN in the nova regime where their accretion and associated X-ray emission will be periodic instead of continuous. For recent observations of super-soft X-ray emissions from novae see Henze et al. (2010), Henze et al. (2011), Schaefer & Collazzi (2010) and Voss et al. (2008).

•Even a steadily-accreting massive WD consistent with a naked, canonical SSS may be obscured by local matter lost from the system, see Nielsen et al. (2013). Several recent studies have found indications of the presence of circumstellar matter, e.g. Gerardy et al. (2004), Immler et al. (2006), Borkowski et al. (2006), Patat et al. (2007), Chiotellis et al. (2012), Sternberg et al. (2011).

•If the progenitor is a rapidly rotating WD of the type suggested in Di Stefano et al. (2011) the X-ray emission of the progenitor would have ceased long before the explosion itself.

•The detailed spectral shape of the SSS is uncertain (Orio 2006), and the assumption of a black-body spectrum used in this study may therefore be inaccurate. Due to the higher sensitivity of Chandra above 1 keV the upper limits are more constraining for harder spectra. This is at most an order of magnitude different compared to our 150 eV data points, for the unrealistic assumption of a powerlaw with photon index $\Gamma = 2$, typical of X-ray binaries (c.f. the limits for power law and black-body in Li et al. (2011a) for 2011fe).

•To make things more difficult, a DD progenitor may also emit soft X-rays for a significant period of time, see Yoon et al. (2007). However, the luminosities expected in this scenario are

approximately an order of magnitude lower than for the steadily-accreting SD progenitor. In any case, the detailed workings of the DD merger are still not fully understood (cf. Pakmor et al. 2010, Lorén-Aguilar et al. 2009, van Kerkwijk et al. 2010). It is currently unclear if the lighter WD forms a disk around the more massive companion, or if both WDs are disrupted in the course of the merging event, and this would have an important effect on the possible X-ray emissions from such systems.

For the above-mentioned reasons the question of a SD vs. DD progenitor cannot be decided based solely on the X-ray brightness (or lack hereof) of a type Ia SN progenitor. However, a direct detection of X-ray emissions from a progenitor would still be interesting, and would provide much needed observational evidence for the progenitors of type Ia SNe with which to compare theoretical work, something that is sorely lacking at the moment.

Conclusions

We have examined archival *Chandra* pre-explosion images corresponding to the position of ten SNe Ia to determine upper limits to the bolometric luminosities of the progenitors.

Disregarding the ambigious case of SN2007on, our study comprises a complete list of nearby SNe that have pre-explosion images in *Chandra*. We compared this sample with known SSSs in the Milky Way and Magellanic Clouds. While most of the luminosities of our sample SNe are too loosely constrained, two SNe (SN2007sr and SN2011fe) probe the luminosity space of known SSSs. The results indicate that the progenitors of these SNe were not bright SSSs shortly before they exploded as SNe Ia. However, our upper limits are not constraining enough to rule out less-bright super-soft X-ray progenitors.

The theoretical picture concerning the super-soft X-ray characteristics of SN Ia progenitors is less than clear. A non-detection does not rule out a SD progenitor, but neither does a positive detection necessarily implicate a SD progenitor or rule out a DD progenitor. Regardless, the archival search method of the *Chandra* archive is highly useful in putting much-needed observational constraints on the progenitors, and is a powerful complement to statistical studies of the characteristics of progenitor populations. The method will become increasingly useful as the sky coverage grows. As SN2011fe shows, if a SN Ia explodes in a nearby galaxy, the chances that several pre-explosion *Chandra* images of the position exist are good, hence affording stringent upper limits to be calculated, or, in the case of an X-ray bright progenitor, a direct detection to be made.

Acknowledgments

The authors are grateful to the referee Martin Henze for carefully reading our first draft and providing many useful comments and suggestions.

This research made use of data obtained from the *Chandra* Data Archive and the CIAO 4.3 software provided by the *Chandra* X-ray Center. We also acknowledge the IAU Central Bureau of Astronomical Telegrams for providing their list of SNe.

This research is supported by NWO Vidi grant 016.093.305.

Additionally, we acknowledge Gijs Roelofs for help with this project in its early stages.

Table 2: *Chandra* observations used in this study. All observations are with the ACIS-S detector.

Chandra observation	exposure time [ks]	pointing (RA, DEC)	SN covered	SN explosion date	observation date date
2760	20.07	(10:18:06.50, +21:49:41.70)	2002cv	2002-05-13	2002-03-14
1614	2.15	(10:14:15.00, +03:27:57.10)	2003cg	2003-03-21	2001-05-02
785	37.35	(12:43:40.30, +11:32:58.00)	2004W	2004-01-28	2000-04-20
400	2.53	(12:22:54.80, +15:49:20.00)	2006X	2006-02-04	1999-11-06
2022	30.23	(03:22:41.70, -37:12:29.00)	2006dd	2006-06-19	2001-04-24
			& 2006mr	2006-11-05	
6783	15.13	(12:01:26.90, +61:53:44.00)	2007gi	2007-07-31	2006-07-24
315	73.17	(12:01:53.70, -18:52:35.50)	2007sr	2007-12-18	1999-12-01
3040	69.93	(12:01:53.70, -18:52:35.50)	2007sr	2007-12-18	2001-12-29
3041	73.85	(12:01:53.70, -18:52:35.50)	2007sr	2007-12-18	2002-11-22
3042	68.14	(12:01:53.70, -18:52:35.50)	2007sr	2007-12-18	2002-05-31
3043	67.96	(12:01:53.70, -18:52:35.50)	2007sr	2007-12-18	2002-04-18
3044	36.97	(12:01:53.70, -18:52:35.50)	2007sr	2007-12-18	2002-07-10
3718	35.16	(12:01:53.70, -18:52:35.50)	2007sr	2007-12-18	2002-07-13
4866	30.16	(07:16:31.20, -29:19:29.00)	2008fp	2008-09-11	2003-12-26
4731	56.96	(14:03:12.90, +54:20:55.60)	2011fe	2011-08-24	2004-01-19
5296	3.23	(14:03:12.90, +54:20:55.60)	2011fe	2011-08-24	2004-01-21
5297	21.96	(14:03:12.90, +54:20:55.60)	2011fe	2011-08-24	2004-01-24
5300	52.76	(14:03:12.90, +54:20:55.60)	2011fe	2011-08-24	2004-03-07
4732	70.69	(14:03:12.90, +54:20:55.60)	2011fe	2011-08-24	2004-03-19
5309	71.68	(14:03:12.90, +54:20:55.60)	2011fe	2011-08-24	2004-03-14
4733	25.13	(14:03:12.90, +54:20:55.60)	2011fe	2011-08-24	2004-05-07
5322	65.53	(14:03:12.90, +54:20:55.60)	2011fe	2011-08-24	2004-05-03
5323	43.16	(14:03:12.90, +54:20:55.60)	2011fe	2011-08-24	2004-05-09
4734	35.93	(14:03:12.90, +54:20:55.60)	2011fe	2011-08-24	2004-07-11
5337	10.07	(14:03:12.90, +54:20:55.60)	2011fe	2011-08-24	2004-07-05
5338	28.93	(14:03:12.90, +54:20:55.60)	2011fe	2011-08-24	2004-07-06
5339	14.51	(14:03:12.90, +54:20:55.60)	2011fe	2011-08-24	2004-07-07
5340	55.12	(14:03:12.90, +54:20:55.60)	2011fe	2011-08-24	2004-07-08
4735	29.15	(14:03:12.90, +54:20:55.60)	2011fe	2011-08-24	2004-09-12
6114	67.05	(14:03:12.90, +54:20:55.60)	2011fe	2011-08-24	2004-09-05
6115	36.2	(14:03:12.90, +54:20:55.60)	2011fe	2011-08-24	2004-09-08
6118	11.61	(14:03:12.90, +54:20:55.60)	2011fe	2011-08-24	2004-09-11
4736	78.34	(14:03:12.90, +54:20:55.60)	2011fe	2011-08-24	2004-11-01
6152	44.66	(14:03:12.90, +54:20:55.60)	2011fe	2011-08-24	2004-11-07
4737	22.13	(14:03:48.20, +54:21:41.00)	2011fe	2011-08-24	2005-01-01
6169	29.75	(14:03:48.20, +54:21:41.00)	2011fe	2011-08-24	2004-12-30
6170	48.56	(14:03:48.20, +54:21:41.00)	2011fe	2011-08-24	2004-12-22
6175	41.18	(14:03:48.20, +54:21:41.00)	2011fe	2011-08-24	2004-12-24

Table 3: Upper limit bolometric luminosities of nearby (< 25 Mpc) SNe Ia with pre-explosion images.

Supernova	position [RA, DEC]	pre-explosion *Chandra* observations	exposure time [ks]	counts in source region	value of exposure map at position [s·cm^2]	unabsorbed 3-σ upper limit bolometric luminosity[4] [erg/s]
2002cv	(10:18:03.68,	2760	20.07	1	$4.99481 \cdot 10^6$	$3.9 \cdot 10^{47}$
	+21:50:06.0)			1	$8.85503 \cdot 10^6$	$1.7 \cdot 10^{44}$
				1	$1.02031 \cdot 10^7$	$4.7 \cdot 10^{41}$
				1	$1.04034 \cdot 10^7$	$1.2 \cdot 10^{41}$
2003cg	(10:14:15.97,	1614	2.15	1	261570	$1.2 \cdot 10^{43}$
	+03:28:02.5)			1	376688	$1.8 \cdot 10^{41}$
				1	605926	$7.8 \cdot 10^{39}$
				1	740782	$3.5 \cdot 10^{39}$
2004W	(12:43:36.52,	785	37.35	1	$6.36082 \cdot 10^6$	$8.5 \cdot 10^{40}$
	+11:31:50.8)			1	$8.75898 \cdot 10^6$	$1.8 \cdot 10^{39}$
				1	$1.29863 \cdot 10^7$	$1.2 \cdot 10^{38}$
				1	$1.54893 \cdot 10^7$	$6.0 \cdot 10^{37}$
2006X	(12:22:53.99,	400	2.53	0	474548	$3.2 \cdot 10^{42}$
	+15:48:33.1)			0	619526	$6.6 \cdot 10^{40}$
				0	855029	$4.3 \cdot 10^{39}$
				0	990341	$2.2 \cdot 10^{39}$
2006dd	(03:22:41.62,	2022	30.23	6	$2.50339 \cdot 10^6$	$1.8 \cdot 10^{40}$
	-37:12:13.0)			6	$3.22214 \cdot 10^6$	$1.1 \cdot 10^{39}$

Continued on next page

[4]for 30 eV, 50 eV, 100 eV, & 150 eV, respectively.

Table 3: Continued from previous page

				6	$5.55312 \cdot 10^6$	$1.4 \cdot 10^{38}$
				6	$7.48767 \cdot 10^6$	$9.1 \cdot 10^{37}$
2006mr	(03:22:42.84,	2022	30.23	44	$2.43645 \cdot 10^6$	$6.9 \cdot 10^{40}$
	-37:12:28.5)			44	$3.14788 \cdot 10^6$	$3.5 \cdot 10^{39}$
				44	$5.46562 \cdot 10^6$	$5.1 \cdot 10^{38}$
				44	$7.39541 \cdot 10^6$	$3.4 \cdot 10^{38}$
2007gi	(12:01:23.42,	6783	15.13	0	444218	$2.1 \cdot 10^{41}$
	+61:53:33.8)			0	743225	$6.8 \cdot 10^{39}$
				0	$1.76997 \cdot 10^6$	$5.5 \cdot 10^{38}$
				0	$2.63497 \cdot 10^6$	$3.0 \cdot 10^{38}$
2007sr	(12:01:52.80,	315, 3040, 3041, 3042,	425.18[5]	4	$1.03024 \cdot 10^7$	$9.3 \cdot 10^{39}$
	-18:58:21.7)	3044, 3044, 3718		4	$1.57593 \cdot 10^7$	$3.7 \cdot 10^{38}$
				4	$3.61044 \cdot 10^7$	$3.7 \cdot 10^{37}$
				4	$5.52568 \cdot 10^7$	$2.1 \cdot 10^{37}$
2008fp	(07:16:32.60,	4866	30.16	1	$1.79972 \cdot 10^6$	$1.0 \cdot 10^{42}$
	-29:19:31.7)			1	$3.07844 \cdot 10^6$	$1.7 \cdot 10^{40}$
				1	$6.00491 \cdot 10^6$	$8.2 \cdot 10^{38}$
				1	$7.93188 \cdot 10^6$	$3.7 \cdot 10^{38}$
2011fe	(14:03:05.81,	4731, 4732, 4733, 4735, 4736,	898.17[6]	4	$7.63589 \cdot 10^6$ / $7.37164 \cdot 10^6$	$6.5 \cdot 10^{38}$ / $4.4 \cdot 10^{38}$
	+54:16:25.4)	4737, 5296, 5297, 5300, 5309,		4	$1.33861 \cdot 10^7$ / $1.23642 \cdot 10^7$	$2.4 \cdot 10^{37}$ / $1.8 \cdot 10^{37}$
		5322, 5323, 5338, 5339, 5340,		4	$3.87832 \cdot 10^7$ / $3.5352 \cdot 10^7$	$2.0 \cdot 10^{36}$ / $1.7 \cdot 10^{36}$
		6114, 6115, 6118, 6152, 6169,		4	$6.49251 \cdot 10^7$ / $6.00846 \cdot 10^7$	$1.0 \cdot 10^{36}$ / $9.3 \cdot 10^{35}$
		6170, 6175				

[5] total exposure time of the combined image.
[6] total exposure time of the combined image.

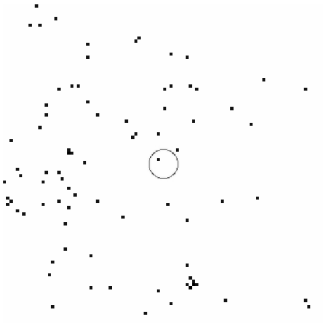

Figure 8: Cut-out of *Chandra* image for observation 2760. The circle corresponds to an aperture of 4.5 pixels at the position of SN2002cv.

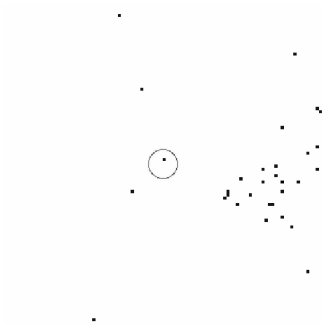

Figure 9: Cut-out of *Chandra* image for observation 1614. The circle corresponds to an aperture of 4.5 pixels at the position of SN2003cg.

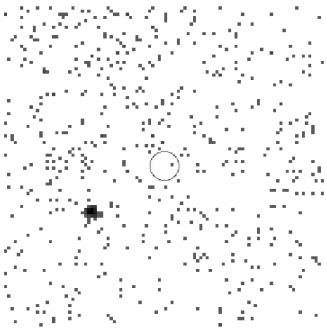

Figure 10: Cut-out of *Chandra* image for observation 785. The circle corresponds to an aperture of 4.5 pixels at the position of SN2004W.

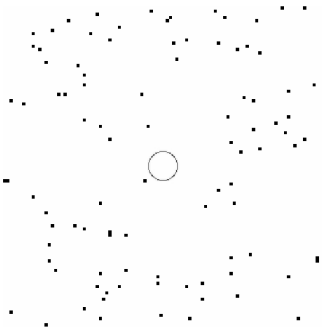

Figure 11: Cut-out of *Chandra* image for observation 400. The circle corresponds to an aperture of 4.5 pixels at the position of SN2006X.

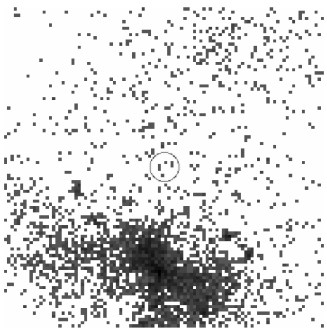

Figure 12: Cut-out of *Chandra* image for observation 2022. The circle corresponds to an aperture of 4.5 pixels at the position of SN2006dd.

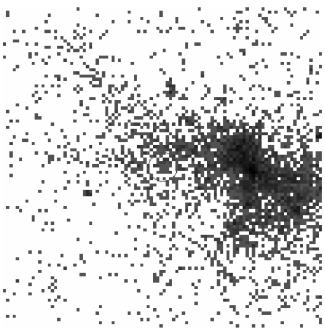

Figure 13: Cut-out of *Chandra* image for observation 2022. The circle corresponds to an aperture of 4.5 pixels at the position of SN2006mr.

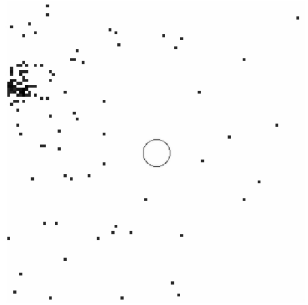

Figure 14: Cut-out of *Chandra* image for observation 6783. The circle corresponds to an aperture of 4.5 pixels at the position of SN2007gi.

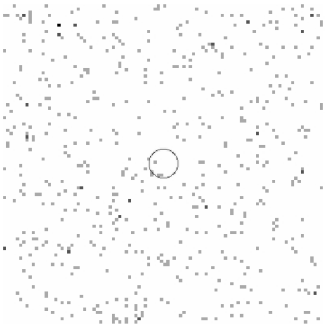

Figure 15: Cut-out of combined image consisting of *Chandra* observations 315 3040 3041 3042 3043 3044 3718. The circle corresponds to an aperture of 4.5 pixels at the position of SN2007sr

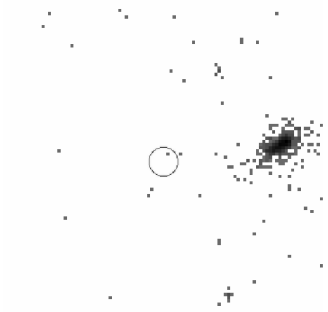

Figure 16: Cut-out of *Chandra* image for observation 4866. The circle corresponds to an aperture of 4.5 pixels at the position of SN2008fp.

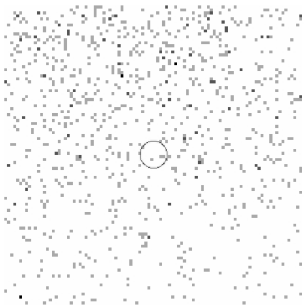

Figure 17: Cut-out of combined image consisting of *Chandra* observations 4731, 5296, 5297, 5300, 4732, 5309, 4733, 5322, 5323, 4737, 5338, 5339, 5340, 4735, 6114, 6115, 6118, 4736, 6152, 4737, 6169, 6170, 6175. The circle corresponds to an aperture of 4.5 pixels at the position of SN2011fe.

Obscuration of supersoft X-ray sources by circumbinary material - A way to hide type Ia supernova progenitors?

M.T.B. Nielsen, C. Dominik, G. Nelemans, R. Voss

Astronomy & Astrophysics 549, A32 (2013)

Abstract

The progenitors of type Ia supernovae are usually assumed to be either a single white dwarf accreting from a non-degenerate companion (the single-degenerate channel) or the result of two merging white dwarfs (the double degenerate channel). However, no consensus currently exists as to which progenitor scenario is the correct one, or whether the observed type Ia supernovae rate is produced by a combination of both channels. Unlike a double degenerate progenitor, a single-degenerate progenitor is expected to emit supersoft X-rays for a prolonged period of time ($\sim$ 1 Myr) as a result of the burning of accreted matter on the surface of the white dwarf. An argument against the single-degenerate channel as a significant producer of type Ia supernovae has been the lack of observed supersoft X-ray sources and the lower-than-expected integrated soft X-ray flux from elliptical galaxies. We wish to determine whether it is possible to obscure the supersoft X-ray emission from a nuclear-burning white dwarf in an accreting single-degenerate binary system. In the case of obscured systems we wish to determine their general observational characteristics. We examine the emergent X-ray emission from a canonical supersoft X-ray system surrounded by a spherically symmetric configuration of material, assuming a black-body spectrum with $T_{bb} = 50$ eV and $L = 10^{38}\mathrm{erg} \cdot \mathrm{s}^{-1}$. The

circumbinary material is assumed to be of solar chemical abundances, and we leave the mechanism behind the mass-loss into the circumbinary region unspecified. We find that relatively low circumstellar mass-loss rates, $\dot{M} = 10^{-9} - 10^{-8} \mathrm{M}_{\odot} \mathrm{yr}^{-1}$, at binary separations of ~ 1 AU or less, will cause significant attenuation of the X-rays from the supersoft X-ray source. These circumstellar mass-loss rates are sufficient to make a canonical supersoft X-ray source in typical external galaxies unobservable in Chandra. If steadily accreting, nuclear-burning white dwarfs are canonical supersoft X-ray sources our analysis suggests that they can be obscured by relatively modest circumbinary mass-loss rates. This may explain the discrepancy of supersoft sources relative to the type Ia supernova rate inferred from observations if the single-degenerate progenitor scenario contributes significantly to the type Ia supernova rate. Recycled emissions from obscured systems may be visible in wavebands other than X-rays. It may also explain the lack of observed supersoft sources in symbiotic binary systems.

Introduction

Type Ia supernovae (SNe Ia) are believed to be carbon-oxygen white dwarfs (WDs) close to the Chandrasekhar mass that undergo thermonuclear runaway in their centers. The resulting explosion produces radioactive iron-group elements, and the subsequent decay of these, most notably of ^{56}Ni, powers characteristic light curves that obey a well-known relation between luminosity at maximum light and fall-off time (Phillips 1993). As a result, SNe Ia are considered standardizable cosmological candles. To this effect they have been utilized to suggest that the expansion of the Universe is accelerating (Riess et al. 1998; Perlmutter et al. 1999), which in turn has given rise to the paradigm of dark energy. Additionally, the energy release of SNe Ia is large enough to influence the dynamics of their host galaxies, and the nucleosynthesis taking place during the explosions is the main source of iron group elements in galactic chemistries.

Despite decades of intense research on the subject, the exact nature of the progenitor systems of these important astrophysical explosions remains unclear. Carbon-oxygen WDs are characteristically formed at masses much lower (~ 0.6 M$_{\odot}$) than that needed for thermonuclear runaway (~ 1.37 M$_{\odot}$), and there is no known process by which an isolated sub-Chandrasekhar mass WD can grow to the critical mass at which it explodes as a SN Ia. Hence, it is usually agreed that SNe Ia can only arise in binary systems, where a WD accretes matter from a companion star. However, the exact method of accretion remains disputed. Two binary progenitor scenarios are usually considered: the single-degenerate (SD), in which a WD accretes mass from a non-degenerate companion (main-sequence or giant star, Whelan & Iben 1973), and the double degenerate (DD), in which two sub-Chandrasekhar mass WDs merge with a mass at or above the mass needed to explode as a SN Ia (Webbink 1984; Iben & Tutukov 1984).

While the DD scenario has garnered considerable attention recently, the SD scenario has been the most popular scenario for a long time, and much work has been done on the physics of this progenitor scenario (e.g. Hachisu et al. 1996). It was shown by Nomoto (1982) that steady nuclear-burning of hydrogen-rich material accreted from a companion onto a massive (~ 1 M$_{\odot}$)

WD can only take place in a fairly narrow interval of accretion rates close to 10^{-7} $M_{\odot}yr^{-1}$. At lower or higher accretion rates it is unclear whether the WD will be able to grow sufficiently in mass for a SN Ia to occur, owing to possible mass-loss from either nova eruptions or stellar winds. This puts rather tight constraints on the parameters of the progenitor systems.

In the 1990s, luminous supersoft X-ray sources (SSSs) were recognized as forming an important new class of X-ray source (Trümper et al. 1991; Greiner et al. 1991)) based on observations of the Large Magellanic Cloud made with the Einstein Observatory in the late 70s and early 80s (Long et al. 1981b). Since then, newer generations of X-ray instruments such as *ROSAT*, *BeppoSAX*, *XMM-Newton*, and *Chandra X-ray Observatory* have found similar sources in other galaxies, including the Milky Way. As the name suggests, SSSs have much softer spectra than those of more commonly known X-ray binaries involving either a neutron star or a black hole. Subsequently, van den Heuvel et al. (1992) showed that a massive WD accreting from a companion star at the steady-burning rate will emit X-rays with a spectrum consistent with that observed for a certain subset of SSSs as a result of thermonuclear-burning of the accreted material. This made SSSs interesting as possible SD progenitor systems of SNe Ia.

If WDs undergoing steady nuclear-burning on their surfaces resemble SSSs, and if the SD progenitor scenario is the dominant contributor to the SN Ia rate, then we should expect - at least naively - to see a corresponding population of SSSs large enough to account for the observed SN Ia rate. However, as has been pointed out, the observed number of SSSs (Di Stefano 2010a) and integrated soft X-ray flux (Gilfanov & Bogdán 2010) observed from external galaxies appear to be at least one and more likely two orders of magnitude too low to account for the SN Ia rate. Furthermore, pre-explosion observations of the positions of nearby ($\lesssim$ 25 Mpc) SNe Ia using archival Chandra data have so far yielded no detections of SSSs (Nielsen et al. 2012). This dearth of SSSs could very well mean that the missing sources are simply not there, and that the SD progenitor scenario is not the dominant contributor to the SN Ia rate. An alternative possibility is that the nuclear-burning WDs appearing as SSS in SD progenitors do exist and produce a significant fraction of the total SN Ia rate, but are somehow with current X-ray instruments during much of their supersoft phase.

In the following, we wish to explore the latter option. We consider a simple model of a massive, accreting WD with a companion star that loses matter into the circumbinary region in addition to the matter it transfers to the accretor. The goal has been to determine how much circumbinary material is needed to render a nuclear-burning WD in a nearby galaxy undetectable as a SSS for a given combination of binary parameters.

We note that we refer to the rate of material that is lost into the circumbinary region as simply the mass-loss rate, $\dot{M}$. This should not be confused with the rate of mass that is transferred to the WD accretor, $\dot{M}_{\rm acc}$. In our notation, the total rate of mass lost from the donor is $\dot{M}_{\rm tot} = \dot{M} + \dot{M}_{\rm acc}$

In section , we describe our model, including the structure of the gas bubble surrounding the SSS and the contributions to the obscuration from neutral gas, ionized gas, and dust. In section , we present the results of our calculations, and section discusses the observational implications of the results. Section discusses the caveats of our model, and section concludes.

Model

We consider the emergent radiation from a massive ($\sim 1 M_\odot$) WD accreting mass from a companion star in a close binary system. The donor may be either a main-sequence or evolved star. The system loses mass into the circumbinary region, and this mass-loss creates a spherical distribution of matter (gas and possibly dust) around the binary that may absorb and/or scatter the X-rays. The mechanism behind the mass-loss from the donor into the circumbinary region is left unspecified in our study, but may be envisioned to be e.g. a stellar wind, wind Roche-lobe overflow (Mohamed & Podsiadlowski 2007), stellar pulsations of the donor, tidal interactions (e.g. Chen et al. 2011), a recently expelled common envelope, or any other process by which material can be deposited into the circumbinary region instead of being accreted by the WD. It is also possible that the material in the circumstellar region may originate from the WD if it emits a wind (Nomoto et al. 1979). Whether the above-mentioned mechanisms are actually capable of producing a spherical circumbinary configuration of matter is a question we do not enter into in this study.

The WD burns accreted material at its surface at the steady burning rate mentioned earlier. The resulting luminosity is that of a typical SSS, i.e. $L_{\rm bol} = 10^{38}$ erg/s, and the spectrum is a black-body with $kT_{bb} = 50$ eV. Our focus is on X-ray observations, and as the companion is not expected to emit appreciably in X-rays, in observational terms our model system reduces to a single nuclear-burning WD within a bubble of circumbinary material.

The gas bubble

We parametrize the mass-loss into the circumbinary region by a wind velocity, u_w, which we assume to be constant in the region outside the position of the WD. We choose a value of $u_w = 10$ km/s, which is typical of the winds of evolved intermediate-mass stars (e.g. Panagia et al. 2006).

As a first approximation, we assume the mass-loss into the circumbinary region is spherically symmetric (see section for a discussion of the caveats of this assumption). The outer extent of the spherical distribution of material depends on the wind velocity and age of the mass-losing phase of the donor star. For the chosen wind velocity, the extent of the obscuring gas bubble is 2.1 AU yr^{-1} $\sim 10^{-5}$ pc yr^{-1}.

Obscuration by neutral gas

In general, the optical depth τ along the line of sight between the source and the observer is the opacity κ times the obscuring column M

$$\mathrm{d}\tau = \kappa \rho dr \qquad \Rightarrow \qquad \tau = \kappa M, \tag{3}$$

where $M = \int \rho dr$, $\rho = \dot{M}/(4\pi r^2 u_w)$, and $\dot{M}$ is the mass-loss rate.

The total neutral column along the line of sight is the sum of the contribution from the local gas bubble, the interstellar medium (ISM) in the host galaxy, the intergalactic medium (IGM) between the Milky Way and the host galaxy, and the ISM in the Milky Way. Therefore, for a given species of neutral gas in our spherically symmetric model the attenuation is formally

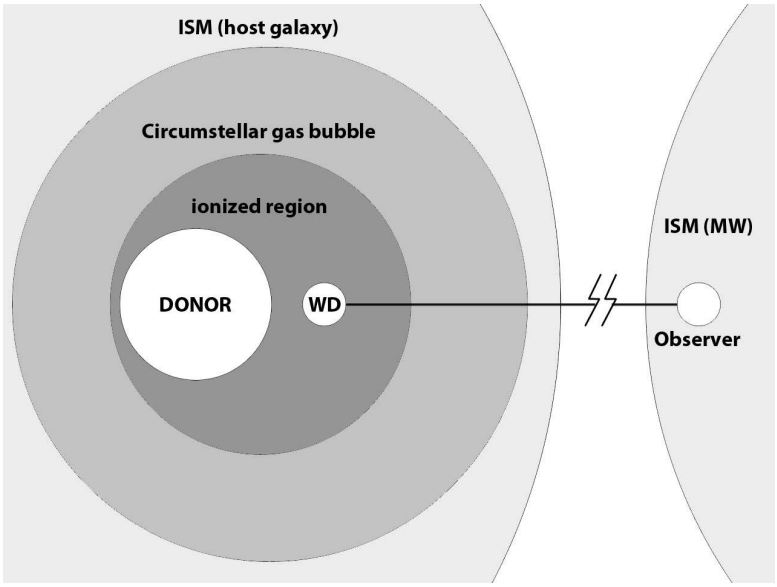

Figure 18: Schematic drawing of the model used in this study. The SSS system consists of a WD accreting material from a donor. The supersoft X-ray emission is the result of steady thermonuclear burning on the surface of the WD. The WD and donor are surrounded by a circumbinary configuration of gas and possibly dust. The radiation from the nuclear-burning WD may ionize a region around the system; in this sketch, the ionized region is localized narrowly around the binary, but for certain configurations the ionized region may extend to or beyond the edge of the circumbinary gas bubble. Before reaching an observer at Earth, photons from the SSS pass through the circumbinary material, the ISM in the host galaxy, the IGM, and the ISM in the Milky Way.

given by

$$\frac{I}{I_0} = \exp\Big(-\kappa_{\rm n}\Big(\quad \frac{\dot{M}}{4\pi u_w}\Big(\frac{1}{r_0} - \frac{1}{r_1}\Big) + \rho_{\rm ISM}(r_{\rm host} - r_1 + r_{\rm obs} - r_{\rm MW}) + \rho_{\rm IGM}(r_{\rm MW} - r_{\rm host})\Big)\Big), \tag{4}$$

where $\kappa_{\rm n}$ is the opacity of the neutral gas, r_0 is the inner radius of the neutral region of the gas species in question, r_1 is the outer radius of the spherical gas bubble, $r_{\rm host}$ is the distance from the source to the edge of the host galaxy, $r_{\rm MW}$ is the distance from the source to the edge of the Milky Way, $r_{\rm obs}$ is the total distance from the source to the observer, and $\rho_{\rm ISM}$ and $\rho_{\rm IGM}$ are the gas densities of the ISM and IGM, respectively. We put $r_0 = a$, where a is the separation between the binary component. For both the wind material, the IGM, and the ISM, we assume solar chemical abundances. X-ray absorption happens by way of K-shell ionizations, and the resulting photon-energy dependent cross-sections are obtained from Morrison & McCammon (1983), as shown in figure 19.

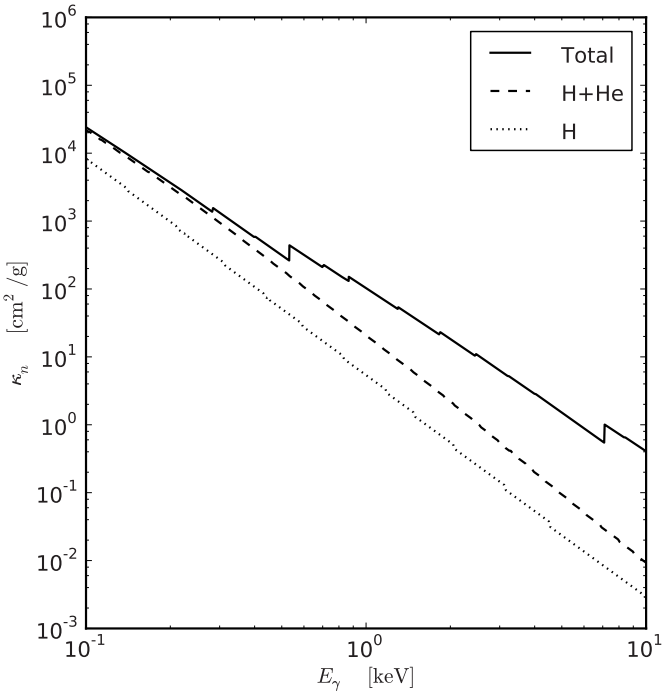

Figure 19: Opacities from K-shell ionizations for neutral gas and atomic metals as a function of photon energy. All values are for solar abundances. The dotted line gives the opacity of hydrogen alone, dashed is the opacity of hydrogen + helium, and solid is the total opacity of all chemical elements at solar abundances. Values are calculated from Morrison & McCammon (1983). As explained in section , the relevant photon energies for Chandra are from 300 eV. Furthermore, for a SSS we do not expect to see any photons above ~ 3 keV.

The formal expression in eq.(4) can be somewhat simplified. The contribution from the IGM is negligible, and we also assume that there is no significant contribution to the column from the host galaxy. This is routinely done for SSS studies (see e.g. Kahabka & van den Heuvel 2006), and many of the galaxies used in the studies of, for example, Gilfanov & Bogdán (2010) and Di Stefano (2010a) are gas poor. Therefore, the column that we consider in our model is just the sum of the column of material in the Milky Way and the circumbinary material.

Obscuration by ionized gas

Close to the source the radiation generated by nuclear-burning on the surface of the WD will photo-ionize the hydrogen in the gas. Since the peak energy of a canonical SSS is low ($kT_{bb} \sim 30 - 100$ eV), heavier elements are unlikely to be appreciably ionized, and certainly

not ionized to K-shell.

To determine the ionization structure of hydrogen around the source, we follow the approach first suggested by Strömgren (1939). The Strömgren sphere is the volume around an ionizing source in which the ionization rate equals the recombination rate. The rate of recombinations to atomic energy level n per unit volume is given by $N_{R,n} = n_e n_p \beta_n(T_e)$, where n_e and n_p are number densities of free electrons and protons, respectively, and β_n is the recombination efficiency of the n'th level, which depends on the electron temperature of the gas, T_e.

If we assume complete ionization within the ionized region, then $n_e = n_p$ for hydrogen. Additionally, we can omit β_1 from the expression, since every recombination directly to the ground level emits a photon capable of causing another ionization, which we assume it will do immediately. The total number of recombinations per unit time is then

$$\begin{aligned} N_{R,\mathrm{tot}} &= \int_{r_0}^{R_I} n_e^2(r)\beta_{2+}(T_e)4\pi r^2 dr \\ &= 4\pi\beta_{2+}(T_e)\int_{r_0}^{R_I} n_e^2(r) r^2 dr \\ &= \frac{\dot{M}^2\beta_{2+}(T_e)}{4\pi u_w^2 m_g^2}\int_{r_0}^{R_I} r^{-2} dr, \end{aligned} \tag{5}$$

where $\beta_{2+} \approx 2{\cdot}10^{-10} T_e^{-3/4}\mathrm{cm}^3/\mathrm{s}$ is the total recombination rate of transitions above the lowest ($\beta_{2+} = \sum_n \beta_n - \beta_1$), and we have assumed that

$$n_e(r) = n_H(r) = \frac{\dot{M}}{4\pi r^2 u_w}\frac{1}{m_g}, \tag{6}$$

where m_g is the mass of the hydrogen gas.

The number of ionizing photons emitted by the SSS per unit time is given by

$$S_* = 4\pi R^2 \int_{13.6\mathrm{eV}}^{\infty} \frac{B_\nu}{h\nu} d\nu = \frac{L}{\sigma T^4}\int_{13.6\mathrm{eV}}^{\infty} \frac{B_\nu}{h\nu} d\nu \tag{7}$$

where h is the Planck constant, σ is the Stefan-Boltzman constant, B_ν is the frequency-dependent Planck function, and ν is the frequency.

Setting S_* equal to $N_{R,\mathrm{tot}}$, we get

$$\begin{aligned} \frac{\dot{M}^2\beta_{2+}(T_e)}{4\pi u_w^2 m_g^2}\left(r_0^{-1} R_I^{-1}\right) &= S_* \\ \Rightarrow r_0^{-1} - \frac{4\pi u_w^2 m_g^2 S_*}{\dot{M}^2\beta_{2+}(T_e)} &= R_I^{-1} \end{aligned} \tag{8}$$

We assume that the temperature of the entire gas bubble is the effective temperature of the SSS. For $kT_{bb} = 50\mathrm{eV}$, the effective temperature is $5.8 \cdot 10^5\mathrm{K}$. This is certainly an overestimation, but as discussed in section the impact of this inaccuracy is negligible.

Eq.(8) clearly only has a physically meaningful solution when r_0^{-1} is larger than the second term on the right-hand side. This gives us a constraint for the mass-loss rate

$$\begin{aligned} \dot{M} &> \left(\frac{S_* 4\pi u_w^2 m_g^2 r_0}{\beta_2(T_e)}\right)^{1/2} \\ &\equiv \dot{M}_{\mathrm{Str}}. \end{aligned} \tag{9}$$

For our model system, $L_{\rm bol} = 10^{38}$ erg/s and $kT_{bb} = 50$ eV, the number of ionizing photons is $1.46 \cdot 10^{47}{\rm s}^{-1}$, and $\dot{M}_{\rm Str} = 2.00 \cdot 10^{-6}{\rm M}_{\odot}{\rm yr}^{-1} \cdot \left(\frac{r_0}{\rm AU}\right)^{1/2}$.

For mass-loss rates higher than $\dot{M}_{\rm Str}$, there is a clearly defined inner ionized region, outside of which only neutral matter exists.

For mass-loss rates lower than $\dot{M}_{\rm Str}$, the expression for the ionized sphere will not be physically meaningful. In this case, the assumption that all photons capable of ionizing the gas are absorbed and cause ionization is inaccurate. For such mass-loss rates, the gas bubble is not dense enough to absorb all photons capable of ionizing the gas, and there is no longer a clearly defined ionized region. Therefore, all hydrogen and helium in the gas bubble is fully ionized, and excess photons seep out into the interstellar medium, possibly causing further ionization there.

In the ionized region, the only contribution to the obscuration from hydrogen and helium will be through Thomson scattering. The cross-section of Thomson scattering is largely independent of photon energy, and therefore the free electrons produced in the ionizations will affect the absorption/scattering at all photon energies at approximately the same amount.

For X-ray binaries involving neutron stars or black holes, the energies and densities involved may sometimes lead to Comptonization of the plasma, which has an impact on the obscuration caused by the Comptonized material. However, for the lower energies and densities involved in our model, Compton scattering plays no role at all.

Obscuration by dust

Depending on the properties and the mass-loss mechanism of the donor star, a fraction of the metals in the gas may be condensed into dust grains, and we need to consider whether the presence of dust changes the total X-ray absorption of the circumbinary material.

As mentioned earlier, X-ray absorption happens by the interaction of photons with K-shell electrons, and in this way the absorption cross-section of an individual atom is largely independent of the location where the atom is found. However, putting atoms into grains represents a form of *clumping* that can decrease absorption if individual grains are already optically thick to X-rays of the considered energy. In this case, a part of the grain does not contribute to the X-ray opacity, because any X-ray photon will already be absorbed in the source-facing side of the grain. This can reduce the opacity by a so-called self-blanketing factor (Fireman 1974) of

$$f_b = \left(1 - e^{-\langle\tau_{\rm gr}\rangle}\right)/\tau_{\rm gr}, \tag{10}$$

Here $\langle\tau_{\rm gr}\rangle$ is the average optical depth of individual grains. However, the effectiveness of this clumping of X-ray opacity is very limited. Even in cold diffuse clouds in the interstellar medium, important elements are hardly depleted into dust grains. For example, nitrogen and neon are abundant elements that remain entirely in the gas phase. In the mass-loss flow of the donor star, this condensation will be even less complete. If the donor star has an oxygen-rich chemistry, the entire carbon content of the wind and an equal amount of oxygen will be trapped in the very stable CO molecule and not participate in the condensation process (Gail & Sedlmayr 1986). For solar-system-like element abundances (Anders & Ebihara 1982), this

means that all of the carbon, all of the nitrogen and neon, and 40% of the oxygen remain in the gas phase. As these are the most important absorbers for soft X-rays, it is clear that the soft X-ray absorption cross-section will be reduced by a factor much less than two. Wilms et al. (2000) conclude that even in the ISM where condensation is rather complete, for grain sizes smaller than 0.3μm, the resulting effect will not exceed 10%. In the donor mass-flow, the effect will be even smaller. Therefore, we can safely ignore this complication and assume that all metals are in the gas phase, fully contributing to the X-ray absorption.

Results

We first present the generic results of our model, i.e. results that do not depend on the instrument being used. We then apply our results to a specific case, that of *Chandra*'s ACIS-S detector.

Generic results: Ionization structure and obscuration

Figure 20 shows how the obscuration depends on orbital separation and mass-loss rate for 350 eV photons emitted from a SSS of $L = 10^{38}$erg/s and $kT_{bb} = 50$eV. Photons at 350 eV are safely above the photon energies at which typical X-ray observations are unreliable, but close enough to the peak of the black-body curve that an unobscured SSS produces appreciable amounts of photons.

Our study shows that for binary separations of around 1 AU a spherically symmetric mass-loss rate of $\sim 10^{-8}$M$_\odot$yr^{-1} is sufficient to fully obscure the supersoft X-ray emission from our model system.

It is evident from figure 20 that for orbital separations around 1 AU a clearly defined ionized region will form at considerably higher mass-loss rates ($\sim 10^{-6}$M$_\odot$yr^{-1}) than those needed for full obscuration. Hence, for 350 eV, at mass-loss rates between those needed for full obscuration and discrete ionization, the SSS will be fully obscured, but the binary will be surrounded by an extended ionized region that may be detectable at wavelengths other than X-rays (see section).

We note that the obscuration curves on fig.20 are for a photon energy of 350 eV. As the photon energy rises, the curves move further to the right in the plot, while the curve for the critical mass-loss rate remains in place (since the critical mass-loss rate does not depend on the photon energy). This means that for higher photon energies one can imagine configurations for which these curves overlap, i.e. there is a clearly defined ionized region around the binary, while the X-ray emission from the binary is not fully obscured. However, this does not happen for our SSS at photon energies below $\sim$ 5 keV, and the number of photons emitted by the system at these energies is miniscule.

Specific results: Chandra's ACIS-S detector

As an application, figure 21 illustrates what our model system will look like if it resides in M101 and is observed with the ACIS-S detector on the *Chandra* X-ray Observatory. The distance to M101 is taken to be 6.4 Mpc (Shappee & Stanek 2011). The contribution to the column from

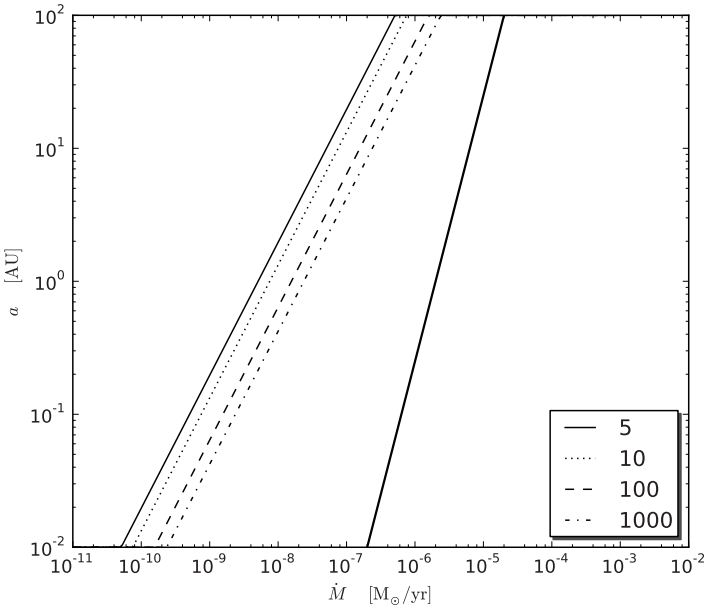

Figure 20: Contour lines showing the dependence of obscuration on mass-loss rate and binary separation, for photons emitted at 350 eV. The left-most solid line corresponds to an attenuation factor of 5, the dotted line to an attenuation of 10, dashed to an attenuation of 100, and dot-dashed to an attenuation of 1000. The right-most solid line is the critical mass-loss rate $\dot{M}_{\rm Str}$; to the left of this line, the wind is insufficiently dense to sustain a clearly defined ionized region around the source. To the right of it, a clearly defined ionized region exists around the source, while the material outside of this region is neutral.

the Milky Way is obtained from Dickey & Lockman (Dickey & Lockman 1990); for M101, we find a column of $1.15 \cdot 10^{20}$ N_H/cm^2. We chose *Chandra*'s ACIS detector as an example, since this is the instrument used by most groups (e.g. Voss & Nelemans 2008, Roelofs et al. 2008, Nelemans et al. 2008, Di Stefano 2010a, Gilfanov & Bogdán 2010, Nielsen et al. 2012).

The photon-energy dependent effective-area function of ACIS-S can be found on the *Chandra* homepage[7]. To find the number of photons detected, we fold the calculated flux of the source with the effective-area before integrating over all photon energies.

Since the launch of *Chandra* in 1999, the sensitivity of the onboard detectors have degraded. We adopt the effective-area function for the earliest possible *Chandra* observations (cycle 3). If a source could be obscured sufficiently to be unobservable to the ACIS detectors when these were new and at their most sensitive, then such a source would also be unobservable to the older, less sensitive ACIS detectors. We note that the detectors on *Chandra* are insensitive to photons below roughly 100 eV. Additionally, *Chandra* detections at photon energies between 100 and 300 eV are known to be unreliable, and analyses should therefore filter out photons

[7] http://cxc.cfa.harvard.edu/cgi-bin/build_viewer.cgi?ea

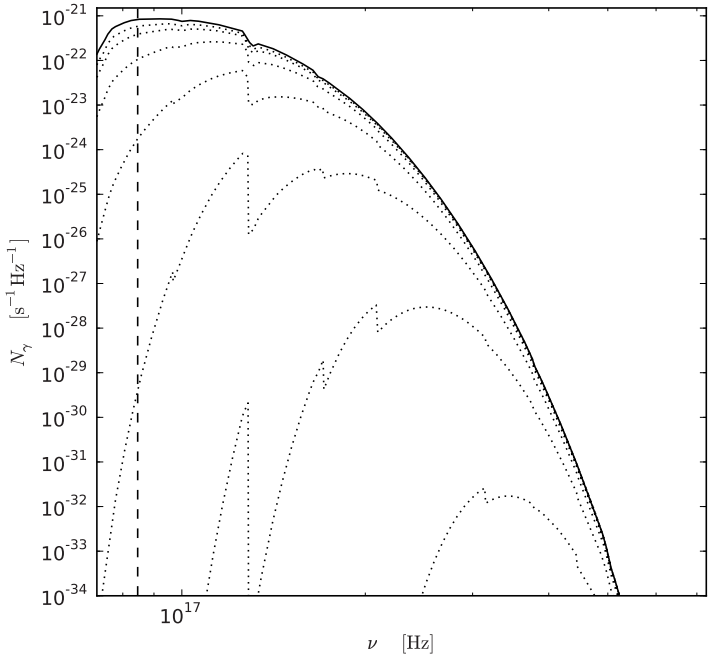

Figure 21: Unabsorbed and absorbed black-body curves of a SSS in M101. The solid curve corresponds to a black-body nuclear-burning WD with $L = 10^{38}$ erg/s, $kT_{bb} = 50$ eV and no obscuring circumstellar matter (i.e. only Galactic N_H), folded with the effective- area function of *Chandra*'s ACIS-S detector. The dotted curves are the absorbed black-body curves of the same source for seven logarithmically equidistant values of $\dot{M}$ from 10^{-9}M$_\odot$yr^{-1} to 10^{-6} M$_\odot$yr^{-1} (see table 4), with the mass-loss rate increasing from left to right. The orbital separation and inner radius of the gas bubble is 1.5 AU. The numbers on each curve give the number of photons expected to be received in ACIS-S for an integration time of 40 ks. For comparison with figure 20, the vertical dashed line is at a photon energy of 350 eV.

at energies below this threshold. This means that observations of SSS spectra are in fact only observations of the high energy tails of their spectra, since the spectral peaks are located far below the detection threshold of *Chandra*.

The number of photons we expect to receive in the relevant energy range (300 eV - 3 keV) for observations with ACIS-S is given in table 4. The mass-loss rates listed in the table correspond to the dotted lines in fig.21. For comparison, the number of photons expected in ACIS-S from the same source integrated over the same energy range in a completely empty environment (i.e. in the absence of galactic or circumbinary material) is $N_0 = 4.4 \cdot 10^{-5}$s^{-1}. Note that the attenuation is for the integrated number of photons, hence not immediately comparable to the values given in fig.20, which are for a single photon energy (350 eV).

Table 4: Attenuation ($N_{\gamma,\mathrm{obs}}/N_0$) of the integrated number of photons from our model system located in M101, as expected for different mass-loss rates and observed with *Chandra*'s ACIS-S detector.

circumbinary $\dot{M}$ [$M_\odot$/yr]	N_{obs}/N_0
0	$9.0 \cdot 10^{-1}$
10^{-9}	$8.0 \cdot 10^{-1}$
$3.1 \cdot 10^{-9}$	$6.2 \cdot 10^{-1}$
10^{-8}	$3.0 \cdot 10^{-1}$
$3.1 \cdot 10^{-8}$	$4.6 \cdot 10^{-2}$
10^{-7}	$6.7 \cdot 10^{-4}$
$3.1 \cdot 10^{-7}$	$6.1 \cdot 10^{-7}$
10^{-6}	$4.1 \cdot 10^{-11}$

Observational implications

In the preceding sections, we have presented the setup of the model and our results. To put our results into an observational context, we now review the current evidence for circumstellar matter around SNe Ia, which would be a signature of the SD progenitor scenario. We also discuss the possible observational implications of our results for SN Ia progenitors.

Evidence of CSM around SN Ia progenitors

Several studies have found evidence of circumstellar matter in SNe Ia explosions.

High-velocity features in early-time optical observations of SN2003du were interpreted by Gerardy et al. (2004) as evidence for the interaction of the outer-most layers of the SN ejecta with a dense circumstellar shell of solar-metallicity material created by mass-loss from the progenitor system prior to the explosion.

In a study of the SN Ia remnants DEM L238 and DEM L249, Borkowski et al. (2006) found bright central X-ray emissions surrounded by fainter shells and interpreted this as remnants of circumstellar media around the progenitors that had been shocked to emission by the SN ejecta.

Chiotellis et al. (2012) compared 2D model simulations with observations of the historical SN Ia SN1604, also known as Kepler's SN. The SN remnant has a peculiar nitrogen-rich shell-like structure in optical images. Simulations by Chiotellis and collaborators assumed a mass-loss of $10^{-7} - 10^{-6} M_\odot \mathrm{yr}^{-1}$ and wind speeds of 5-20 km/s, typical of thermally pulsating asymptotic giant stars. The observed shell-like features are reproduced by their simulations, and interpreted as a shocked interaction layer between the progenitor's wind-blown circumstellar bubble and the SN ejecta. If correct, their results are consistent with a SD progenitor emitting a stellar wind prior to explosion.

A study by Patat et al. (2007) found blue-shifted absorption features of the Na I doublet (5896 Å and 5890 Å) in optical spectra of SN2006X, which was interpreted as evidence of gas outflows from the progenitor system. Their results were generalized by Sternberg et al. (2011),

who found similar features in an unbiased sample of 35 SNe Ia, indicating that these features, while not demonstrably present for other types of SNe, may be characteristic of SNe Ia.

Upper limits

In contrast, a number of studies have looked for, and failed to find, evidence of circumstellar matter in SN Ia explosions. These non-detections have led to upper limits being placed on the possible mass-loss from SN Ia progenitor systems in several wave-bands.

Using optical spectra of SN2001el, Mattila et al. (2005) found upper limits of $\dot{M} \lesssim 9 \cdot 10^{-6}$ and $5 \cdot 10^{-5} \mathrm{M}_{\odot}\mathrm{yr}^{-1}$ for the progenitor system of the SN, for wind speeds of 10 km/s and 50 km/s, respectively.

Studies aimed at finding radio emission from the interaction between SN ejecta and circumstellar matter have been undertaken by several groups. No direct detection has been made at this point, but upper limits are reaching interesting values. Using the VLA, Panagia et al. (2006) found upper limits of $\sim 10^{-6} \mathrm{M}_{\odot}\mathrm{yr}^{-1}$ based on observations of 27 SNe Ia. Their analysis is extrapolated from the assumption that the process behind radio emission from SNe Ia are similar to those of SNe Ib/c.

Using more recent radio observations, Chomiuk et al. (2011) analyzed EVLA observations of early SN Ia spectra. From their non-detections, they found typical upper limits $\dot{M}/u_w \lesssim 10^{-7} \mathrm{M}_{\odot}\mathrm{yr}^{-1}/(100\mathrm{km/s})$ for most sources (private communication). Chomiuk et al. (2012) reported upper limits of $\dot{M}/u_w = (6 \cdot 10^{-10} - 3 \cdot 10^{-9}) \mathrm{M}_{\odot}/\mathrm{yr}/(100\mathrm{km/s})$ for non-detections of radio emission from SN2011fe, the closest SN Ia in 25 years. For the lower wind speed used in our model, the upper limits are correspondingly lower, hence the upper limit of the wind mass-loss rate of the donor becomes $10^{-8} \mathrm{M}_{\odot}\mathrm{yr}^{-1}$ for typical SD SN Ia progenitors, and $(6 \cdot 10^{-11} - 3 \cdot 10^{-10}) \mathrm{M}_{\odot}/\mathrm{yr}$ for SN2011fe.

Observational predictions

We note that except for SN2011fe the upper limits found in the studies mentioned above are all higher than what we require for the full obscuration of systems with binary separations of $\lesssim 10$AU. The upper limits found by Chomiuk and collaborators come closest to constraining our results, and if their general limits are correct then our model cannot explain the obscuration of systems with binary separations larger than 1 AU. If their limits for SN2011fe are correct, then the non-detection of X-ray emission from that particular SN cannot be explained by obscuration from circumbinary material in our model for a giant donor, since that would require binary separations of $\lesssim 10^{-2}$AU, effectively placing the WD within the envelope of the giant. A MS donor cannot be ruled out by these radio upper limits, nor can a WD wind. Hopefully, future observations will provide either a detection of the shocked region or stronger general constraints with which to compare our model.

Another important point is that even relatively small circumbinary gas bubbles are able to fully obscure the system: As can be seen from the r_0-dependence in eq.(4), the obscuration is caused mainly by material in a very narrow region around the SSS. The outer extent of the circumstellar gas bubble is essentially irrelevant, except for very small bubbles where r_0 is comparable in size to r_1. This means that even quite compact systems, say up to a gas

bubble radius of ~ 10 AU, would be capable of obscuring a SSS, provided that the mass-loss rate is high enough. It follows that the mass-loss does not have to have been 'on' for very long to obscure the system in X-rays. We emphasize that this does not solve the problems raised in Di Stefano (2010a) and Gilfanov & Bogdán (2010), as the source still needs to be 'on' for a significant period ($\sim 10^6$ years) to be able to grow significantly in mass. However, it may explain why many SSS appear to be highly variable.

In general, observations to detect or constrain the mass-loss rate of the progenitor systems of SNe Ia need to be performed a very short time after the SN explosion. The bulk of the SN ejecta moves at $\sim 10,000$ km/s, corresponding to roughly 6 AU per day. Therefore, the interaction shock from a nuclear-burning WD shrouded in an fully obscuring gas bubble with a radius in the range of a couple of tens of AU is unlikely to be detected by anything but the very earliest (1-2 days after explosion) observations. Since radio appears able to provide the most robust upper limits, the ideal observing scheme would be to obtain EVLA observations of SNe Ia within a day or less of the explosion.

If the companion in our model system is evolved, we can disregard orbital separations smaller than $\sim 0.5-1$AU, since these will be inside the outer layers of the companion. At such small separations, the WD is more likely to spiral into the companion or cause the envelope to be expelled, rather than go through a stable period as a SSS. However, several studies argue against the possibility of giant companions. For example, using pre-explosion archival *Hubble Space Telescope* (HST) images Li et al. (2011a) ruled out a luminous giant or supergiant as the companion to SN2011fe, although a sub-giant companion could not be excluded by the data.

If the companion is a main-sequence (MS) star, the system can exist stably at much smaller orbital separations, and the mass-loss rates required for obscuration are correspondingly lower, as is clearly evident from figure 20. However, the mass-loss rate from such systems may also be much lower than for systems containing evolved stars.

There is also the possibility that the mass-loss from the system is caused by a wind from the WD itself. This could happen if the mass-loss from the donor to the accretor is slightly higher than the maximal steady-burning accretion rate. The accreted mass could be supplied by either a MS or evolved donor. If the accretion rate is higher than the steady-burning rate, the WD will 'puff up' from the accretion and emit a wind of its own, while possibly still burning some of the material on its surface (see Nomoto et al. 1979). The 'orbital separation' in figure 20 should then instead be perceived as the difference in radius between the nuclear-burning layer and the wind-emitting layer of the WD. For such small separations, full obscuration can be achieved even with fairly low ($10^{-11}-10^{-10}\mathrm{M}_\odot\mathrm{yr}^{-1}$) mass-loss rates. If we envision a WD accreting at slightly above the maximal steady-burning rate and emitting a weak, spherical wind of this magnitude, such a source would be completely obscured in our model. More generally, if the accretion process feeding a steady burning WD is not 100% efficient, or if the X-ray emitting surface of the WD loses a very small fraction of the accreted material to the circumstellar region while it burns, the result could be significant or complete obscuration. These WD wind scenarios could therefore potentially explain the absence of a large fraction of the SSSs that become type Ia SNe in the SD scenario.

A possible observational characteristic of our model could be H-α emission caused by recombination in the ionized gas bubble. This emission may be visible in archival optical images of nearby SNe Ia, and it would be logical to suggest a systematic archival search for this kind of emission in pre-explosion images at the position of nearby SN Ia progenitors. However, such a search of the HST archive was performed by Voss et al. (2012, in prep.), who found no evidence of optical counterparts for nearby SNe Ia progenitors, so it is unclear whether such a search is actually feasible. Another option is to search for H-α emission in regions where such emission is not to be expected, i.e. outside of young, star-forming regions. It may be possible to perform an analysis similar to the SSS 'counting' done by Di Stefano (2010a), but in H-α instead of X-rays. We note, however, that even though dust is unimportant for the obscuration of X-rays from our model system it could possibly obscure the H-α emission, since dust is a more efficient absorber at optical wavelengths. Depending on the tenuousness of the outer parts of the gas bubble, there may also be forbidden lines, but this depends heavily on the gas density.

Symbiotics

WDs in symbiotic binary systems are expected to be massive and to accrete mass at rates comparable to the steady-burning interval. However, only three symbiotic SSSs are currently known (SMC3, Lin 358 and AG Dra). Somewhat analogous to the evidence for circumbinary matter around SN Ia progenitors, observations of outbursts from recurrent novae in symbiotic systems also appear to detect the presence of significant amounts of circumbinary material, providing absorbing columns large enough to fully obscure the systems in quiescence (e.g. Shore et al. 1996). The physical parameters of typical symbiotic systems are $L_{bol} = 10^3 - 10^4 \mathrm{L}_\odot = 4 \cdot 10^{35} - 4 \cdot 10^{36}$ erg/s and $a = 2 - 5$ AU, while the red giant wind emitted by the donor in such systems is roughly $10^{-7} \mathrm{M}_\odot$/yr (see e.g. Mikołajewska 2012). If we assume that this type of source has a black-body spectrum comparable to a canonical SSS, then Figure 20 shows that even if the luminosities of these systems were as high as those expected for the nuclear-burning SD SN Ia progenitors, the systems would be completely obscured. That they are observed to be one to two orders of magnitude less luminous only serves to make them even easier to obscure.

Discussion

As mentioned earlier, we use a number of simplifying assumptions in our calculations. Here we discuss the caveats introduced by these assumptions.

Density profile

The assumption of a constant wind speed from the surface of the companion star is probably incorrect. In reality, the wind is accelerated by a variety of processes until it reaches its terminal velocity, and this is not expected to happen until well beyond the orbit of the binary. Therefore, our wind speed is probably too high. If the wind is accelerated through the system and does not reach the constant value used in our simulations until some time later, i.e. further

away from the source, the density close to the source will be higher. Thus, the assumption also underestimates the amount of obscuration.

In addition, we have assumed a spherically symmetric distribution of matter around the binary. This is in general not observed in symbiotic systems, where disk-like structures in the orbital plane are expected, possibly accompanied by bipolar outflows (e.g. Solf & Ulrich 1985; Corradi & Schwarz 1993; Munari & Patat 1993). It is difficult to say, overall, whether the assumption of sphericity is likely to over- or underestimate the amount of obscuration. In the case of a non-spherical structure, the obscuration in specific cases depends sensitively on the inclination of the observer to the sight-line. This uncertainty could be dealt with if we had a firm understanding of the symmetries of the matter in the relevant binary systems. Given the absence of that understanding, combined with the earlier mentioned finding that only the material very close to the system has a significant effect on the obscuration, we believe that our spherically symmetric model is a reasonable first approximation. Hopefully, further studies will provide a clearer understanding of the density structures of the systems in question.

Temperature

In our calculations, we have a assumed constant temperature throughout the entire gas bubble, i.e. the temperature of the surface of the WD. In reality, the temperature of the gas bubble falls off with the distance from the emitting SSS. However, even at a temperature corresponding to the T_{bb} of the SSS, the elements of importance to absorption and scattering in the observationally relevant interval, i.e. elements heavier than helium but lighter than iron, will not be fully ionized. Our simplified temperature assumption only plays a role for hydrogen and helium, which are unimportant absorbers at the photon energies where *Chandra* is sensitive. We therefore estimate that this effect is negligible for our purposes.

Dust and stellar winds

As explained in section , dust appears to be fairly unimportant to the possible obscuration of a SSS.

However, if the X-ray source manages to ionize a large region in the circumbinary gas, in this region dust formation will be impossible. If radiation pressure on dust is an important factor for driving the wind in the first place, introducing the X-ray source may have significant effects on the mass-loss rate from the companion. If dust has already formed, it may be destroyed again, for example by thermal evaporation due to the X-ray heating of the grains (e.g. Fruchter et al. 2001), by charge explosions produced by massive photo-electric ionizations (ibid), or by thermal sputtering in hot gas (e.g. Tielens et al. 1994). In this study, we have not considered these effects in detail. We have instead used a fixed mass-loss rate as a model parameter and disregarded the consequences for X-ray absorption if part of the heavier atoms are present in the form of dust grains.

Metallicity

By using the model of Morrison & McCammon (1983), we have assumed solar metallicity for the obscuring material (both the wind material and ISM). As mentioned, the most important

obscuring elements for the photon energies accessible with *Chandra* are elements heavier than helium but lighter than iron. For metallicities different from the one used in this study, the obscuration will scale accordingly.

Spectrum

Following the original work of van den Heuvel et al. (1992) we assumed the SSS to be a simple black-body. This is probably not an entirely accurate description of a nuclear-burning WD (e.g. Ness et al. 2003, Rauch 2003, Rauch & Werner 2010), and by assuming a black-body spectrum we may well overestimate the temperature of the actual surface of the WD. However, deviations of the actual spectra from that of a black-body is negligible in this context, since we have analyzed obscurations of several orders of magnitude. In addition to this, the temperature dependence in our calculations is quite weak (e.g. the number of ionizing photons in the calculation of the extent of the ionized region depends on temperature as $\sim T^{-3/4}$). Observations of SSSs have often assumed black-body spectra (e.g. Greiner 2000), so comparisons of such observations with our model will in a sense be consistent. We note that the question of WD atmospheres is not particularly well understood at this point, so a very detailed analysis with additional assumptions would not necessarily improve the applicability of our results.

Conclusions

To date, it has mostly been assumed that nuclear-burning WDs in SD progenitor systems would be more or less 'naked'. Consequently, the absence of a large enough number of these sources has been seen as a problem for the SD model, as there seem to be too few of these sources to account for the observed SN Ia rate.

We have examined a model system of a canonical SSS embedded in a spherical, circumbinary gas bubble. The mechanism behind the formation of the gas bubble has been left unspecified, but could be the result of e.g. a stellar wind from an evolved companion, wind-RLOF, pulsations of the donor, or tidal effects between the binary components.

We have shown that for a certain critical mass-loss rate (e.g. $\dot{M} \sim 10^{-6}\mathrm{M}_{\odot}\mathrm{yr}^{-1}$ for $a \sim 1\mathrm{AU}$) a clearly defined, narrowly situated ionized region will form around the SSS. For systems with mass-loss rates below this critical value, the SSS will be surrounded by extended ionized regions that may extend into the ISM.

Our results suggest that for systems with $a \sim 1\mathrm{AU}$ quite modest circumbinary mass-loss rates ($\sim 10^{-9} - 10^{-8}\mathrm{M}_{\odot}\mathrm{yr}^{-1}$) are sufficient to significantly obscure the nuclear-burning WD SSS. This mass-loss is in addition to the mass the donor loses to the accreting WD. For wider systems, higher mass-loss rates are needed. Even at orbital separations on the order of 100 AU, the mass-loss rates required for significant obscuration ($\sim 10^{-7}\mathrm{M}_{\odot}\mathrm{yr}^{-1}$) are not unrealistic for some late red giants or asymptotic giant branch stars. However, such wide systems are unlikely to be able to supply the mass-loss rate required for steady burning.

The mass-loss rate required for the ionized region to become clearly defined is several orders of magnitude higher than the mass-loss rates needed for total obscuration at the relevant photon energies ($\lesssim 1\mathrm{keV}$). This means that SSS systems with sufficient mass-loss rates to fully obscure

the X-ray emission will have extended regions of ionized material surrounding them. According to our model, for binary separations $\sim$ 1AU, mass-loss rates between 10^{-8} and 10^{-6}M$_{\odot}$yr^{-1} produce these systems. While not observable as SSSs, these systems may instead be observable in IR, radio, or H-α as recombination nebulae. To the extent that they are available, multi-wavelength archival searches of pre-explosion images at the positions of nearby SNe Ia may find these types of emission, even if no sources have been found in archival Chandra images. We also propose that H-α emissions outside of young regions may be evidence of obscured SSSs.

If a steady burning WD emits a small amount of the accreted material, on the order of $\sim 10^{-11} - 10^{-10}$M$_{\odot}$yr^{-1}, our calculations show that it may be completely undetectable in X-rays. We have no way of determining whether steady burning WDs accrete at 100% efficiency, but if it does not then even such a small amount of material will have important consequences for the X-ray signature of such objects.

The full obscuration constraints for binary separation and mass-loss rate presented above are probably too strict. Our model examined an observational best-case scenario, and when simplifying assumptions have been made they have consistently been made to favor a minimal amount of obscuration. For these reasons, even lower mass-loss rates may be sufficient to fully obscure more realistic systems.

Our results may have implications for the SD scenario for type Ia SNe. That it is comparatively easy to hide the X-ray emission from nuclear-burning WDs may help to explain some of the 'missing' systems mentioned in the Introduction. If a significant fraction of the progenitor systems could be shown to be severely or completely obscured by circumbinary material originating in the binaries themselves, then it would explain the discrepancy between the SN Ia rate and the small number of observed SSS systems and integrated X-ray luminosity of ellipticals.

Our study may also explain why so few symbiotic systems are visible as SSSs, since typical symbiotic systems are embedded in a dense wind and are less luminous than the expected SD SSS systems.

In future work, we plan to include our model in population synthesis simulations to determine whether systems with the parameters required for obscuration are produced in large enough numbers to account for a significant fraction of the 'missing' SSSs.

Acknowledgements
This research is supported by NWO Vidi grant 016.093.305. The authors would like to thank the anonymous referee for constructive criticism and suggestions that have significantly improved the quality of this manuscript. Additionally, MN is grateful to Jan Kuijpers, Rosanne Di Stefano, Joanna Mikolajewska, and Laura Chomiuk for helpful comments and suggestions.

Upper limits on bolometric luminosities of three type Ia supernova progenitors - New results in the ongoing *Chandra* archival search for type Ia supernova progenitors

M.T.B. Nielsen, R. Voss, G. Nelemans

Monthly Notices of the Royal Astronomical Society 435, 187 (2013)

Abstract

We present analysis of *Chandra* archival, pre-explosion data of the positions of three nearby (< 25 Mpc) type Ia supernovae, SN2011iv, SN2012cu & SN2012fr. No sources corresponding to the progenitors were found in any of the observations. Combining all sources with well defined backgrounds does not reveal any evidence for X-ray emission from the progenitors either. We calculated upper limits on the bolometric luminosities of the progenitors, under the assumption that they were black bodies with effective temperatures between 30 and 150 eV, corresponding to 'canonical' supersoft X-ray sources. The upper limits of SN2012fr straddles the Eddington luminosity of canonical supersoft sources, but fainter canonical supersoft sources cannot be ruled out by this study. We also compare our upper limits with known compact binary supersoft X-ray sources. This study is a continuation of the campaign to directly detect or constrain the X-ray characteristics of pre-explosion observations of nearby type Ia supernova progenitors; with the results reported

in Nielsen et al. (2012), the number of nearby type Ia supernovae for which pre-explosion images are available in the *Chandra* archive is now 13 and counting.

Introduction

Type Ia supernovae (SNe) are of crucial imporance for both cosmology and galactic chemical evolution. However, the nature of the progenitor systems giving rise to type Ia SNe remains unresolved. Two scenarios are normally considered: the single-degenerate (SD), in which a carbon-oxygen white dwarf (WD) grows in mass by accreting hydrogen-rich material from a companion (Whelan & Iben 1973), and the double-degenerate (DD) scenario, where a double WD binary system slowly spirals in and finally merges (Webbink 1984; Iben & Tutukov 1984). Beyond these two major scenarios, there are also a number of alternative scenarios, such as the 'core degenerate' scenario (Kashi & Soker 2011). In all scenarios, the end result is a carbon-oxygen WD with a mass at or above a critical mass ($\sim 1.38 M_{\odot}$), where the density and temperature of the WD interior is high enough to facilitate a runaway of unstable thermonuclear burning, which completely unbinds the WD in a supernova explosion. The process produces radioactive iron-group elements, and the subsequent decay of these powers a characteristic light-curve that can be used as standardizable cosmological candles (Phillips 1993), e.g. to measure the accelerating expansion of the Universe (Riess et al. 1998; Perlmutter et al. 1999).

In the SD scenario, the accreting WD is expected to be a supersoft X-ray source (SSS), with a black body temperature between 30 and 150 eV, and luminosity of $\sim 10^{37} - 10^{38}$erg/s (van den Heuvel et al. 1992; Kahabka & van den Heuvel 1997). For sources closer than $\sim$ 25 Mpc, such sources should be detectable with the *Chandra* X-ray observatory. With the aim of directly detecting a progenitor of a type Ia SN immediately prior to the explosion, a search of archival pre-explosion *Chandra* images was undertaken by Voss & Nelemans (2008), resulting in the possible, but ambiguous (Roelofs et al. 2008) detection of the X-ray emission of the progenitor of SN2007on. Since then, a systematic search has been conducted, resulting in upper limits of the bolometric luminosities of ten additional nearby type Ia SNe, SN2002cv, SN2003cg, SN2004W, SN2006X, SN2006dd, SN2006mr, SN2007gi, SN2007sr, SN2008fp, and SN2011fe, presented in Nielsen et al. (2012).

In this article, we expand on the results of Nielsen et al. (2012) by presenting upper limits on the bolometric luminosities of three additional supernovae: SN2011iv (detected by Drescher (CBET 2940), classified by Chen & Wang and Stritzinger (CBET 2940)), SN2012cu (detected by Itagaki (CBET 3146), classified by Marion & Milisavljevic (CBET 3146)), and SN2012fr (detected by Klotz and the *TAROT* collaboration (CBET 3275) and classified by Childress et al. (CBET 3275)). Based on the *Chandra* observations, we calculate upper limits on the bolometric luminosities of the progenitors, assuming black-body spectra for four effective temperatures in the super-soft range ($kT_{\rm BB}$ = 30, 50, 100, and 150 eV). The method used is identical to the one used in Nielsen et al. (2012), so the results are immediately comparable, and together the 13 upper limits, plus the ambiguous case of SN2007on (see Voss & Nelemans 2008; Roelofs et al. 2008), constitute the complete set of currently known nearby ($<$ 25 Mpc) type

Ia SNe with pre-explosion observations in the *Chandra* archive. We compare the calculated upper limits with the luminosities of known SSS in nearby galaxies.

We note that the current ambiguity concerning the possible direct detection of the progenitor of SN2007on is unlikely to be resolved until new *Chandra* observations of the position of the SN are available. Because of this, we do not include SN2007on in our sample of nearby type Ia SNe with pre-explosion *Chandra* observations.

In Section the *Chandra* observations used in this study will be described. Section explains the methods employed in the data analysis of the observations, and gives the results. Section discusses our results, and Section concludes.

Observations

We searched the *Chandra* Data Archive and found pre-explosion observations with the Advanced CCD Imaging Spectrometer (ACIS-S) at the positions of three nearby (>25 Mpc) type Ia SNe: SN2011iv, SN2012cu, and SN2012fr. No obvious sources corresponding to X-ray emitting progenitors were found on any of the pre-explosion images.

For SN2012cu, only a single pre-explosion observation exists, while several epochs of pre-explosion observations are available for SN2012cu and SN2012fr. For SN2012fr two additional, pre-explosion observations (obs IDs 13920 & 13921), both of them relatively deep (90 and 110 kiloseconds, respectively), will become available in april 2013. Our analyses do not take these two, currently proprietary observation epochs into account.

The observations used in this study are listed in Table 5.

Data Reduction & Results

The observations mentioned above were analyzed with the CIAO 4.3 software suite, and followed the same procedure as the one described in Nielsen et al. (2012). For ease of reference, all tables have been kept in the same format as that used in Nielsen et al. (2012).

All images were checked for photons of any energy at the positions of the SNe. No indications of the presence of sources were found. The images were then filtered to only include photons between 300 and 1000 eV, since below approximately 300 eV, the *Chandra* ACIS detector is unreliable, and above 1 keV, we expect no photons from the sources.

As our data model, we assumed an absorbed black-body and used the spectral models `xsphabs` and `xsbbody` (corresponding to `phabs` and `bbody` in XSPEC). Spectral weights files were generated for four different black-body temperatures, $kT_{\rm BB} = 30$, 50, 100 & 150 eV, taking into account the absorbing columns mentioned below. We then generated exposure maps from the spectral weights files. Multiple, pre-explosion epochs of observations exits for SN2011iv and SN2012fr, and for these SNe we combined the binned images to get deeper observations.

The distances to the SNe were taken to be identical to those of their host galaxies, as found in the NED online database[8]

[8] http://ned.ipac.caltech.edu/

Table 5: *Chandra* observations used in this study. All observations are with the ACIS-S detector.

Chandra observation	exposure time [ks]	pointing (RA, DEC)	SN	SN explosion date	observation date
2942	29.24	(03:38:52.00, -35:35:34.00)	2011iv	2011-12-02	2003-02-13
4174	45.67	(03:38:49.58, -35:34:36.34)	2011iv	2011-12-02	2003-05-28
9798	18.3	(03:38:51.00, -35:34:31.00)	2011iv	2011-12-02	2007-12-24
9799	21.29	(03:38:51.00, -35:34:31.00)	2011iv	2011-12-02	2007-12-27
3999	4.71	(12:53:29.20 +02:10:06.20)	2012cu	2012-06-14	2003-02-14
3554	14.61	(03:33:36.40 -36:08:25.00)	2012fr	2012-10-27	2002-12-24
6868	14.61	(03:33:36.40 -36:08:25.00)	2012fr	2012-10-27	2006-04-17
6869	15.54	(03:33:36.40 -36:08:25.00)	2012fr	2012-10-27	2006-04-20
6870	14.55	(03:33:36.40 -36:08:25.00)	2012fr	2012-10-27	2006-04-23
6871	13.36	(03:33:36.40 -36:08:25.00)	2012fr	2012-10-27	2006-04-10
6872	14.62	(03:33:36.40 -36:08:25.00)	2012fr	2012-10-27	2006-04-12
6873	14.64	(03:33:36.40 -36:08:25.00)	2012fr	2012-10-27	2006-04-14
13920	88.53	(03:33:36.40 -36:08:25.00)	2012fr	2012-10-27	2012-04-09
13921	108.2	(03:33:36.40 -36:08:25.00)	2012fr	2012-10-27	2012-04-12

Table 6: Host galaxies, distances and total hydrogen columns for each of the SNe analyzed in this study.

supernova	host galaxy	distance [Mpc] (from NED)	absorbing column [N_H cm^{-2}]	reference for column values
2011iv	NGC 1404	25.0	$1.51{\cdot}10^{20}$	Dickey & Lockman (1990)
2012cu	NGC 4772	13.3	$1.72{\cdot}10^{20}$	Dickey & Lockman (1990)
2012fr	NGC 1365	20.7	$1.24{\cdot}10^{20}$	Schlafly & Finkbeiner (2011)

For SN2012fr, Schlafly & Finkbeiner (2011) give the V-band absorption (in magnitudes) in the direction of the SN as $A_V = 0.056$ (see also ATEL#4535), and from this the neutral hydrogen column can be calculated, using the relation $N_H = 2.21 \cdot 10^{21} A_V$, where N_H is the neutral hydrogen column in cm^{-2} (Güver & Özel 2009). For SN2011iv, Foley et al. (2012) found negligible extinction in the host galaxy, and for SN2012cu, no values for the hydrogen column, reddening or extinction could be found in the literature. Therefore, for SN2011iv and SN2012cu we used the value for the Galactic column found in Dickey & Lockman (1990), which is referenced with CIAO's COLDEN tool. The host galaxies, distances, and columns for the SNe analysed in this study are summarised in Table 6.

For each observation, we used a circular aperture of 4.5 pixel radius, which covers more than 90% of the point-spread function of a theoretical point source. This aperture contains the background plus a Poissonian realization of the expected number of photons from a source.

For this photon count, $N_{\rm obs}$, we found the maximum average number of counts μ, for which the probability P of observing $N_{\rm obs}$ photons is within 3σ, under the assumption of Poissonian statistics, see e.g. Gehrels (1986): $P\left(\mu, N \leq N_{\rm obs}\right) \leq 0.0013$. This μ represents the 3σ upper limit of any progenitor including background. We found the upper limit to the luminosity of the source according to the formula,

$$L_{X,UL} = 4\pi \frac{(\mu - b)\,\langle E_\gamma \rangle d^2}{\zeta} \tag{11}$$

where b is the expected background for a circular aperture of radius 4.5 pixels, $\langle E_\gamma \rangle$ is the average energy of the photons found from the absorbed XSPEC model for the assumed spectrum, d is the distance to the SN and ζ is the value of the exposure map for the given spectrum at the position of the SN on the detector.

We then corrected the calculated luminosities for interstellar absorption, using the columns listed in Table 6, to obtain the unabsorbed luminosities of the sources. As a last step, we scaled the calculated supersoft X-ray luminosities to obtain bolometric luminosities.

Table 7 lists the results of our analysis. The individual *Chandra* images are shown on Figures 26-28. For SN2011iv and SN2012fr, these images are the combined images for all the available observation epochs, while Figure 27 shows the single pre-explosion *Chandra* observation in existence of the position of SN2012cu.

Table 7: Nearby (< 25 Mpc) SNe Ia with pre-explosion images, upper limit bolometric luminosities.

Supernova	SN position [RA, DEC]	pre-explosion *Chandra* observations	exposure time [ks]	total counts in source region[10]	3-σ counts in source region region	value of exposure map at position [s·cm^2]	unabsorbed 3-σ upper limit bolometric luminosity[9] [erg/s]
2011iv	(03:38:51.35, -35:35:32.0)	2942, 4174, 9798, 9799	114.5	243	289.8	$3.65{\cdot}10^6$	$1.22{\cdot}10^{41}$
						$5.51{\cdot}10^6$	$5.55{\cdot}10^{39}$
						$1.31{\cdot}10^7$	$6.07{\cdot}10^{38}$
						$2.06{\cdot}10^7$	$3.56{\cdot}10^{38}$
2012cu	(12:53:29.35, +02:09:39.0)	3999	4.71	1	8.9	236537	$6.89{\cdot}10^{40}$
						327195	$3.38{\cdot}10^{39}$
						651910	$4.35{\cdot}10^{38}$
						941337	$2.77{\cdot}10^{38}$
2012fr	(03:33:35.99, -36:07:37.7)	3554, 6868, 6869, 6870, 6871, 6872, 6873, 13920, 13921	298.66	5	16.03	$7.41{\cdot}10^6$	$6.64{\cdot}10^{39}$
						$1.13{\cdot}10^7$	$3.00{\cdot}10^{38}$
						$2.74{\cdot}10^7$	$3.27{\cdot}10^{37}$
						$4.32{\cdot}10^7$	$1.93{\cdot}10^{37}$

[9] for 30 eV, 50 eV, 100 eV, & 150 eV, respectively.
[10] for combined image if several observation epochs exits

Discussion

This study is a continuation of that presented in Nielsen et al. (2012). It increases the total number of nearby (< 25 Mpc) type Ia SNe with pre-explosion images in *Chandra* to 13. None of these show any evidence for an X-ray progenitor. We note that for SN2007on an X-ray source was detected, see Voss & Nelemans (2008), however, whether this actually was a detection or a chance alignment remains undetermined, as explained in Roelofs et al. (2008). We therefore disregard SN2007on in the following.

In Figure 22 we compare the upper limits found in this study and in Nielsen et al. (2012) with the known SSSs of the Magellanic Clouds and the Milky Way. As can be seen, the upper limits of SN2012fr are comparable to those of SN2007sr, which narrowly straddles the parameter space where we expect to find canonical SSSs, i.e. $kT_{\rm BB} = 30 - 100$ eV & $L_{\rm bol} \simeq 10^{37} - 10^{38}$ erg/s. Even for SN2012fr, we can rule out the brightest SSSs as progenitors, provided they are unobscured by local material. However, for all the SNe in the sample, a progenitor with a low effective temperature and/or bolometric luminosity would be permitted by the observations. SN2011fe remains the most constraining case by far, which primarily stems from the fact that it was the most nearby type Ia SN since the launch of *Chandra*, and it took place in a well-observed galaxy (M101).

Rather than just looking at the individual upper limits, we can use the fact that we now have a 13 consistently calculated upper limits to study the sample of objects. The first thing to note is that the comparison in Figure 22 is in a sense inconsistent: we compare 3-σ upper limits with data with 1-σ error bars. For individual systems, that is probably the right thing to do, but as a sample, a comparison using 1-σ upper limits may be more relevant. Therefore, we show the same plot with 1-σ upper limits in Figure 23. The 1-σ upper limits of SN2007sr and SN2012fr are probing the $kT_{\rm BB}$, $L_{\rm bol}$-parameter space of known SSSs. Furthermore, we can have a look in more detail at the individual observations and how they compare to the expected background as a sample. In Figure 24 we compare the observed counts in the source region for the SNe in our sample, except SN2006mr and SN2011iv, with the number of counts expected from the background in the same region. Evidently, the pre-explosion source counts for all the SNe on the figure are consistent with background only (i.e. no source) to within 2-σ confidence; this is also the case for SN2011iv (not shown on the figure). We note that at this confidence level, the pre-explosion source count on the position of SN2006mr (also not shown) is formally a detection; however, for a sample of 13 systems, ~ 4.2 of them are expected to be detections when considering 1-σ limits, and we should even expect one 2-σ detection as well. So, for purely statistical reasons, the fact that SN2006mr is a 2-σ detection should not come as a big surprise. Furthermore, SN2006 is located on a very uneven background region close to the center of its host galaxy, and the exact number of background photons is difficult to determine without additional information concerning the X-ray background (see Nielsen et al. 2012 for details).

Figure 25 shows a stacked image of the SNe that are located on a reasonably even background (i.e. excluding SN2006mr, S2006dd and SN2011iv). If there were a general tendency towards more photons in the source regions of each image it would become gradually clearer as the images are added. We find no evidence for such a stack-up of photons.

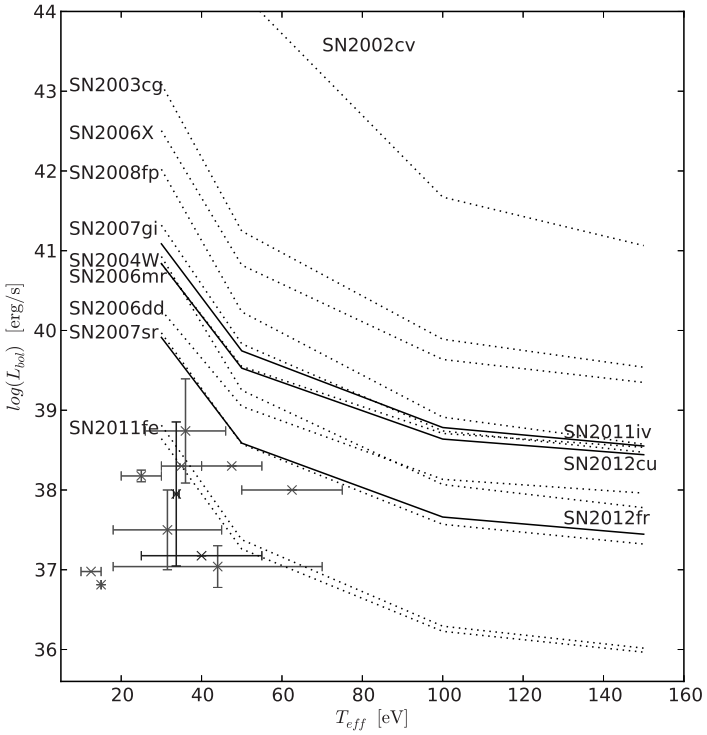

Figure 22: Comparison between bolometric luminosity 3-σ upper limits found in this paper and Nielsen et al. (2012) with bolometric luminosities of known supersoft X-ray sources in nearby galaxies, as taken from Greiner (2000). The dotted lines and SN designations on the left (center for SN2002cv) are for the 10 upper limits from the 2012 paper, while the 3 new upper limits presented in this paper are plotted with solid lines and SN designations on the right. The green, blue and red crosses are known compact binary and symbiotic SSSs in the Milky Way, SMC and LMC, respectively.

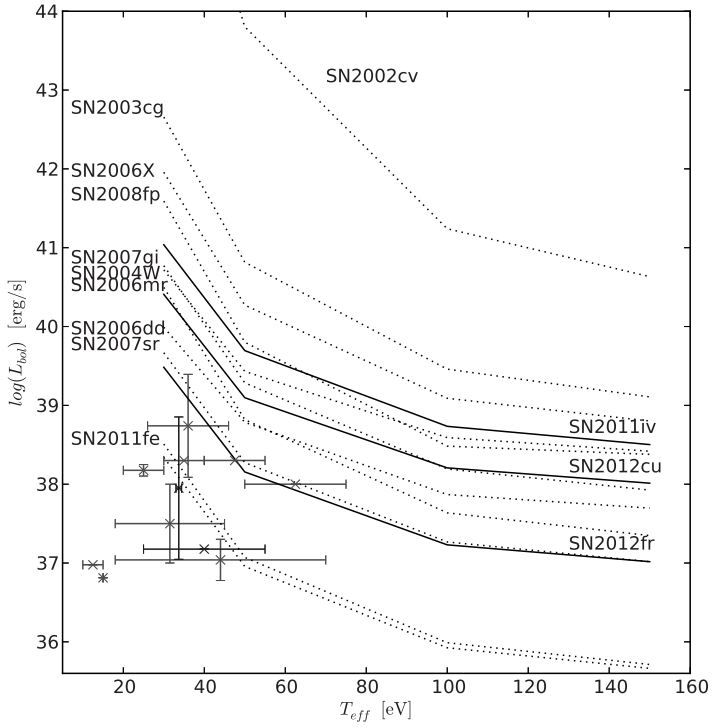

Figure 23: 1-σ version of Figure 22.

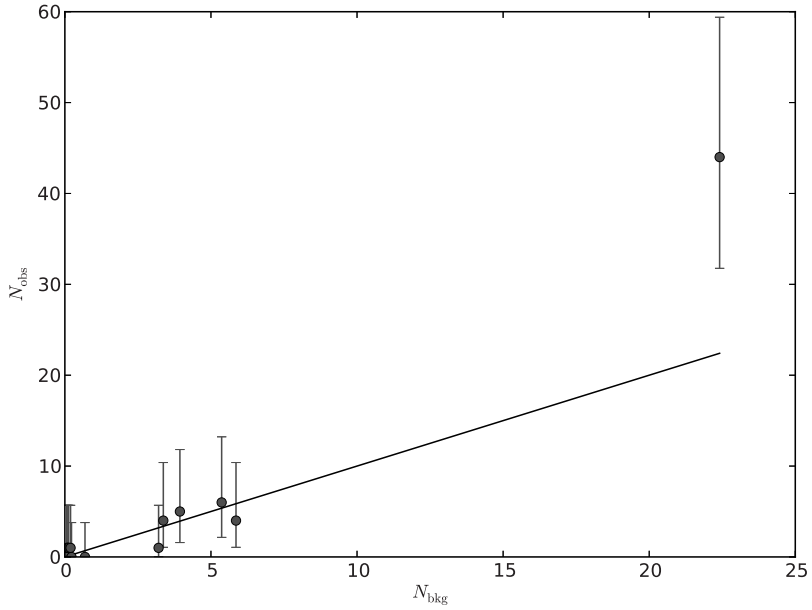

Figure 24: Source counts ($N_{\rm obs}$) vs. expected background counts in the 4.5 pixel aperture source region ($N_{\rm bkg}$). Error bars correspond to 2-σ confidence level. For ease of reference, the point corresponding to SN2011iv is not shown, as the count rates is very large (243) in comparison to the other points. The outlying point corresponds to SN2006mr.

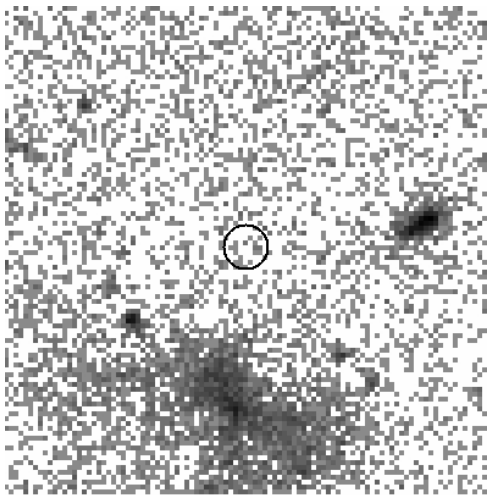

Figure 25: Stacked pre-explosion images of SN2002cv, SN2003cg, SN2004W, SN2006X, SN2006dd, SN2007gi, SN2007sr, SN2008fp, SN2011fe, SN2012cu, and SN2012fr. Pre-explosion images of SN2006mr and SN2011iv were excluded due to uneven backgrounds.

To make a more qualitative statement, we compared the number of observed pre-explosion photons for each SN position with two hypotheses: the null hypothesis (hypothesis H_0) that there is no source at the position of the SNe prior to the SN explosion. The alternative hypothesis (hypothesis H_1) is that there is a naked (i.e. unobscured by local phenomena), 'canonical' SSS ($L_{\rm bol} = 10^{38}$ erg/s, $kT_{\rm BB} = 50$ eV) at the positions of the SNe prior to the SN explosion. We calculated the expected number of counts for canonical SSSs at the distances given in Table 6 and Table 1 in Nielsen et al. (2012). We rescaled this bolometric flux to the supersoft X-ray flux in *Chandra*'s 0.3-1.0 keV band, then found the absorbed flux using the relevant absorbing column given in Table 6 and Table 1 in Nielsen et al. (2012), and inserted this into Equation 11 to find the expected number of photons from such a source. The number of photons expected if no source is present is simply the number of background photons. We then calculated the Poissonian probabilities P of detecting the observed number of counts for the two hypotheses. The ratio P_{H_1}/P_{H_0} is the likelihood ratio. Table 8 shows the likelihood ratios for the alternative and null hypotheses for the entirety of our nearby SN sample. In general, a likelihood ratio larger than 1 favours hypothesis 1, i.e. that there is a canonical SSS present at the position of the SN prior to the explosion. Conversely, a number smaller than 1 favours the null hypothesis that there is no source present. Values close to 1 indicate that we cannot discriminate between the two hypotheses.

The strongest conclusion we can make from the individual likelihood ratios in Table 8 is that for SN2011fe the presence of a naked, canonical SSS is strongly ruled out. For SN2007sr and SN2012fr, it appears that we can rule out a source, but not with very strong confidence. Conversely, for SN2008fp, SN2011iv, and SN2012cu, the presence of sources are favoured, but again, only weakly so. For SN2006mr, we seem to have a strong indication of the presence of a source, however, as Fig. 7 in Nielsen et al. (2012) shows, the background of the position of the progenitor is quite uneven. Therefore, whether this is actually a detection of a source is unclear. We also note that for SN2002cv the probabilities for either hypotheses are the same. This is due to the large absorbing column for that SN, and it essentially means that including the pre-explosion observations for SN2002cv in our analysis confers no information as to whether there is a source present or not.

By taking the product of the likelihood ratios, i.e. $\Pi(P_{H_1}/P_{H_0})$, we can determine whether or not the sample as a whole gives us reason to believe that sources are actually present in the pre-explosion observations. Due to the extremely small likelihood ratio for SN2011fe, the combined likelihood ratio of the entire sample is tiny ($\sim 2.2 \cdot 10^{-12}$). However, if we accept that we can rule out a naked, canonical SSS as the progenitor of SN2011fe and leave it out, along with the problematic case of SN2006mr, we get a combined likelihood ratio of $\sim$0.99. To properly interpret this number, we conduct a simulation to assess the probability that this combined likelihood ratio could have been observed by chance even if in reality there were canonical SSSs present in all osbervations. In order to do so, we assumed that a source was present and simulated 100,000 Poissonian realisations of the source counts for each pre-SN observation with expectation values as per a canonical SSS. These were multiplied into combined likelihood ratios for the subsample excluding SN2011fe and/or SN2006mr. We then counted the fraction of cases where the simualtions resulted in a likelihood ratio lower than

Table 8: Comparison of hypotheses H_0 and H_1 (see text for details).

SN	counts observed	photons expected, canonical SSS	photons expected, no source	P_{H_1}	P_{H_0}	P_{H_1}/P_{H_0}
2002cv	1	$1.01{\cdot}10^{-1}$	$1.01{\cdot}10^{-1}$	$9.13{\cdot}10^{-2}$	$9.13{\cdot}10^{-2}$	1.00
2003cg	1	$6.98{\cdot}10^{-2}$	$6.48{\cdot}10^{-2}$	$6.51{\cdot}10^{-2}$	$6.07{\cdot}10^{-2}$	1.07
2004W	1	3.53	3.21	$1.03{\cdot}10^{-1}$	$1.30{\cdot}10^{-1}$	$7.92{\cdot}10^{-1}$
2006X	0	$6.98{\cdot}10^{-1}$	$6.89{\cdot}10^{-1}$	$4.98{\cdot}10^{-1}$	$5.02{\cdot}10^{-1}$	$9.92{\cdot}10^{-1}$
2006dd	6	6.68	5.37	$1.55{\cdot}10^{-1}$	$1.55{\cdot}10^{-1}$	1.00
2006mr	44	23.7	22.4	$5.87{\cdot}10^{-5}$	$1.83{\cdot}10^{-5}$	3.21
2007gi	0	$3.21{\cdot}10^{-1}$	$2.27{\cdot}10^{-1}$	$7.26{\cdot}10^{-1}$	$7.97{\cdot}10^{-1}$	$9.10{\cdot}10^{-1}$
2007sr	4	6.29	3.37	$1.21{\cdot}10^{-1}$	$1.85{\cdot}10^{-1}$	$6.54{\cdot}10^{-1}$
2008fp	1	$1.81{\cdot}10^{-1}$	$1.30{\cdot}10^{-1}$	$1.51{\cdot}10^{-1}$	$1.14{\cdot}10^{-1}$	1.33
2011fe	4	41.7	5.86	$9.66{\cdot}10^{-14}$	$1.40{\cdot}10^{-1}$	$6.89{\cdot}10^{-13}$
2011iv	243	198	197	$1.77{\cdot}10^{-4}$	$1.28{\cdot}10^{-4}$	1.38
2012cu	1	$4.52{\cdot}10^{-1}$	$1.94{\cdot}10^{-1}$	$2.88{\cdot}10^{-1}$	$1.60{\cdot}10^{-1}$	1.80
2012fr	5	7.97	3.94	$9.26{\cdot}10^{-2}$	$1.54{\cdot}10^{-1}$	$6.01{\cdot}10^{-1}$

the observed value. For the full sample, there is no chance to find the extremely low likelihood ratio by chance (0 instances out of 100,000). For the sub-sample that excludes SN2011fe and SN2006mr, we find a value of $\sim$0.99 or lower in only $\sim$ 14% of the cases, i.e. the low value could be found by chance even if there were sources present in the pre-SN observations, but it is rather unlikely. This confirms our interpretation of the likelihood ratio, that it is a hint against canonical SSS progenitors being present for *all* supernovae, but not a very strong hint.

We conclude that the sample as a whole strongly disfavours the hypothesis that there are sources present, but this is dominated by the strong upper limits of SN2011fe. If we accept SN2011fe as a non-detection and exclude it from our sample, it essentially becomes impossible to determine with a high level of confidence whether sources are present or not. Removing the problematic case of SN2006mr favours the non-presence of sources, to approximately the 1-σ level.

In general, the currently-used assumptions concerning the thermonuclear processing of accreted material on the surface of a massive WD are probably too simplistic to provide a good model for the X-ray emissions from such systems. The accretion process and the interaction between a luminous X-ray source and the material being accreted is bound to be complicated. What is needed is a better understanding of the detailed physics of the burning of hydrogen- and helium-rich material on the surface of massive WDs, realistic modelling of the radiative transfer processes in the entire WD+donor system, resulting in reliable observational predictions.

Conclusions

With the results reported in this study, and disregarding the ambiguous case of SN2007on, we currently have thirteen pre-explosion *Chandra* obervations of the positions of type Ia SNe. None of them show evidence of a supersoft X-ray progenitor. However, as discussed in Section , the upper limits of the bolometric luminosities of even the best of these observations place only weak constraints on the supersoft X-ray characteristics of the progenitor systems of the SNe in question: for SN2007sr, SN2011fe and SN2012fr we can rule out only the brightest of the suggested canonical SSS progenitors.

Our search was initially started in an attempt to solve the question of the SD or DD nature of type Ia SN progenitors, since SD were expected to be SSSs, while DD progenitors were not. However, there may be several reasons for the lack of supersoft X-ray emissions from the progenitors of type Ia SNe, besides the obvious one that they are not SSS. A number of recent studies have shown the question of whether type Ia SN progenitors are X-ray sources to be somewhat more involved than what was initially assumed, for details see Section in this paper and the discussion in (Nielsen et al. 2012). Also, it has been suggested that DD progenitors may also emit soft X-rays for a significant period of time during the merger leading to the SN explosion, see Yoon et al. (2007). However, the luminosities expected in such cases are approximately an order of magnitude lower than for a steadily-accreting SD progenitor. Also, Di Stefano (2010b) found that if the DD scenario is the dominant contributor to the type Ia SN rate, then a significant population of X-ray bright proto-DD systems should exist as a result of wind accretion before the second WD forms. However, a study by Nielsen et al. (accepted) involving recent population synthesis codes fails to reproduce a significant population of SSS proto-DD progenitor systems as was suggested by Di Stefano (2010b), and in any case, any emission from this type of system would cease long before the SN itself.

The campaign to use archival *Chandra* images to constrain the soft X-ray characteristics of type Ia SNe continues, and the number of nearby type Ia SNe for which archival images exist continues to grow. While other studies have provided upper limits to the luminosities of indivdual type Ia SN progenitors, our archival search campaign provides the only consistently executed study of the upper limits of the X-ray and bolometric luminosities of nearby (< 25 Mpc) type Ia SN progenitors.

Acknowledgments

We thank the IAU Central Bureau of Astronomical Telegrams for providing a list of SNe. This research made use of data obtained from the *Chandra* Data Archive and the ciao 4.3 software provided by the *Chandra* X-ray Center.

This research is supported by NWO Vidi grant 016.093.305.

Additionally, we acknowledge Gijs Roelofs for help with this project in its early stages.

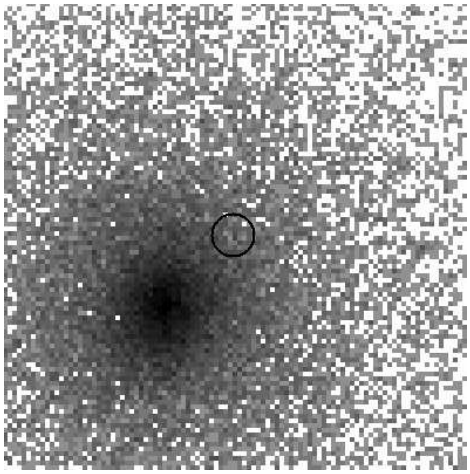

Figure 26: Part of *Chandra* observations 2942, 4174, 9798 & 9799. The circle corresponds to an aperture of 4.5 pixels at the position of SN2011iv.

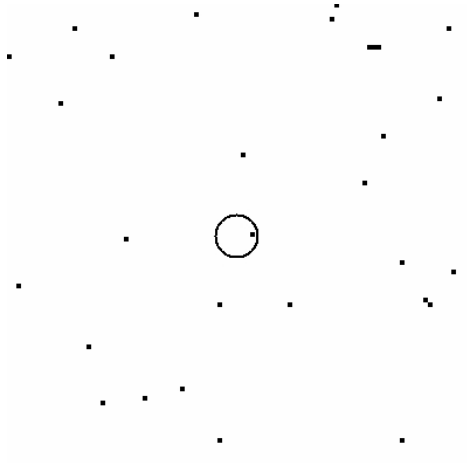

Figure 27: Part of combined image consisting of *Chandra* observation 3999. The circle corresponds to an aperture of 4.5 pixels at the position of SN2012cu

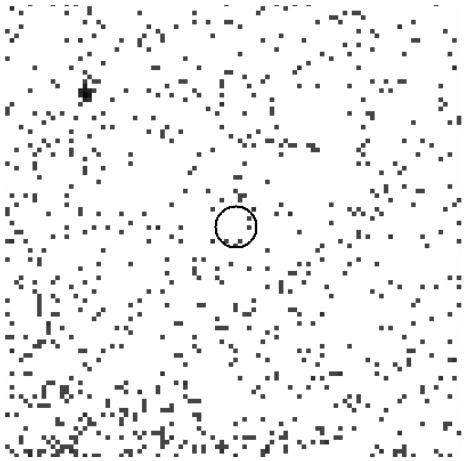

Figure 28: Part of *Chandra* observations 3554, 6868, 6869, 6870, 6871, 6872, 6873, 13920, & 13921. The circle corresponds to an aperture of 4.5 pixels at the position of SN2012fr.

On double-degenerate type Ia supernova progenitors as supersoft X-ray sources - A population synthesis analysis using SeBa

M.T.B. Nielsen, G. Nelemans, R. Voss, S. Toonen

Astronomy & Astronphysics (accepted)

Abstract

The nature of the progenitors of type Ia supernova progenitors remains unclear. While it is usually agreed that single-degenerate progenitor systems would be luminous supersoft X-ray sources, it was recently suggested that double-degenerate progenitors might also go through a supersoft X-ray phase. We aim to examine the possibility of double-degenerate progenitor systems being supersoft X-ray systems, and place stringent upper limits on the maximally possible durations of any supersoft X-ray source phases and expected number of these systems in a galactic population. We employ the binary population synthesis code SeBa to examine the mass-transfer characteristics of a possible supersoft X-ray phase of double-degenerate type Ia supernova progenitor systems for 1) the standard SeBa assumptions, and 2) an optimistic best-case scenario. The latter case establishes firm upper limits on the possible population of supersoft source double-degenerate type Ia supernova progenitor systems. Our results indicate that unlike what is expected for single-degenerate progenitor systems, the vast majority of the material accreted by either pure wind mass-transfer or a combination of wind and RLOF mass-transfer is helium rather than hydrogen. Even with extremely optimistic assumptions concerning the mass-transfer and retention efficiencies, the average mass

accreted by systems that eventually become double-degenerate type Ia supernovae is small. Consequently, the lengths of time that these systems may be supersoft X-ray sources are short, even under optimal conditions, and the expected number of such systems in a galactic population is negligible.The population of double-degenerate type Ia supernova progenitors that are supersoft X-ray sources is at least an order of magnitude smaller than the population of single-degenerate progenitors expected to be supersoft X-ray sources, and the supersoft X-ray behaviour of double-degenerate systems typically ceases long before the supernova explosions.

Introduction

Type Ia supernovae (SNe) are of critical importance to cosmological distance measurements and galactic evolution. Despite decades of intense research the nature of the progenitors giving rise to these explosions remains unclear (e.g. Maoz & Mannucci 2012). From observational evidence, it is inferred that the exploding objects are carbon-oxygen white dwarfs (WDs) with masses close to the Chandrasekhar mass ($M_{Ch} \sim 1.38 M_{\odot}$) that undergo thermonuclear runaway as carbon and oxygen is processed to radioactive iron-group elements. However, most single carbon-oxygen WDs are born at masses much smaller than M_{Ch}, typically ~ 0.6 $M_{\odot}$. Consequently, the fundamental problem surrounding type Ia SN progenitors revolves around how newly-formed, initially sub-M_{Ch} WD can grow sufficiently in mass to eventually explode as type Ia SNe. It is commonly agreed that the progenitors are binary systems where the WD that eventually explodes accretes mass from a companion. Two progenitor scenarios (or 'channels') are usually considered: in the single-degenerate (SD) scenario, a single WD accretes hydrogen-rich material from a non-degenerate companion (usually a giant, although main sequence or helium-stars are also sometimes considered) and processes the accreted material to carbon and oxygen, eventually reaching the required mass where it explodes Whelan & Iben (1973). In the double-degenerate (DD) scenario, a binary system consisting of two sub-M_{Ch} WDs spiral in via emission of gravitational radiation and eventually merge, forming a single carbon-oxygen WD with a combined mass at or above the required mass (Iben & Tutukov 1984; Webbink 1984). From the observational data currently available, it is not possible to clearly discriminate which scenario is the correct one, or whether both scenarios contribute to the SN Ia rate. Beyond the two main scenarios, there are a number of alternative scenarios considered by various groups, e.g. the 'core degenerate' scenario (Kashi & Soker 2011).

As shown by van den Heuvel et al. (1992), the accretion and thermonuclear processing of H-rich material on the WD in the SD scenario is expected to emit copious amounts of supersoft X-rays ($L_{\rm bol} \sim 10^{38}$erg/s at black-body spectral fits corresponding to $T_{\rm BB} = 30 - 150$ eV), provided the material is accreted at high enough rates (Nomoto 1982). This potentially makes nearby progenitor systems observable to current X-ray instruments like *Chandra* and *XMM-Newton*. An archival search for *Chandra* pre-explosion observations at the positions of nearby type Ia SNe is being undertaken (see Voss & Nelemans 2008; Nielsen et al. 2012, 2013), but so far, no unambiguous direct detections of supersoft X-ray sources (SSSs) at the positions of type Ia SNe have been made. Additionally, when compared to the population that

should be expected if the SD scenario is responsible for the observed SN Ia rate, the observed population of SSSs in nearby galaxies falls short by at least one, and quite likely two orders of magnitude (Di Stefano 2010a). Likewise, the integrated soft X-ray luminosity measured from elliptical galaxies falls similarly short (Gilfanov & Bogdán 2010), assuming SSS SD systems are the progenitors of type Ia SNe. Taken at face value, these points should be considered serious problems for the SD scenario (however, see the Discussion section for alternative explanations of the absence of SSSs).

To complicate matters further, it has been suggested that even if the DD scenario is the dominant one in terms of supplying progenitors of type Ia SNe, a large population of SSSs would still be expected to exist (Di Stefano 2010b). The motivation for this is that most of the binary systems that eventually become DD progenitors of type Ia SNe should pass through a stage where they consist of a WD and a non-degenerate companion, before the latter becomes a WD. This configuration mimics the late stages of a SD system where it could be a SSS. If DD progenitor systems are also SSSs for a significant amount of time ($\sim$ Myr), there could be an observationally significant number of such systems at any one time in a galactic population like the Milky Way. If correct, this would mean that the absence of a large population of SSS could potentially be a problem for both progenitor scenarios, not just for the SD scenario.

If we wish to understand the nature of the progenitors of type Ia SNe, we must obtain a better understanding of the observational characteristics of the progenitor scenarios. We need to settle whether either of the scenarios give rise to supersoft X-ray emission. In the present study, we examine the hypothesis that DD progenitors are SSS, using the SeBa binary evolution code (Portegies Zwart & Verbunt 1996; Nelemans et al. 2001; Toonen et al. 2012). In Section we review the theory behind SSSs and the proposed SSS nature of DD type Ia SN progenitor systems. In Section we explain the details of our method. Section lists our results, and Section discusses the implications of these results. Section concludes.

A word on terminology: we use 'mass-transfer' to denote the transfer of material from donor to accretor, regardless of whether some of that material is subsequently lost from the accretor. By 'retention efficiency' we mean the fraction of the transferred material that remains on the accretor. By 'accretion' we refer to transferred material that remains on the accretor. So, a mass-transfer rate of 10^{-7} $M_\odot$/yr that is retained at 25% retention efficiency results in an accretion rate of $2.5 \cdot 10^{-8}$ $M_\odot$/yr, for example. Note that retention efficiency and accretion efficiency are not the same; the accretion efficiency is the ratio of the total amount of matter lost from the donor that remains on the accretor, while retention efficiency is the ratio of the transferred material that remains on the accretor.

Theory

For an initially sub-M_{Ch} WD to grow in mass and eventually become a type Ia SN, material from the donor star needs to be transferred and retained on the WD. While a wide range of mass-transfer rates are possible, the retention of transferred material depends on the mass of the accretor and the mass-transfer rate; for WDs above 0.6 $M_\odot$, the transfer of hydrogen-rich material can only take place in a stable manner in a narrow interval of mass-transfer rates,

between $1.7 \cdot 10^{-7}$ $M_\odot$/yr and $4.1 \cdot 10^{-7}$ $M_\odot$/yr (Nomoto 1982). Outside of this interval, the transferred material is unlikely to be retained on the WD; for mass transfer rates above the steady-burning rate, the material is transferred onto the WD faster than it can be processed, and the WD consequently swells up, likely stopping or severely hampering the mass-transfer process, see also Nomoto et al. (1979). For mass-transfer rates below the steady-burning rate, the material burns unstably (Fujimoto & Sugimoto 1979, 1982), i.e. in nova eruptions, causing the WD to lose most of the accreted mass, plus possibly some additional mass from the WD itself.

A similar constraint governs the mass-transfer of helium-rich material, i.e. very high mass-transfer rates cause the accretor to swell up, somwehat lower mass-transfer rates allow steady burning, while low mass-transfer rates result in helium-novae. The question of helium steady burning was examined by Hachisu et al. (1999); Kato & Hachisu (1999); Iben & Tutukov (1996) (see also review by Bours et al. 2013). Because of the higher temperatures and densities required for helium burning, higher mass-transfer rates are required for helium to burn steadily, as compared to hydrogen mass-transfer. The exact value of the steady burning rate is somewhat disputed, but for a 1 $M_\odot$ WD, the interval of steady burning mass-transfer rates that agrees with all of three studies mentioned above is between $2.5 \cdot 10^{-6}$ $M_\odot$/yr and $4.0 \cdot 10^{-6}$ $M_\odot$/yr (see Fig.2 in Bours et al. 2013).

To get the initially sub-M_{Ch} to the mass needed for a type Ia SN explosion in the SD scenario, an extended period of steady mass-transfer is required after the formation of the WD. Since carbon-oxygen WDs are not expected to form at masses larger than $1 - 1.2$ $M_\odot$, the steady mass-transfer and processing of material must last on the order of a few million years or longer. The mechanism of mass-transfer can be anything that is capable of supplying a transfer of matter at the steady-burning rate; usually, it is assumed to happen either through a wind or by Roche-lobe overflow (RLOF).

In the case of DD progenitors, a binary system evolves to consist first of a single WD and a non-degenerate companion, and later two WDs that eventually merge to form a single WD with a mass sufficient to explode as a type Ia SN (however, see our comment concerning 'double-CE' systems in Section below). At some intermediate point during its evolution, before the merger happens, such proto-DD systems will consist of a WD and a non-WD companion star, and hence may be considered conceptually similar to a SD system. Since we expect SD type Ia SN progenitor systems to be SSSs as a result of the thermonuclear processing of the accreted material, we may also consider the prospect that such 'SD-like', proto-DD type Ia SN progenitors could display similar behaviour in this phase of their evolution, if they accrete material from their companions at sufficiently high rates. In Di Stefano (2010b) it was suggested that a significant fraction of these systems should be expected to accrete H-rich material from their companions at a rate large enough to sustain steady burning, corresponding to a population of 'thousands' in a spiral galaxy like the Milky Way. They would therefore also emit supersoft X-rays, similarly to a SSS SD type Ia SN progenitor system, for an extended period of time ($\sim$ Myr). The mechanism behind this mass-transfer is wind mass-transfer, and Di Stefano (2010b) assumed a wind accretion efficiency of 25%, i.e. one-fourth of the material lost from the non-degenerate companion is accreted unto the WD.

Two key requirements need to be met for the SD-like proto-DD type Ia SN progenitor systems to constitute a significant population of observable SSSs. Firstly, the mass-transfer rate needs to be high enough for the transferred material to be burned steadily on the surface of the WD, thereby giving rise to supersoft X-ray emission. If this requirement is not met, the sources may still accrete material (albeit at much smaller retention efficiency, as described in Nomoto 1982), but they will presumably not emit much in terms of supersoft X-rays. Secondly, the accretion of material at the steady-burning rate needs to take place over a long enough period of time, so that at any one time there will be a significant population of these sources present for us to observe.

Before the merger and SN can take place the second WD needs to form, after which the decay of the orbit will lead to the merger. Due to the time needed for this process (during which the system no longer is SD-like and not expected to emit supersoft X-rays), it will not be possible to directly associate a given SN with a previously observed SSS if DD systems are the dominant progenitor channel for type Ia SNe.

Method

We employed the binary population synthesis code SeBa (Portegies Zwart & Verbunt 1996; Nelemans et al. 2001; Toonen et al. 2012) to simulate the evolution of a large number of binaries. The evolution is followed for a Hubble time starting from the zero-age main-sequence. At every timestep, stellar winds, mass transfer, common envelopes (CEs), angular momentum loss, and gravitational waves are taken into account with appropriate recipes. We assume solar metalicities, and the initial primary masses are distributed according to the Kroupa initial mass function (Kroupa et al. 1993) between 0.95-10 $M_\odot$ and the initial mass ratio distribution is flat. The distribution of orbital separations is flat in log-space citepAbt.1983 out to 10^6 $R_\odot$, and the eccentricities are distributed thermally between 0 and 1 (Heggie 1975). Due to uncertainties in the physics of CEs (for an overview, see Ivanova et al. 2013), several prescriptions for the CE-phase exist that are based on the energy budget (the α-prescription, see Tutukov & Yungelson 1979; Webbink 1984) or on the angular momentum balance (the γ-prescription, see Nelemans et al. 2000). In SeBa, the α-formalism is used in all cases where the binary contains a compact object, or when a CE is triggered by a tidal instability. For all other CE-events, the γ-formalism is used. The results given below (in the main text, not in the Appendix) use these assumptions. For both the standard and optimistic cases (see below) we assume $\gamma = 1.75$ (Nelemans et al. 2001) and $\alpha\lambda = 2$ (Nelemans et al. 2001), where λ is the envelope-structure parameter (de Kool et al. 1987). For completeness, in the Appendix we also include results for a model that applies the α-formalism to all CE-events.

We note that for the α-CE formulation, there are systems that develop directly into DD systems from the giant phase, thereby avoiding the SD-like phase; for the standard γ-CE formulation used here, this does not happen. See Toonen et al. (2012) for details.

We ran a SeBa simulation for a total of 500,000 binary systems. From the resulting outputs we conducted analyses for two separate cases: a 'standard' and an 'optimistic' case. In the former, we simply took the SeBa outputs at face value. In the latter case, we manually

imposed optimistic conditions concerning transfer and retention of material (see below). The motivation for the second analysis was to calculate solid upper limit for the populations of DD progenitor systems that could possibly be SSSs, and specifically to compare with the results of Di Stefano (2010b), whose study used more generous assumptions concerning the efficiency of wind mass-transfer than assumed by SeBa. The reason it is possible to manually impose a different retention efficiency from the SeBa outputs in the optimistic case is that SeBa explicitly outputs the mass loss from both binary components in each calculation step. By finding the difference in donor mass in each step in which the donor is not transferring mass stably we can find the amount of material lost in a wind. We then assume a given retention efficiency to find the fraction of this material that ends up being accreted unto the donor. As long as the masses accreted in this way are small compared to the mass of the accretor - which they always are - this approach does not significantly change the general physical and evolutionary behaviour of the binaries, which means that the subsequent SeBa steps are still correct.

In both cases, we examined all systems consisting of a single WD and a non-degenerate companion that would later merge to a final mass above the Chandrasekhar mass, i.e. systems that could be said to be SD-like before becoming DD type Ia SNe. We calculated the accreted masses of both hydrogen- and helium-rich material.

In the standard case, the masses accreted from wind and RLOF is directly given by the code. For wind mass-transfer, SeBa only considers Bondi-Hoyle-Lyttleton wind accretion, the accretion efficiency of which is quite small (typically, $< 1\%$, see Edgar (2004). For both wind and RLOF mass-transfer, SeBa follows the steady-burning constraints of Nomoto (1982), i.e. material transferred at rates different from the steady-burning rate is unlikely to be appreciably retained on the WD. We refer to Bours et al. (2013) for further details on the assumptions concerning wind and stable mass-transfer in SeBa.

For the optimistic case, we relaxed the assumptions concerning both wind and RLOF mass-transfer to enable comparison with Di Stefano (2010b) and establish upper limits on the possible lifetime and number of SSS proto-DD type Ia SN progenitor systems. For wind transfer, we counted the total mass transferred as the mass lost from the donor star while the the accretor is a WD and the binary components are detached (i.e. not in a CE or inspiraling phase). Only a fraction of this material will actually be accreted by the accretor, and the rest of it will be lost from the system. The exact amount accreted depends on the model used. Di Stefano (2010b) assumed an accretion efficiency of 25% for wind mass-transfer. To get strong upper limits we adopted the same wind accretion efficiency as Di Stefano, i.e. 25%. For both wind and RLOF we assumed a retention efficiency of 100%, i.e. all the mass that ends up on the accretor stays there. This is obviously quite an optimistic assumption, since, as mentioned above, the material needs to be accreted at a fairly narrow range of mass-transfer rates in order to facilitate full retention. However, in the context of the current study, we are content to establish an upper limit of the number of SD-like proto-DD type Ia SN progenitor systems that could conceivably be SSSs.

If we assume that all the accreted material (hydrogen or helium) is transferred at the steady-burning rate appropriate for that type of material, the average SSS lifetime $\tau_{\rm accr}$ of a

DD SN progenitor in a given stellar population is given by:

$$\tau_{\rm accr}/{\rm SN} = \sum_{X}^{H,He} \frac{\Delta M_X}{\dot{M}_{X,{\rm steady}}} \tag{12}$$

where ΔM_X is the total accreted mass of material X, and $\dot{M}_{X,{\rm steady}}$ is the minimum mass-transfer rate required for steady-burning of material X.

The donors in SeBa can be either hydrogen- or helium-rich. As mentioned in Section , for helium-rich material, the mass-transfer rate needed to sustain steady burning and avoid significant mass loss through nova eruptions is roughly an order of magnitude larger than for hydrogen-rich material. This larger steady-burning mass-transfer rate translates into a shorter SSS life-time for the same mass of material, as compared with a system transferring hydrogen. Since we want to determine an upper limit to the number of possible DD progenitors that can be SSSs at any given time, we take the minimum steady-burning rates mentioned above, i.e. $\dot{M}_{\rm H,steady} = 1.7 \cdot 10^{-7}$ M$_\odot$/yr and $\dot{M}_{\rm He,steady} = 2.5 \cdot 10^{-6}$ M$_\odot$/yr. For simplicity, we assume the material transferred from H-rich donors (i.e. main sequence stars, Herzsprung gap stars, first giant branch stars, core helium-burning stars, and asymptotic giant stars) to consist of a 25% helium and 75% hydrogen (by mass), while the material transferred from helium-rich systems (helium-stars and helium-giants) is exclusively helium.

The average number of sources $N_{\rm accr}$ is calculated by scaling the average SSS lifetime with the average occurrence rate of type Ia SNe in a galaxy:

$$N_{\rm accr} = 3.0 \cdot 10^{-3} \tau_{\rm accr} \left(\frac{L_{\rm B}}{10^{10} {\rm L}_{\rm B,\odot}} \right) \tag{13}$$

where $L_{\rm B}$ is the B-band luminosity of the galaxy, L$_{\rm B,\odot}$ is the B-band luminosity of the Sun, and we have assumed an type I SN rate of 3 per millennium, typical of a spiral galaxy like the Milky Way. We limit ourselves to considering a population similar to the Milky Way, which means that the last term in Eq.(13) is equal to 1.

Results

In this section, we present the results for the standard and the optimistic cases. The former gives realistic estimates of the mass accretion, according to our best current understanding. The latter gives strong upper limits to the mass accretion which should be applicable no matter which assumptions are made concerning mass-transfer and retention efficiencies.

Of the simulated 500,000 binary systems, 2290 systems resulted in double carbon-oxygen WD mergers with a combined mass above 1.38 M$_\odot$ for the γ-CE prescription in the standard case (see Section for further information on when the α- and γ-formalisms are used in SeBa). When we relaxed our mass-transfer and retention efficiency assumptions, 175 systems that were DD type Ia progenitors in the standard case experience enough mass transfer to bring their WDs above 1.38 M$_\odot$ before the systems merge. Under our optimistic assumptions, these systems would therefore become SD (instead of DD) type Ia SNe. Consequently, we removed them from our optimistic case sample, leaving us with 2115 systems for this case.

For general applicability, rather than giving our results in total numbers, we list them in terms of solar masses per SN. This enables the reader to scale the results with any particular supernova rate and progenitor life-time of their choice. The total masses can be found by multiplying the average numbers by the number of progenitor systems in each sample.

In the following, we only discuss the results for the γ-CE formulation. However, the results for the α-CE are quite similar and yield essentially the same conclusions. The results for the α-CE are given in the Appendix.

All systems

The average masses accreted per SN in our entire sample are given in Table 9. Figure 29 shows the accretion histories of these systems. Clearly, helium-accreting systems dominate in terms of the amount of mass being transferred for both the standard and optimistic assumptions.

Table 9 also gives the average SSS life-time of the progenitor systems, based on the average mass accreted per SN in the total sample. This SSS life-time assumes that all material is burned at the steady-burning rate, and takes the different steady-burning rates for hydrogen and helium into account. For both the standard and optimistic cases, the average life-times are roughly 0.05 Myr, significantly smaller than both the expected total life-time of an average DD type Ia SN progenitor system (e.g. Maoz et al. Maoz et al. (2010)), and the expected supersoft X-ray life-time of SD progenitors. The SSS life-times translate into a number of accreting SSS systems expected to be 'on' in Milky Way-type spiral galaxy at any time, according to Eq.(13). Table 9 lists this number for both of the examined cases. We also list the Poissonian errors on these numbers, with the caveat that at the end of the day, the accreted masses, and thereby the calculated $N_{\rm accr}$ depend on the assumptions used in SeBa. For a detailed discussion of these assumptions we refer to Toonen et al. (2012).

Figure 29 shows the accretion history for all the systems in our sample for the optimistic case. Supersoft behaviour can only take place during periods where the systems are accreting. As can be seen, systems where the initially most massive star evolves into a WD first generally finish transferring mass earlier than is the case for the systems where the initially least massive star evolves into a WD first. This is to be expected, since in the latter type of system, the initially most massive star becomes a long-lived helium-star, and so the initially least massive star needs time to evolve to a WD before mass-transfer can start. This type of 'evolution-reversed' systems will therefore be slow to form, and will not start transferring mass until somewhat later than systems where the most massive star becomes a WD first (see Toonen et al. 2012 for more details on this type of evolution).

Table 10 gives the time from the last mass-transfer event until the SN explosion for all the systems in our sample for the optimistic assumptions. For the vast majority (99.999%) of the systems, mass-transfer ceases a Myr or more before the SN explosion. So, even under the optimistic assumption that all of the involved systems are transferring mass at exactly the right steady-burning rate to emit supersoft X-rays, it would not be possible to observationally associate any of these systems with SN explosions, as they would have ceased to be SSSs long (millions to billions of years) before the SNe take place. This is expected, as the second white dwarf needs time to form before the system can merge and explode.

Table 9: Mass accreted by the first-formed WDs in all DD progenitor systems (2290 for the standard case; 2115 for the optimistic case), split by donor type. The bottom rows give the SSS life-time of the average ΔM, if all material is accreted at the component-specific (for H and He, respectively) steady-burning mass-transfer rates, and the resulting expected number of accreting systems (with Poisson errors). Both columns use the γ-CE prescription.

donor stellar type	standard SeBa case: ΔM/SN [$M_\odot$]	upper limit case: ΔM/SN [$M_\odot$]
main sequence star	0.0	$5.98 \cdot 10^{-5}$
Herzsprung gap star	0.0	$2.61 \cdot 10^{-5}$
first giant branch star	$7.14 \cdot 10^{-5}$	$2.87 \cdot 10^{-5}$
core He-burning star	0.0	$1.81 \cdot 10^{-4}$
asymptotic giant branch star	0.0	$3.91 \cdot 10^{-5}$
He-star	$4.98 \cdot 10^{-5}$	$2.31 \cdot 10^{-3}$
He-giant star	$8.54 \cdot 10^{-2}$	$1.17 \cdot 10^{-1}$
Total, all types	$8.55 \cdot 10^{-2}$	$1.19 \cdot 10^{-1}$
$\tau_{\rm accr}$ [yr]	$3.5 \cdot 10^4$	$4.9 \cdot 10^4$
$N_{\rm accr}$ (10^{10} $L_{B,\odot}$ galaxy)	$1.0 \cdot 10^2 \pm 10$	$1.5 \cdot 10^2 \pm 12$

Table 10: Time from last mass-transfer event to SN explosion, all accreting systems, optimistic case. Compare with tables 12 and 14

time since last accr	no. of systems	fraction of total
t < 1 Myr	2	$9.46 \cdot 10^{-4}$
1 Myr < t < 10 Myr	14	$6.62 \cdot 10^{-3}$
10 Myr < t < 100 Myr	117	$5.53 \cdot 10^{-2}$
100 Myr < t < 400 Myr	171	$8.09 \cdot 10^{-2}$
t > 400 Myr	1811	$8.56 \cdot 10^{-1}$
Total	2115	1.00

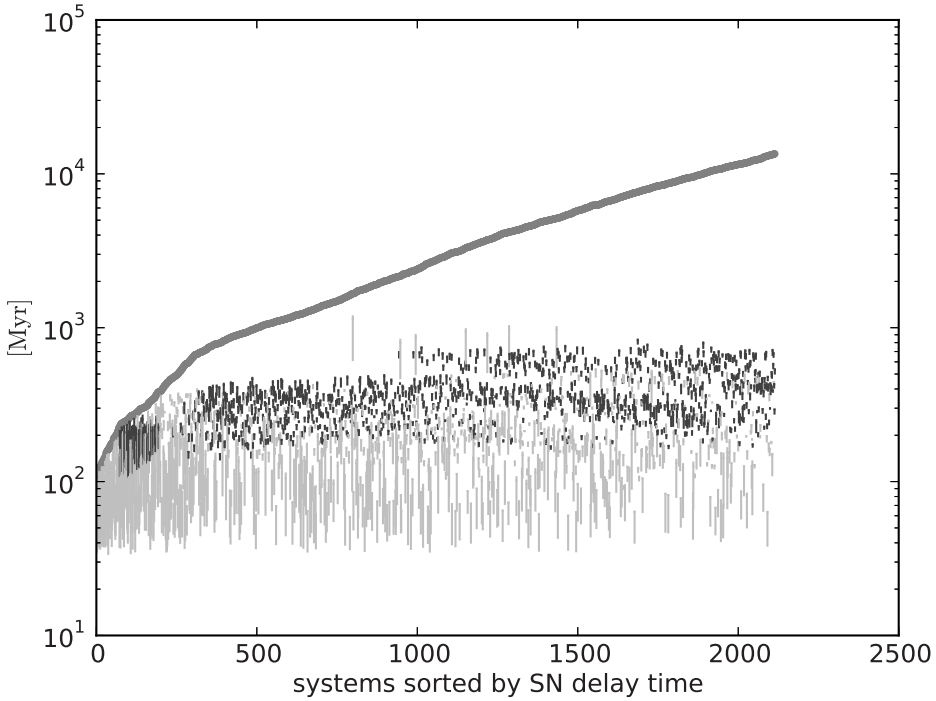

Figure 29: Accretion history for all systems in the optimistic case, using the γ-CE formulation. The y-axis gives the delay time from formation of the system until the SN explosion. Each column in the plot corresponds to one system, and the systems are ordered according to delay time, with delay times increasing towards the right; the dark grey line delineates the SN explosions. Light grey vertical lines show accretion events in systems where the initially most massive star is the accretor, black is for systems where the initially least massive star is the accretor. Compare with Figures 30 & 31

Wind accreting / symbiotic systems

Some systems never experience stable mass-transfer from the donor to the accretor while they are in the SD-like configuration, and instead accrete exclusively via a wind. Such systems could be considered roughly similar to symbiotic SD type Ia supernova progenitors during this phase.

Table 11 lists the mass accreted per supernova for all systems of this type. As expected, wind mass-transfer is a negligible contributor to WD growth in the standard case, so we expect no SSSs powered by this type of mass-transfer for that case. With the relaxed assumptions in the optimistic case, the systems do accrete some material (and a small number become SD type Ia SNe as a result, as mentioned), although still quite small amounts compared to systems experiencing RLOF (see below). The majority of the accreted material is helium-rich. The average amount of material accreted for this type of system corresponding to an average SSS

Table 11: Mass accreted via wind mass-transfer by the first-formed WDs in DD progenitor systems in our sample (924 for the standard case; 902 for the optimistic case), split by donor type. The bottom row gives the SSS life-time of the average ΔM, if all material is accreted at the component-specific (for H and He, respectively) steady-burning mass-transfer rates, and the resulting expected number of accreting systems (with Poisson errors). Both columns use the γ-CE prescription.

donor stellar type	standard SeBa case: ΔM/SN [$M_\odot$]	upper limit case: ΔM/SN [$M_\odot$]
main sequence star	0.0	0.0
Herzsprung gap star	0.0	$2.44 \cdot 10^{-5}$
first giant branch star	0.0	$4.23 \cdot 10^{-5}$
core He-burning star	0.0	$3.21 \cdot 10^{-6}$
asymptotic giant branch star	0.0	$2.47 \cdot 10^{-6}$
He-star	0.0	$1.03 \cdot 10^{-3}$
He-giant star	0.0	$3.50 \cdot 10^{-3}$
total, all types	0.0	$4.60 \cdot 10^{-3}$
$\tau_{\rm accr}$ [yr]	0.0	$2.16 \cdot 10^{3}$
$N_{\rm accr}$ (10^{10} $L_{B,\odot}$ galaxy)	0	6.5 ± 2.5

life-time of roughly 5000 years. This is completely negligible compared to both the total life-times of even the shortest-living systems that become DD type Ia SNe, and the expected SSS phase of a SD progenitor. The expected number of these SSSs active in a galactic population is therefore also tiny. The considerations concerning errors on $N_{\rm accr}$ mentioned in Subsection are clearly applicable for Table 11 as well.

Figure 30 shows the accretion history of the systems of this type, andTable 12 gives the time from the last mass-transfer event until the SN explosion for the optimistic assumptions. For systems transferring mass via a wind, mass-transfer ceases at least 10 Myrs before the SN explosion. For ∼83% of the systems, this time interval is larger than 100 Myrs. Wind accretors generally finish their accretion earlier than RLOFing systems (see next section).

RLOF-accreting systems

Table 13 lists the mass accreted per supernova for systems that experience mass-transfer via RLOF, at some point during their evolution. All of these systems also experience wind mass-transfer at some point.

As with wind accreting systems, RLOF-transferring systems accrete predominantly helium and only negligible amounts of hydrogen. The average mass accreted by these systems is significantly larger than that accreted by purely wind-accreting systems. The expected SSS life-time of these systems is correspondingly larger, slightly less than 10^5 years, however, this is still significantly less than the expected total life-time of a DD type Ia SN progenitor system, and at least an order of magnitude smaller than the SSS period expected for SD progenitor

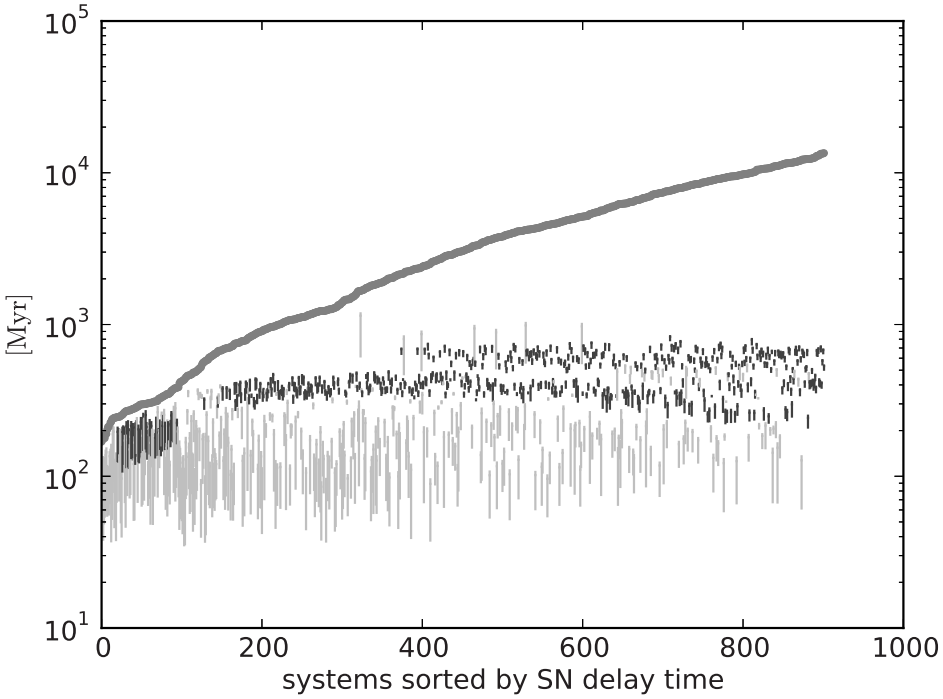

Figure 30: Accretion history for detached, purely wind-accreting systems (i.e. systems that never experience stable mass-transfer) in the optimistic case, using the γ-CE formulation. The y-axis gives the delay time from formation of the system until the SN explosion. Each column in the plot corresponds to one system, and the systems are ordered according to delay time, with delay times increasing towards the right; the dark grey line delineates the SN explosions. Light grey vertical lines show accretion events in systems where the initially most massive star is the accretor, black is for systems where the initially least massive star is the accretor. Compare with Figures 29 & 31.

systems. The expected number of these systems in a Milky Way-type galactic population at any time is therefore still smaller than what was estimated in Di Stefano (2010b). See subsection for considerations concerning errors on $N_{\rm accr}$.

Figure 31 shows the accretion history of these systems.

Table 14 gives the time from the last mass-transfer event until the SN explosion for all the systems experiencing mass-transfer via RLOF in our sample, for the optimistic assumptions. For systems transferring mass via RLOF, $\sim$1% of the systems explode less than 10 Myrs after the cessation of mass-transfer.

Table 12: Time from last mass-transfer event to SN explosion, detached / wind-accreting systems, optimistic case. Compare with tables 10 and 14.

time since last accr	no. of systems	fraction of total
t < 1 Myr	0	0.0
1 Myr < t < 10 Myr	0	0.0
10 Myr < t < 100 Myr	56	$6.21 \cdot 10^{-2}$
100 Myr < t < 400 Myr	94	$1.04 \cdot 10^{-1}$
t > 400 Myr	752	$8.34 \cdot 10^{-1}$
Total	902	1.00

Table 13: Mass accreted by the first-formed WDs in DD progenitor systems in our sample that experience a combination of RLOF and wind mass-transfer (1366 for the standard case; 1213 for the optimistic case), split by donor type. The bottom row gives the SSS life-time of the average ΔM, if all material is accreted at the component-specific (for H and He, respectively) steady-burning mass-transfer rates, and the resulting expected number of accreting systems (with Poisson errors). Both columns use the γ-CE prescription.

donor stellar type	standard SeBa case: ΔM/SN [$M_\odot$]	upper limit case: ΔM/SN [$M_\odot$]
main sequence	0.0	$1.04 \cdot 10^{-4}$
Herzsprung gap	0.0	$2.74 \cdot 10^{-5}$
first giant branch	$1.20 \cdot 10^{-4}$	$1.86 \cdot 10^{-5}$
core He-burning	0.0	$3.12 \cdot 10^{-4}$
asymptotic giant branch	0.0	$6.63 \cdot 10^{-5}$
He-star	$8.35 \cdot 10^{-5}$	$3.26 \cdot 10^{-3}$
He-giant	$1.43 \cdot 10^{-1}$	$2.01 \cdot 10^{-1}$
total, all types	$1.43 \cdot 10^{-1}$	$2.05 \cdot 10^{-1}$
$\tau_{\rm accr}$ [yr]	$5.8 \cdot 10^4$	$8.42 \cdot 10^4$
$N_{\rm accr}$ (10^{10} $L_{B,\odot}$ galaxy)	$1.7 \cdot 10^2 \pm 13$	$2.5 \cdot 10^2 \pm 16$

Table 14: Time from last mass-transfer event to SN explosion, systems experiencing mass-transfer via RLOF at least once, optimistic case. Compare with tables 10 and 12.

time since last accr	no. of systems	fraction of total
t < 1 Myr	2	$1.65 \cdot 10^{-3}$
1 Myr < t < 10 Myr	14	$1.15 \cdot 10^{-2}$
10 Myr < t < 100 Myr	61	$5.03 \cdot 10^{-2}$
100 Myr < t < 400 Myr	77	$6.35 \cdot 10^{-2}$
t > 400 Myr	1059	$8.73 \cdot 10^{-1}$
Total	1213	1.00

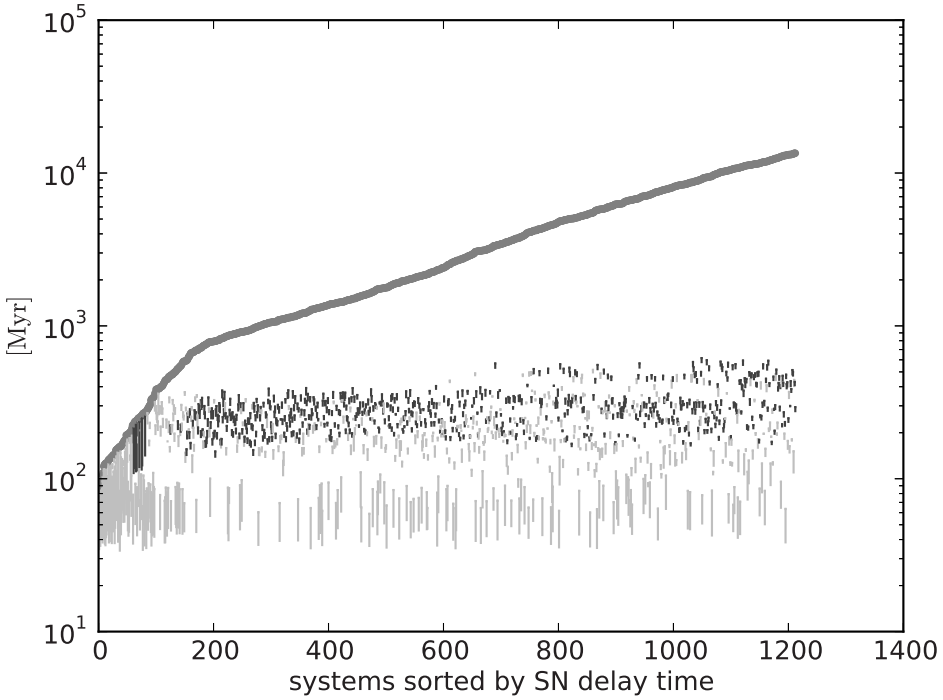

Figure 31: Accretion history for systems that experience stable mass-transfer at some point during their evolution in the optimistic case, using the γ-CE formulation. Most of the systems in this category will also experience wind mass-transfer. The y-axis gives the delay time from formation of the system until the SN explosion. Each column in the plot corresponds to one system, and the systems are ordered according to delay time, with delay times increasing towards the right; the dark grey line delineates the SN explosions. Light grey vertical lines show accretion events in systems where the initially most massive star is the accretor, black is for systems where the initially least massive star is the accretor. Compare with Figures 29 & 30.

Discussion

The aim of this study was to determine whether DD progenitor systems of type Ia SNe could conceivably constitute a significant population of SSSs during the SD-like part of their evolution. If they would, then the observationally inferred absence of SSSs would strongly limit the DD progenitor scenario. Our results indicate that DD progenitors do not make up a significant population of SSSs for either of the cases we have examined. As mentioned in Section , the mass-transfer and retention efficiencies assumed in the optimistic case are probably not realistic, but even with such optimistic assumptions, we estimate a total galactic population of just 6-7 wind accreting proto-DD SN progenitors in large spiral galaxies like the Milky Way. In contrast, the study by Di Stefano (2010b) predicted 'thousands' of wind-accreting SSS proto-DD progenitors. The number of RLOFing systems that could be SSSs under our optimistic assumptions is larger, around ~ 250, but still quite negligible compared to Di Stefano's estimate. For the standard SeBa case, we find no wind accreting SSSs, and ~ 170 SSSs from RLOFing progenitors. We stress that all numbers estimated in the optimistic case should be considered generous upper limits. The cause of the disagreement between the results of our study and that of our comparison study may be the somewhat general assumptions concerning the donor mass loss rates used by Di Stefano, although this can hardly explain the difference completely. As mentioned, that study predicts thousands) of donor stars capable of supplying a large mass loss rate, and combined with a large enough retention efficiency this leads to an appreciable population of SSS proto-DD type Ia SN progenitor systems accreting over a long period of time. But it is unclear to the authors of this article how such a large population of long-lived, large $\dot{M}$-donors arises, and a similar population is not reproduced by SeBa, despite using the same accretion efficiency.

Our study predicts a different chemical composition of the accreted material for proto-DD accretors. Contrary to what is expected for the SD scenario, helium mass-transfer dominates the SD-like phase of proto-DD type Ia supernova progenitors. As mentioned, this has a significant effect on the maximal life-times of any SSS phases of such systems. This is not just a feature of the optimistic case; also for the standard case, the vast majority of the accreted material is helium.

In our study, the average masses accreted in systems experiencing RLOF ($\sim$0.2 $M_\odot$) is similar to the accreted masses hypothesised for the most massive carbon-oxygen WDs in the SD scenario. However, the fact tha the majority of the accreted material is helium results in significantly shorter SSS life-times. Our results therefore hinge on the details concerning the mass-transfer and steady-burning of helium, which are currently less well-understood than for hydrogen. However, due to the higher temperatures and densities required for helium-burning, the steady-burning rate that we have assumed is probably not unreasonable.

The studies by Di Stefano (2010a) and Gilfanov & Bogdán (2010) indicated that the observed numbers of SSSs in nearby galaxies and the integrated supersoft luminosity in ellipticals are one to two orders of magnitude too small compared to what should be expected if luminous SSS SD progenitors were the main contributors to the type Ia SN rate. According to our study, we expect a factor 10-20 fewer SSS DD progenitors compared to SSS SD progenitors, for the same SN rate. If we accept the more constraining case, i.e. that the difference between the

observed number and/or integrated luminosities of SSSs fall two orders of magnitude short of the expected value, then the lack of SSSs would also be a problem for the DD progenitor scenario, at least under the assumption that all accreted material is burned at the steady-burning rate, although it would still be a lot smaller problem than for the SD scenario. However, one should be careful, as the long delay between the SSS phase and the actual explosion would make a direct comparison between the current SSS population and the current type Ia SN rate impossible. What would then be needed is to take the details of the star formation history of the galaxies for which the SSS populations have been determined into account and use these to calculate the expected SSS population for the DD scenario. That is beyond the scope of the present paper.

Because of the time required for the second WD to form in a DD progenitor system, we expected to find the cessation of accretion long before the merger that leads to the type Ia SN. The accretion history plots in Figures 29-31 and Tables 10-14 show that even if our optimistic assumptions were correct, the SSS behaviour would have ceased millions of years before the SN explosion for most systems. We note that systems accreting exclusively via a wind generally stop accreting earlier (with respect to the merger) than systems accreting via a combination of wind and RLOF.

The applicability of our results depends on the correctness of the assumptions on which SeBa is based. For the evolution towards type Ia SNe, Toonen et al. (2012) and Bours et al. (2013) found that the most crucial assumptions for the SD channel are the retention efficiency and the CE-prescription, whereas the DD channel is relatively insensitive to the latter assumption. Our results explicitly vary the retention efficiency (from realistic to extremely optimistic values in the two cases) and we note that our results hardly depend on which CE-formalism is used.

The SN rate inferred from earlier observations is approximately a factor 10 larger than what can be produced with the current version of SeBa with DD progenitors (Toonen et al. 2012), although recent observations indicate that the observed rate may be smaller than previously thought, and therefore the discrepancy between the simulated DD populations may fall correspondingly less short, to within a factor of a few of the observed type Ia SN rate (Bours et al. 2013). This means that, theoretically, our results could underestimate the numbers of SSS progenitors for the DD scenario. However, if the DD scenario really is the dominant progenitor scenario the discrepancy between the theoretical rates and the observed rates must be either due to an incorrect normalisation with the correct binary evolution channels, or to completely new binary evolution channels that have yet to be identified. Although difficult to prove, we believe the discrepancy is more likely due to a normalisation issue, and certainly there is no strong reason to believe that any additional DD binary evolution channels would produce very long SSS phases. Whatever the exact reason for and magnitude of the discrepancy, in our analysis we implicitly assumed that we can scale our results from the current (too small) SeBa DD type Ia rate to the actual SN rate, to compare with SSS SD progenitors.

On a fundamental note, we emphasise that the discussion concerning SSS usually implicitly assumes that such sources are more or less 'naked', i.e. unobscured by local material. If, for whatever reason, the sources in question are significantly obscured by local matter (as would

likely be the case if the systems were transferring mass via a wind, where a large fraction of the matter lost from the donor would not be accreted unto the accretor), the situation may well be different (see Nielsen et al. accepted). That local, circumbinary material may have been present around at least some type Ia SNe immediately prior to the explosion has been established by a number of studies (Gerardy et al. 2004; Borkowski et al. 2006; Patat et al. 2007; Sternberg et al. 2011; Chiotellis et al. 2012).

Conclusions

The key to solving the type Ia SN progenitor question is a better understanding of the observational characteristics of the accretion process which eventually brings the accreting WD to the mass required for the SN. While observational data of the SNe themselves is rapidly growing as a result of several large-scale SN surveys, the theoretical understanding of what a nuclear burning WD looks like remains a sticky point. Without a better grasp on this issue, the riddle of the SN Ia progenitors is going to remain unsolved, presumably until such a time when direct confirmation of a (very) nearby SN Ia progenitor can be made.

We performed an analysis of the accretion behaviour of DD type Ia SN progenitor systems in the evolutionary stage prior to the formation of the second WD, where the systems may conceivably be similar to SD type Ia SN progenitors, and hence possibly SSSs. For this, we simulated 500,000 binary systems with the population synthesis code SeBa. We made our analysis for two cases: 1) a conservative / realistic case using the standard SeBa assumptions concerning mass-transfer and retention efficiencies, and 2) a more optimistic case using less constrained assumptions for wind accretion (i.e. 25% mass-transfer efficiency, 100% retention efficiency) to establish firm upper limits on the possible SSS behaviour of proto-DD type Ia SN progenitor systems. For both cases, we calculated the average accreted mass per SN, the corresponding SSS life-time, and the expected number of accreting SSSs in a Milky Way-type galactic population at any given time, assuming all mass-transfer happens at the rate required for steady burning for the type of material in question (hydrogen or helium).

For wind accretion we observe the following:

1. In the standard case, no mass is accreted via wind, so we expect no SSS behaviour at all for DD progenitors of type Ia SNe if the standard SeBa assumptions concerning wind accretion are generally correct.

2. For the relaxed assumptions in the optimistic case, the average mass accreted per supernova via pure wind mass-transfer is tiny.

3. Unlike what is likely the case for SD progenitors, the majority of the accreted material is helium, not hydrogen. Even if this material were accreted at the steady-burning rate (which it most likely is not) it would not be sufficient to make the systems luminous SSSs for very long; in our estimate, the average SSS lifetime is on the order of a couple of thousands of years. Translated into numbers of systems in a Milky Way-type galaxy, this corresponds to less than 10 luminous SSSs originating from proto-DD type Ia SN progenitors accreting via a wind.

The conclusions we make from this is that we do not expect a significant number of proto-DD type Ia SN progenitor to be observable as SSSs as a result of pure wind mass-transfer. This goes contrary to what was concluded in the study by Di Stefano (2010b), which predicted thousands of these sources.

For systems transferring mass via a wind and RLOF, the basic conclusions are rather similar to those concerning pure wind-accreting systems, with a few modifications:

1. For both the standard and optimistic cases, the average masses accreted per supernova may be significantly (more than an order of magnitude) larger than for pure wind-accreting systems.

2. As for wind accreting systems, the vast majority of the transferred mass is helium.

3. The length of the supersoft X-ray emitting phase for these systems will be of the order of $10^5 - 10^4$ years, if all mass-transfer happens at the steady-burning rates. While this is significantly longer than for pure wind-accreting systems, it is still negligible compared to the total life-time of DD type Ia SN progenitor systems, and at least an order of magnitude smaller than the expected SSS life-time of SD progenitors. The expected number of accreting systems present in a galactic population is correspondingly smaller.

To sum up: on the basis of our study, we do not find support for the existence of a significant population of SSS proto-DD type Ia SN progenitor systems. This holds for both wind- and RLOF-accreting systems, although the tendency is stronger for wind accretors. Since no SSSs are expected if the DD progenitor scenario of type Ia SNe, the absence of observed SSSs is not a strong argument against the DD progenitor scenario.

Acknowledgements

This research is supported by NWO Vidi grant 016.093.305. We thank the anonymous referee for a careful reading, and many constructive suggestions.

Appendix

Table 15: Mass accreted by the first-formed WDs in all DD progenitor systems (3298 for the standard case; 2920 for the optimistic case), split by donor type. The bottom row gives the SSS life-time of the average ΔM, if all material is accreted at the component-specific (for H and He, respectively) steady-burning mass-transfer rates. Both columns use the α-CE prescription.

donor stellar type	standard SeBa case: ΔM/SN [$M_\odot$]	upper limit case: ΔM/SN [$M_\odot$]
main sequence star	0.0	$4.61 \cdot 10^{-5}$
Herzsprung gap star	0.0	$3.64 \cdot 10^{-5}$
first giant branch star	$5.77 \cdot 10^{-5}$	$4.39 \cdot 10^{-5}$
core He-burning star	0.0	$8.05 \cdot 10^{-5}$
asymptotic giant branch star	0.0	$1.62 \cdot 10^{-5}$
He-star	$8.27 \cdot 10^{-4}$	$3.10 \cdot 10^{-3}$
He-giant star	$8.46 \cdot 10^{-2}$	$1.09 \cdot 10^{-1}$
Total, all types	$8.54 \cdot 10^{-2}$	$1.13 \cdot 10^{-1}$
$\tau_{\rm accr}$ [yr]	$3.4 \cdot 10^{4}$	$4.6 \cdot 10^{4}$
$N_{\rm accr}$ (10^{10} $L_{B,\odot}$ galaxy)	$1.0 \cdot 10^{2}$	$1.4 \cdot 10^{2}$

Table 16: Mass accreted via wind mass-transfer by the first-formed WDs in DD progenitor systems in our sample (1384 for the standard case; 1363 for the optimistic case), split by donor type. The bottom row gives the SSS life-time of the average ΔM, if all material is accreted at the component-specific (for H and He, respectively) steady-burning mass-transfer rates. Both columns use the α-CE prescription.

donor stellar type	standard SeBa case: ΔM/SN [$M_\odot$]	upper limit case: ΔM/SN [$M_\odot$]
main sequence star	0.0	0.0
Herzsprung gap star	0.0	$3.51 \cdot 10^{-5}$
first giant branch star	0.0	$4.37 \cdot 10^{-5}$
core He-burning star	0.0	$2.28 \cdot 10^{-6}$
asymptotic giant branch star	0.0	$1.86 \cdot 10^{-6}$
He-star	0.0	$9.84 \cdot 10^{-4}$
He-giant star	0.0	$3.00 \cdot 10^{-3}$
total, all types	0.0	$4.07 \cdot 10^{-3}$
$\tau_{\rm accr}$ [yr]	0.0	$2.0 \cdot 10^{3}$
$N_{\rm accr}$ (10^{10} $L_{B,\odot}$ galaxy)	none	6.0

Table 17: Mass accreted by the first-formed WDs in DD progenitor systems in our sample that experience a combination of RLOF and wind mass-transfer (1914 for the standard case; 1557 for the optimistic case), split by donor type. The bottom row gives the SSS life-time of the average ΔM, if all material is accreted at the component-specific (for H and He, respectively) steady-burning mass-transfer rates. Both columns use the α-CE prescription.

donor stellar type	standard SeBa case: ΔM/SN [$M_\odot$]	upper limit case: ΔM/SN [$M_\odot$]
main sequence star	0.0	$8.64 \cdot 10^{-5}$
Herzsprung gap star	0.0	$3.75 \cdot 10^{-5}$
first giant branch star	$9.95 \cdot 10^{-5}$	$4.40 \cdot 10^{-5}$
core He-burning star	0.0	$1.49 \cdot 10^{-4}$
asymptotic giant branch star	0.0	$2.87 \cdot 10^{-5}$
He-star	$1.42 \cdot 10^{-3}$	$4.96 \cdot 10^{-3}$
He-giant star	$1.46 \cdot 10^{-1}$	$2.02 \cdot 10^{-1}$
Total, all types	$1.48 \cdot 10^{-1}$	$2.08 \cdot 10^{-1}$
$\tau_{\rm accr}$ [yr]	$5.9 \cdot 10^{4}$	$8.5 \cdot 10^{4}$
$N_{\rm accr}$ (10^{10} $L_{B,\odot}$ galaxy)	$1.8 \cdot 10^{2}$	$2.5 \cdot 10^{2}$

The type Ia supernova rate in the Local Universe

M.T.B. Nielsen, G. Nelemans

(in prep.)

Abstract

The rate of type Ia and core-collapse supernovae are well-measured at intermediate and cosmological distances. However, these rates are less well determined in the Local Universe. This may affect the conclusions about their progenitors drawn from local (progenitor) samples. We want to determine the type Ia supernova rate and the type Ia to core-collapse supernova ratio in the Local (< 50 Mpc) Universe. We want to compare this with the corresponding values for intermediate and cosmological distances. We count the number of supernovae of all types in the Local Universe and compare the rate with the two-component model of a prompt and a tardy component. We compare the type Ia to core-collapse supernova rate to determine how well it agrees with the rate found for the intermediate distance Universe. We find that the local type Ia supernova rate agrees well with the estimates from the more distant Universe, at least when disregarding Poisson noise for the very nearby sample (<10-15 Mpc). We find that the ratio of type Ia to core-collapse supernovae approaches a constant value above 20 Mpc, despite the likely different selection biases. We find some evidence of an overpopulation of core-collapse supernovae in the nearby Universe or alternatively a somewhat low value of the type Ia to core-collapse supernova ratio. The supernova rates inferred from observations of intermediate and cosmological distance populations appear to describe the nearby Universe quite well although incompleteness is an issue already at short distances. We thus conclude that the supernovae in the Local Universe are a representative

sample for the whole population and thus can well be used to study supernova progenitors. The type Ia supernovae in the Local Universe predominantly have short delay times.

Introduction

Every year several type Ia supernovae (SNe) and core-collapse (CC) SNe are discovered in the Local Universe, i.e. the volume within several tens of Mpc. These SNe are often studied in detail and can give valuable information about their progenitors (e.g. Smartt 2009; Li et al. 2011a; Nielsen et al. 2012). While the nature of the progenitors of CC SNe are fairly well established (Smartt 2009), for type Ia SNe the situation is unclear (see Maoz & Mannucci 2012 for a review).

For type Ia SNe, the progenitor models fall roughly into two categories: accretion of matter onto a white dwarf from a non-degenerate companion, the so-called single-degenerate channel (Whelan & Iben 1973). Or the merger of two white dwarfs in the so-called double-degenerate channel (Iben & Tutukov 1984; Webbink 1984). One way to study the progenitor issue is via the rate at which SNe explode as a function of host galaxy properties such as star-formation rate (SFR) and total mass (e.g. Maoz 2008). Based on this delay time distributions (DTDs, e.g. Yungelson & Livio 2000) determined from SN rates obtained via dedicated SN surveys, studies have shown that many type Ia SNe explode within about 1 Gyr from the formation of their progenitor stars ("prompt" type Ia SNe), but with a tail extending to 10 Gyr (e.g. Totani et al. 2008; Maoz et al. 2011). This means that the progenitors either must have a large range in masses (high mass for the prompt component, low masses for the late time explosions) or that there can be a significant delay from the end of the evolution of the star to the actual SN explosion. The latter is a natural consequence in the double-degenerate channel, due to the time it takes for the white dwarfs to merge.

Alternative ways to study the progenitor issue are to examine nearby type Ia SNe in detail, study the properties of supernova remnants in the Galaxy and determine the properties of Galactic candidate progenitor populations such as accreting white dwarfs and short-period double white dwarfs. In all these approaches the information about SN rates (SNRs), determined at intermediate distances is directly compared to very local SN, their remnants or progenitor populations. In this article we aim to determine if the number of observed SN in the Local Universe is consistent with the rates determined further away.

Method

A straightforward way to compare the observed number of SNe in the Local Universe with SN rates determined from supernova surveys is to compare the CC SNe with the SFR in the volume and compare the type Ia SNe with both the SFR as well as the mass in the volume. We use the convenient parametrisation of Scannapieco & Bildsten (2005):

$$\frac{\mathrm{SNR}}{100\mathrm{yr}^{-1}} = A\left(\frac{M_\star(t)}{10^{10}\mathrm{M}_\odot}\right) + B\left(\frac{\dot{M}_\star(t)}{10^{10}\mathrm{M}_\odot\mathrm{Gyr}^{-1}}\right) \quad (14)$$

where $M_\star$ and $\dot{M}_\star$ are the stellar mass and star formation rate, respectively.

The dimensionless coefficients A and B are found by fitting with observed SN rates as described by e.g. Mannucci et al. (2005). For the CC SNR, $A = 0$ and B is estimated at 7.5 ± 2.5 by Scannapieco & Bildsten (2005). For type Ia SNe, the A-value comes from type Ia SNe in galaxies that show no sign of recent star formation and is found to be $4.4^{+1.6}_{-1.4} \cdot 10^{-2}$. The B-value comes from the relation between the CC SNR and SFR given above combined with the observed ratio of type Ia SNe to CC in star-forming galaxies of $\sim$0.35 (Mannucci et al. 2005). We adopt the values of $A = 4.4 \cdot 10^{-2}$ and $B = 2.6$, given in Scannapieco & Bildsten (2005) although a more recent determination of the ratio of type Ia SNe to CC SNe (Li et al. 2011b) finds a somewhat lower ratio of 0.25, which would lower the B value.

For the stellar mass, we assume a constant mass density throughout our nearby volume and adopt the estimate of $M_\star = 5.3 \cdot 10^8 h$ M$_\odot$ Mpc^{-3}. given in Bell et al. (2003). Following recent cosmological parameter determinations based on *Planck* observations of the cosmic microwave background radiation, we adopt a value for h of 0.7 (Planck Collaboration et al. 2013). This yields a stellar mass density of $3.7 \cdot 10^8$M$_\odot$Mpc^{-3}.

To get the star formation rate, we use the Gravitational Wave Galaxy Catalogue (GWGC), which is designed to be complete out to 100 Mpc, see White et al. (2011). The catalogue includes absolute B-magnitude, from which we can calculate the total B-band luminosity, L_B. Although L_B is known not directly to sample the SFR, we can use the detailed work of Botticella et al. (2012) who determined the SFR in a volume out to 11 Mpc using several SFR indicators. Assuming that up to the slightly larger distances we probe here the average galaxy properties are similar to those within 11 Mpc, we can then use the SFR and L_B given in Table 1 in Botticella et al. (2012) to find a conversion factor from our L_B to SFR. The results are the following:

$$\mathrm{SFR}_{\mathrm{H}\alpha} = 6.46 \cdot 10^{-11} / L_{B,\odot} \quad (15)$$

$$\mathrm{SFR}_{\mathrm{FUV}} = 1.05 \cdot 10^{-10} / L_{B,\odot} \quad (16)$$

$$\mathrm{SFR}_{\mathrm{TIR+H}\alpha} = 7.29 \cdot 10^{-11} / L_{B,\odot} \quad (17)$$

$$(18)$$

where the SFR subscripts refer to the frequency bands used in Botticella et al. (2012) (apart from the self-explanatory H$_\alpha$, FUV and TIR are far ultraviolet and infrared, respectively). Interestingly, Botticella et al. (2012) conclude that the higher rate implied by the FUV observations need to be the right one, given the observed CC SNR. In the remainder of the paper we assume the lower H$_\alpha$ values as we will find below that those match quite well, but we discuss the higher FUV values also.

We analyse the rate of both type Ia and CC SNe within 50 Mpc. To find the SNRs in this distance interval, we use Harvard's SN list[11], which lists the SN type and host galaxy, when available. For named host galaxies we find the distances from NED, using the galaxy velocities relative to the center of the Milky Way (D Galactocentric GSR)). These distances are taken at face value (i.e. no error bars) as the distances to the SNe in our distance cuts. We discard

[11] http://www.cfa.harvard.edu/supernova/finders/Supernovae.html

Table 18: Overview of the most important quantities involved in the calculations of the SNRs, for four separate distance intervals.

	11 Mpc	20 Mpc	30 Mpc	50 Mpc
$V_{\rm tot}$ [Mpc^3]	$5.58{\cdot}10^{3}$	$3.35{\cdot}10^{4}$	$1.13{\cdot}10^{5}$	$5.24{\cdot}10^{5}$
$N_{\rm gal}$	1227	4406	8264	15878
$L_{B,\rm tot}$ [L$_\odot$]	$1.67{\cdot}10^{12}$	$9.76{\cdot}10^{12}$	$2.43{\cdot}10^{13}$	$7.13{\cdot}10^{13}$
$M_\star$ [10^{10}M$_\odot$Mpc^{-3}]	$3.71{\cdot}10^{-2}$	$3.71{\cdot}10^{-2}$	$3.71{\cdot}10^{-2}$	$3.71{\cdot}10^{-2}$
$\dot{M}_\star$ [10^{10}M$_\odot$Gyr^{-1}Mpc^{-3}]	$1.94{\cdot}10^{-3}$	$1.88{\cdot}10^{-3}$	$1.39{\cdot}10^{-3}$	$8.79{\cdot}10^{-4}$
$N_{\rm Ia}$	7	33	89	177
SNR$_{\rm meas.}$ [Mpc^{-3}(100yr)$^{-1}$]	$5.23{\cdot}10^{-3}$	$4.10{\cdot}10^{-3}$	$3.28{\cdot}10^{-3}$	$1.41{\cdot}10^{-3}$
SNR$_{\rm exp.}$ [Mpc^{-3}(100yr)$^{-1}$]	$6.66{\cdot}10^{-3}$	$6.52{\cdot}10^{-3}$	$5.24{\cdot}10^{-3}$	$3.92{\cdot}10^{-3}$
$N_{\rm CC}$	36	109	206	418
SNR [Mpc^{-3}100yr^{-1}]	$2.69{\cdot}10^{-2}$	$1.36{\cdot}10^{-2}$	$7.59{\cdot}10^{-3}$	$3.33{\cdot}10^{-3}$
SNR$_{\rm exp.}$ [Mpc^{-3}(100yr)$^{-1}$]	$1.46{\cdot}10^{-2}$	$1.41{\cdot}10^{-2}$	$1.04{\cdot}10^{-2}$	$6.6{\cdot}10^{-3}$
$N_{\rm unid.SNe}$	4	8	16	38
SNR [Mpc^{-3}100yr^{-1}]	$2.99{\cdot}10^{-3}$	$9.95{\cdot}10^{-4}$	$5.89{\cdot}10^{-4}$	$3.02{\cdot}10^{-4}$
Ia-to-CC rate	$1.94{\cdot}10^{-1}$	$3.03{\cdot}10^{-1}$	$4.32{\cdot}10^{-1}$	$4.23{\cdot}10^{-1}$

SNe for which the hosts are unidentified ('Anon.' in Harvard's list), or those with named host galaxies for which no reliable distance estimate exist. As such, our results give lower limits to the actual SNR.

To get reliable rates, we need to deliminate our sample in terms of observation years (Harvard's SN list goes back to the first registered SNe during the Middle Ages). A certain trade-off needs to be made: to avoid Poisson noise in our nearby rates we need a sample of a certain size, however, the further we go back in time the less complete the sky-coverage becomes. We have chosen to limit ourselves to a period from 1990 to the present. This delimination is arguably somewhat arbitrary, but corresponds to the time when significant numbers of SN were discovered per year.

Results

Supernova sample and star formation estimates

For 1990 to 2013, Harvard's list contains a total of 5168 SNe of all types. Most of these are either out of range or do not have reliable distance estimates: 700 type Ia SNe, 718 CC SNe and 110 SNe of unidentified type take place in host galaxies at distances larger than 50 Mpc. In addition, the numbers of SNe to take place in anonymous galaxies are 1889, 668 and 426, for type Ia, CC and unidentified SNe, respectively. Lastly, a small number (11, 11 and 2, for the same SN types) of SNe takes place in named galaxies without reliable distance estimates. These are also removed from our sample. This leaves us with a total of 633 SNe of all types in galaxies for which reliable distance estimates within 50 Mpc. Table 18 gives the statistics for these SNe.

Figure 32 shows the cumulative distribution of observed numbers of SNe of all types in the 1990-2013 time interval. For reference we also plot the total volume. Apart from the unavoidable fluctuations due to low numbers at short ranges, the rate of all types of SNe roughly follows the volume, as would be expected.

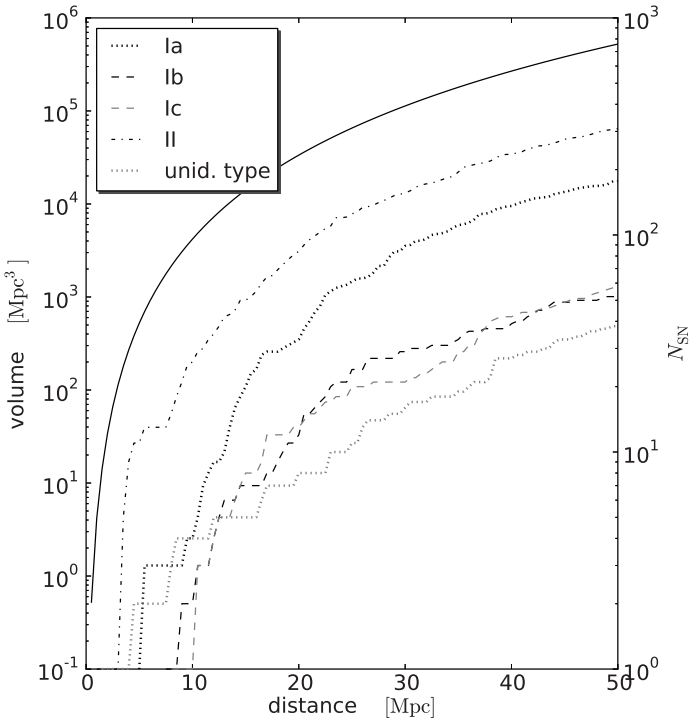

Figure 32: The observed number of SNe in our sample within 50 Mpc (units on right y-axis). The dashed line is the total volume (units on left y-axis).

Figure 33 shows the total B-luminosity and B-luminosity density of our sample galaxies within 50 Mpc that we need to estimate the SFR. As is well-known in cosmology, we expect the Universe to approach homogeneity at scales larger than ~ 100 Mpc. In our nearby sample, however, the density is clearly not constant, although there is an approach to constancy at the last ~ 10 Mpc of our sample. The high peak at very low distances is an artifact of our position within the over-density of the Local Group.

To determine if there are local deviations from homogeneity, we compare the total volume and total B-luminosity on Fig. 34. If the Local Universe were completely homogeneous, the two quantities should be completely proportional. However, there appears to be a slight over-density between roughly 20 and 40 Mpc. To the extent that B-luminosity traces star formation,

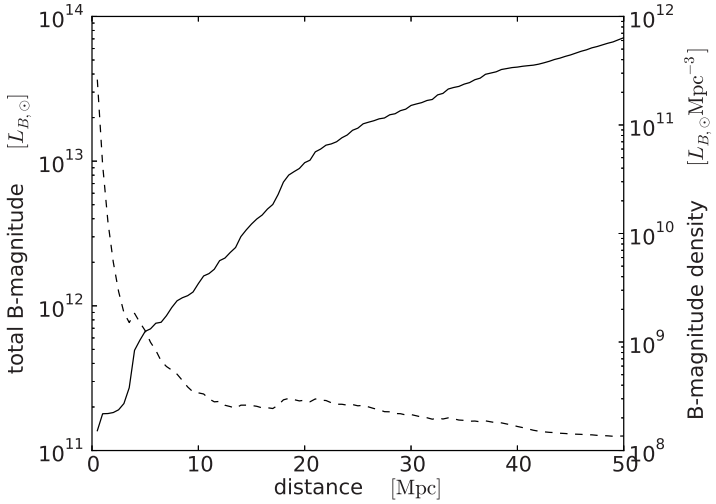

Figure 33: Total B-luminosity (full line, units on left y-axis) and B-luminosity density (dashed line, units on right y-axis) with distance.

we would therefore expect more young, massive stars, and consequently more CC SNe, in this distance interval. By the second term in Eq. (14) we would also expect more type Ia SNe.

Comparison of SN sample with expected numbers

Figure 35 shows a comparison between the observed number of type Ia SNe in the 1990-2013 time interval with the number expected from the local mass and SFR as given above (Eq. 14). For type Ia SNe, disregarding unavoidable Poisson noise at short distances, the observed rate match quite well with the expected rate of Scannapieco & Bildsten (2005), up to approximately 20 Mpc if we use the H_α SFR values. Using the FUV values gives a expected rate that is ∼60 per cent higher. Beyond 20 Mpc, the observed rate drops faster than the expected rate. This suggest that either we miss some type Ia SNe, or we overestimate $M_\star$ or $\dot{M}_\star$. We expect the former option to be the most likely. For CC SNe, we find that within the volume corresponding to 11 Mpc the observed rate is higher by about a factor two than expected if we use the H_α SFR, a conclusion also found by Botticella et al. (2012). They therefore argue that the FUV SFR estimate should be used. However, the discrepancy quickly disappears at slightly larger distances of about 20 Mpc. This suggest either that we start missing some half of the CC SN at 20 Mpc due to selection effects such as obscuration, or alternatively that the large number of CC SN within 11 Mpc is peculiar.

We further investigate this issue in terms of the relative number of type Ia versus CC SNe. Figure 36 shows an effectively constant ratio beyond ∼ 20 Mpc, at a value quite close to the value given in Mannucci et al. (2005) and thus somewhat higher than the Li et al. (2011b) value. The plot shows that between 10 and 15-20 Mpc there is a large change in the type Ia to CC SN ratio making it unclear what the intrinsic ratio is since differential selection effects

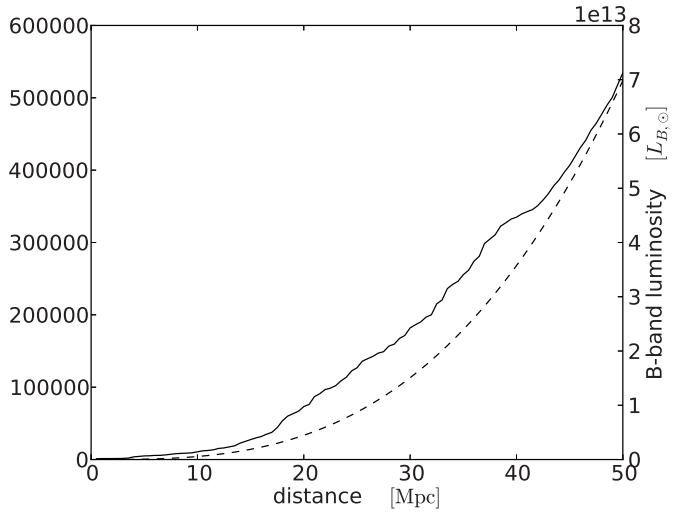

Figure 34: Comparison between the total volume (dashed line, units on left y-axis) and total B-luminosity (full line, units on right y-axis).

may influence the measurement.

On Figure 37, we plot the distances and apparent magnitudes of nearby type Ia SNe. Evidently, some type Ia SNe are discovered when they are quite faint, i.e. $\sim$ 19 magnitude, even in the nearby Universe. Such discoveries could in principle happen both before and after maximum light, but since the fall-off time is considerably longer ($\sim$months) compared to the rise time ($\sim$week), it is more likely that the faint SNe are discovered after maximum. The fact that even nearby SNe aren't discovered until they are quite faint suggests that at larger distances we would expect to miss SNe, even more so for CC SNe that are intrinsically fainter.

Finally, in Fig. 36 we also show the fraction of type Ia SN that should come from the prompt component according to the theoretical estimate. It shows that in the volumes we study here, the prompt component should dominate the number of type Ia SN that are discovered.

Discussion

Our analysis makes a few simplifying assumptions, in particular the constant stellar mass density from Bell et al. (2003) and the constant SFR-to-L_B ratio from the 11 Mpc value of Botticella et al. (2012). The first assumption is certainly not correct at the smallest distances, but the argument to use it anyway is that the mass density should average out in the end and, more importantly, that the number of type Ia SNe is dominated by the prompt component. The second assumption is known not to be correct on large scales, but since the galaxy content in the 50 Mpc volume is probably not very different from that in the 11 Mpc volume, this assumption is likely not very inaccurate.

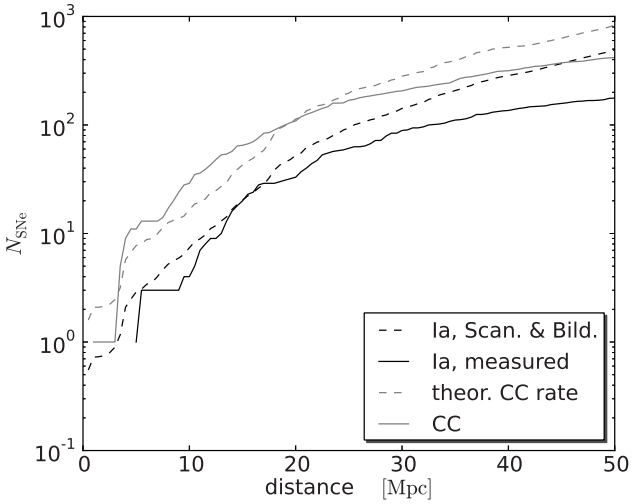

Figure 35: Comparison between the observed number of SN and theoretical rates. The measured type Ia rate (solid black line) is compared to the Scannapieco & Bildsten (2005) rate (dashed black line). The measured core-collapse rate (solid grey line) is compared to the theoretical CC rate (dashed grey line), given by the $\dot{M}_\star$-term in the same model (see Eq.(14)), scaled with the type Ia to core-collapse SN rate of 0.35 from Mannucci et al. (2005).

Boissier & Prantzos (2009) study the relative frequencies of the different types of SNe in the Local Universe in detail in order to relate them to the host galaxy properties such as size and metallicity. They therefore also determined the type Ia to CC SNe ratio for the Local Universe and found a more gradual increase than what we find between 10 and 20 Mpc. It should be noted that the number of SNe in this interval is small, so we should be careful not to over-interpret this results. Boissier & Prantzos (2009) find that the type Ia to CC SN ratio is a function of galaxy brightness and conclude that a higher value is due to the lower specific star formation rate in these galaxies (i.e. a larger contribution from the tardy component). However, this should also have shown up in our expected rate, in which the tardy component plays an insignificant role.

We can compare our results with the detailed study of Botticella et al. (2012) that dealt with CC SN only. In fact, we use the results of that study extensively to calibrate our SFR estimate. Botticella et al. (2012) conclude that in order for the CC rate to make sense, the FUV estimate of the SFR should be the right one, as the one based on H_α underestimates the number by a factor $\sim$2. We also find that within 11 Mpc the observed number of CC SNe is larger than expected based on the H_α estimate. Conversely we find that the number of type Ia SNe within $\sim$15 Mpc agrees well with that estimate, although the number of type Ia SNe is relatively small ($\sim$10). Also, if we look further, at 20 Mpc the number of CC SNe already agrees well with the estimate based on the H_α SFR, so either the completeness of

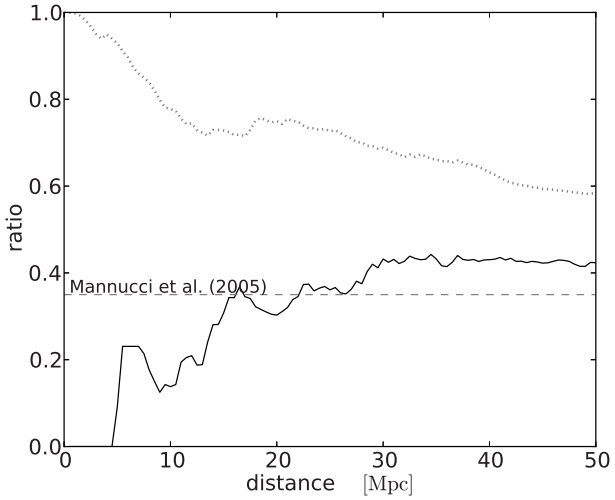

Figure 36: Comparison between the observed type Ia to CC SN rate (solid line) to the expected rate given in Mannucci et al. (2005) (dashed line). The contribution (as a fraction between 0 and 1) to the type Ia SN rate from the "prompt" or $\dot{M}_\star$ component of Eq.(14 is shown as well (dotted line).

the CC SN sample drops very quickly beyond 11 Mpc, or the situation is more complicated than the conclusion that the H_α SFR estimate is too low. Boissier & Prantzos (2009) show the absolute magnitudes for the different types of SNe in their figure 1, and although the CC SNe become incomplete at shorter distances than the type Ia SNe, the effect at distances of 20-30 Mpc (1400-2100 km/s) seems not so pronounced that it could cause the CC sample to become highly incomplete (while the type Ia SN sample remains more or less complete). The fact that the type Ia to CC SN ratio remains roughly constant to 50 Mpc also suggests that the completeness of the two samples is not a very strong function of distance in this interval.

Finally, we can compare the type Ia to CC SN ratio that we find with the ones found before. Our ratio agrees well with the value of 0.35 found by Mannucci et al. (2005) and is somewhat higher than the value of 0.25 found by Li et al. (2011b).

Conclusions

We studied the sample of SNe discovered in the Local Universe (within 50 Mpc) in the past 25 years. We compare the number of type Ia and CC SNe with each other and with an estimate of the expected number based on the SFR and mass enclosed in that volume. We assume a constant mass density and determine the SFR from the B-band magnitude of the galaxies assuming the average B-band to SFR ratio found within 11 Mpc is a good estimate also within 50 Mpc.

Our main conclusion is that the nearby type Ia SN rate is in agreement with what is

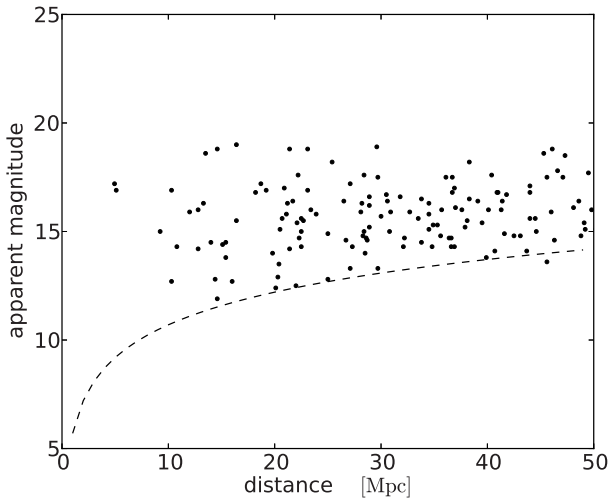

Figure 37: Distances to nearby type Ia SNe, plotted against apparent magnitudes at discovery. For comparison, we include a (dashed) line corresponding to the peak of a canonical $M_V = -19.3$ type Ia SN.

expected from the two-component model in Scannapieco & Bildsten (2005) up to 20 Mpc or so if we assume a relatively low value for the SFR to B-band magnitude conversion. The majority of the type Ia SN arise from the prompt component, that explodes within 1 Gyr after star formation. This means the type Ia SN Local Universe should be representative of the general population.

We confirm the result of Botticella et al. (2012) for the CC SN that within 15 Mpc the observed number is too high, favouring a larger value for the SFR to B-band magnitude conversion. This means the ratio of Ia to CC SNe in that volume is lower than expected, which suggest either that there is a surplus of very nearby CC SNe, or that the type Ia to CC SN ratio is lower than expected.

At larger distances the number of both type Ia and CC SNe drops below the expectations, suggesting incompleteness in the samples. Interestingly, the type Ia to CC SN ratio levels off at a value close to the one found by Mannucci et al. (2005) from $\sim$ 15-20 Mpc and up to at least our distance cut-off of 50 Mpc. Whether this reflects the intrinsic ratio, supporting the conclusion that there is a local surplus of CC SNe, or a value that is higher due to selection biases but surprisingly remains constant, is difficult to tell.

Acknowledgements

This research is supported by NWO Vidi grant 016.093.305.

Bibliography

E. Anders & M. Ebihara. "Solar-System Abundances of the Elements: A New Table." *Meteoritics*, 17:180, 1982.

P. Astier, et al. "The Supernova Legacy Survey: measurement of Ω_M, $\Omega_{\dot{I}\dot{Z}}$ and w from the first year data set." *A&A*, 447:31–48, 2006.

E. F. Bell, et al. "The Optical and Near-Infrared Properties of Galaxies. I. Luminosity and Stellar Mass Functions." *ApJS*, 149:289–312, 2003.

S. Boissier & N. Prantzos. "Relative frequencies of supernovae types: dependence on host galaxy magnitude, galactocentric radius, and local metallicity." *A&A*, 503:137–150, 2009.

K. J. Borkowski, et al. "Dense, Fe-rich Ejecta in Supernova Remnants DEM L238 and DEM L249: A New Class of Type Ia Supernova?" *ApJ*, 652:1259–1267, 2006.

M. T. Botticella, et al. "A comparison between star formation rate diagnostics and rate of core collapse supernovae within 11 Mpc." *A&A*, 537:A132, 2012.

M. C. P. Bours, et al. "Single degenerate supernova type Ia progenitors. Studying the influence of different mass retention efficiencies." *A&A*, 552:A24, 2013.

D. Branch, et al. "On the relative frequencies of spectroscopically normal and peculiar type IA supernovae." *AJ*, 106:2383–2391, 1993.

N. R. Butler, et al. "X-ray Upper Limit for PTF11kly in M101 from Historical Chandra Imaging." *The Astronomer's Telegram*, 3587:1, 2011.

E. Cappellaro, et al. "The Rate of Supernovae - Part Two - the Selection Effects and the Frequencies Per Unit Blue Luminosity." *A&A*, 273:383, 1993.

X. Chen, et al. "Tidally Enhanced Stellar Wind: a Way to Make the Symbiotic Channel to Type Ia Supernova Viable." *ApJ*, 735:L31, 2011.

A. Chiotellis, et al. "The imprint of a symbiotic binary progenitor on the properties of Kepler's supernova remnant." *A&A*, 537:A139, 2012.

L. Chomiuk, et al. "EVLA Constraints on the Progenitors of Supernovae Type Ia." In *American Astronomical Society Meeting Abstracts 217*, volume 43 of *Bulletin of the American Astronomical Society*, page 304.05. 2011.

L. Chomiuk, et al. "EVLA Observations Constrain the Environment and Progenitor System of Type Ia Supernova 2011fe." *ApJ*, 750:164, 2012.

R. L. M. Corradi & H. E. Schwarz. "Bipolar nebulae and binary stars - The family of crabs He 2-104, BI Crucis, and MyCn 18." *A&A*, 268:714–725, 1993.

M. de Kool, et al. "An evolutionary scenario for the black hole binary A0620-00." *A&A*, 183:47–52, 1987.

K. M. Desai, et al. "Supernova Remnants and Star Formation in the Large Magellanic Cloud." *AJ*, 140:584–594, 2010.

R. Di Stefano. "The Progenitors of Type Ia Supernovae. I. Are they Supersoft Sources?" *ApJ*, 712:728–733, 2010a.

R. Di Stefano. "The Progenitors of Type Ia Supernovae. II. Are they Double-degenerate Binaries? The Symbiotic Channel." *ApJ*, 719:474–482, 2010b.

R. Di Stefano, et al. "Spin-up/Spin-down Models for Type Ia Supernovae." *ApJ*, 738:L1, 2011.

J. M. Dickey & F. J. Lockman. "H I in the Galaxy." *ARA&A*, 28:215–261, 1990.

R. Edgar. "A review of Bondi-Hoyle-Lyttleton accretion." *New A Rev.*, 48:843–859, 2004.

N. Elias-Rosa, et al. "Anomalous extinction behaviour towards the Type Ia SN 2003cg." *MNRAS*, 369:1880–1900, 2006.

N. Elias-Rosa, et al. "SN 2002cv: a heavily obscured Type Ia supernova." *MNRAS*, 384:107–122, 2008.

E. L. Fireman. "Interstellar Absorption of X-Rays." *ApJ*, 187:57–60, 1974.

R. J. Foley, et al. "The First Maximum-light Ultraviolet through Near-infrared Spectrum of a Type Ia Supernova." *ApJ*, 753:L5, 2012.

A. Fruchter, et al. "X-Ray Destruction of Dust along the Line of Sight to γ-Ray Bursts." *ApJ*, 563:597–610, 2001.

M. Y. Fujimoto & D. Sugimoto. "Asymptotic Strength of Thermal Pulses in the Helium Shell Burning." *PASJ*, 31:1–10, 1979.

M. Y. Fujimoto & D. Sugimoto. "Helium shell flashes and evolution of accreting white dwarfs." *ApJ*, 257:291–302, 1982.

H.-P. Gail & E. Sedlmayr. "The primary condensation process for dust around late M-type stars." *A&A*, 166:225–236, 1986.

N. Gehrels. "Confidence limits for small numbers of events in astrophysical data." *ApJ*, 303:336–346, 1986.

C. L. Gerardy, et al. "SN 2003du: Signatures of the Circumstellar Environment in a Normal Type Ia Supernova?" *ApJ*, 607:391–405, 2004.

M. Gilfanov & Á. Bogdán. "An upper limit on the contribution of accreting white dwarfs to the typeIa supernova rate." *Nature*, 463:924–925, 2010.

J. Greiner. "Catalog of supersoft X-ray sources." *New A*, 5:137–141, 2000.

J. Greiner, et al. "ROSAT observation of two supersoft sources in the Large Magellanic Cloud." *A&A*, 246:L17–L20, 1991.

T. Güver & F. Özel. "The relation between optical extinction and hydrogen column density in the Galaxy." *MNRAS*, 400:2050–2053, 2009.

I. Hachisu, et al. "A New Model for Progenitor Systems of Type IA Supernovae." *ApJ*, 470:L97, 1996.

I. Hachisu, et al. "A New Evolutionary Path to Type IA Supernovae: A Helium-rich Supersoft X-Ray Source Channel." *ApJ*, 519:314–323, 1999.

I. Hachisu, et al. "Supersoft X-ray Phase of Single Degenerate Type Ia Supernova Progenitors in Early-type Galaxies." *ApJ*, 724:L212–L216, 2010.

D. C. Heggie. "Binary evolution in stellar dynamics." *MNRAS*, 173:729–787, 1975.

M. Henze, et al. "X-ray monitoring of classical novae in the central region of M 31. I. June 2006-March 2007." *A&A*, 523:A89, 2010.

M. Henze, et al. "X-ray monitoring of classical novae in the central region of M 31. II. Autumn and winter 2007/2008 and 2008/2009." *A&A*, 533:A52, 2011.

W. Hillebrandt & J. C. Niemeyer. "Type IA Supernova Explosion Models." *ARA&A*, 38:191–230, 2000.

W. Hillebrandt, et al. "Towards an understanding of Type Ia supernovae from a synthesis of theory and observations." *Frontiers of Physics*, 8:116–143, 2013.

D. Homeier, et al. "An analysis of DA white dwarfs from the Hamburg Quasar Survey." *A&A*, 338:563–575, 1998.

I. Iben, Jr. "More on carbon burning in electron-degenerate matter - Within single stars of intermediate mass and within accreting white dwarfs." *ApJ*, 253:248–259, 1982.

I. Iben, Jr. & A. V. Tutukov. "Supernovae of type I as end products of the evolution of binaries with components of moderate initial mass (M not greater than about 9 solar masses)." *ApJS*, 54:335–372, 1984.

I. Iben, Jr. & A. V. Tutukov. "On the Evolution of Symbiotic Stars and Other Binaries with Accreting Degenerate Dwarfs." *ApJS*, 105:145, 1996.

S. Immler, et al. "X-Ray Observations of Type Ia Supernovae with Swift: Evidence of Circumstellar Interaction for SN 2005ke." *ApJ*, 648:L119–L122, 2006.

N. Ivanova, et al. "Common envelope evolution: where we stand and how we can move forward." *A&A Rev.*, 21:59, 2013.

P. Kahabka & E. P. J. van den Heuvel. "Luminous Supersoft X-Ray Sources." *ARA&A*, 35:69–100, 1997.

P. Kahabka & E. P. J. van den Heuvel. *Super-soft sources*, pages 461–474. 2006.

A. Kashi & N. Soker. "A circumbinary disc in the final stages of common envelope and the core-degenerate scenario for Type Ia supernovae." *MNRAS*, 417:1466–1479, 2011.

M. Kato & I. Hachisu. "A New Estimation of Mass Accumulation Efficiency in Helium Shell Flashestoward Type IA Supernova Explosions." *ApJ*, 513:L41–L44, 1999.

P. Kroupa, et al. "The distribution of low-mass stars in the Galactic disc." *MNRAS*, 262:545–587, 1993.

W. Li, et al. "Exclusion of a luminous red giant as a companion star to the progenitor of supernova SN 2011fe." *Nature*, 480:348–350, 2011a.

W. Li, et al. "Nearby supernova rates from the Lick Observatory Supernova Search - II. The observed luminosity functions and fractions of supernovae in a complete sample." *MNRAS*, 412:1441–1472, 2011b.

W. D. Li, et al. "The Lick Observatory Supernova Search." In *American Institute of Physics Conference Series*, editors S. S. Holt & W. W. Zhang, volume 522 of *American Institute of*

Physics Conference Series, pages 103–106. 2000.

Jifeng Liu, et al. "On the Nature of the Progenitor of the Type Ia SN2011fe in M101." *ApJ*, 749:141, 2012.

K. S. Long, et al. "A soft X-ray study of the Large Magellanic Cloud." *ApJ*, 248:925–944, 1981a.

K. S. Long, et al. "A soft X-ray study of the Large Magellanic Cloud." *ApJ*, 248:925–944, 1981b.

L. A. Lopez, et al. "Typing Supernova Remnants Using X-Ray Line Emission Morphologies." *ApJ*, 706:L106–L109, 2009.

P. Lorén-Aguilar, et al. "High-resolution smoothed particle hydrodynamics simulations of the merger of binary white dwarfs." *A&A*, 500:1193–1205, 2009.

K. Maeda, et al. "An asymmetric explosion as the origin of spectral evolution diversity in type Ia supernovae." *Nature*, 466:82–85, 2010.

F. Mannucci, et al. "The supernova rate per unit mass." *A&A*, 433:807–814, 2005.

D. Maoz. "On the fraction of intermediate-mass close binaries that explode as Type Ia supernovae." *MNRAS*, 384:267–277, 2008.

D. Maoz & F. Mannucci. "A search for the progenitors of two TypeIa Supernovae in NGC 1316." *MNRAS*, 388:421–428, 2008.

D. Maoz & F. Mannucci. "Type-Ia Supernova Rates and the Progenitor Problem: A Review." *PASA*, 29:447–465, 2012.

D. Maoz, et al. "The Supernova Delay Time Distribution in Galaxy Clusters and Implications for Type-Ia Progenitors and Metal Enrichment." *ApJ*, 722:1879–1894, 2010.

D. Maoz, et al. "Nearby supernova rates from the Lick Observatory Supernova Search - IV. A recovery method for the delay-time distribution." *MNRAS*, 412:1508–1521, 2011.

S. Mattila, et al. "Early and late time VLT spectroscopy of SN 2001el - progenitor constraints for a type Ia supernova." *A&A*, 443:649–662, 2005.

J. Mikołajewska. "Symbiotic Stars: Observations Confront Theory." *Baltic Astronomy*, 21:5–12, 2012.

S. Mohamed & P. Podsiadlowski. "Wind Roche-Lobe Overflow: a New Mass-Transfer Mode for Wide Binaries." In *15th European Workshop on White Dwarfs*, editors R. Napiwotzki & M. R. Burleigh, volume 372 of *Astronomical Society of the Pacific Conference Series*, page 397. 2007.

R. Morrison & D. McCammon. "Interstellar photoelectric absorption cross sections, 0.03-10 keV." *ApJ*, 270:119–122, 1983.

U. Munari & F. Patat. "Search for Resolved Hα Nebulae around Symbiotic Stars and Their Formation Mechanisms." *A&A*, 277:195, 1993.

R. Napiwotzki, et al. "SPY - the ESO Supernovae type Ia Progenitor survey." *The Messenger*, 112:25–30, 2003.

K. Nariai & K. Nomoto. "Recurrence of Nova Explosions." In *IAU Colloq. 53: White Dwarfs and Variable Degenerate Stars*, editors H. M. van Horn & V. Weidemann, page 525. 1979.

G. Nelemans, et al. "Reconstructing the evolution of double helium white dwarfs: envelope loss without spiral-in." *A&A*, 360:1011–1018, 2000.

G. Nelemans, et al. "Population synthesis for double white dwarfs . I. Close detached systems." *A&A*, 365:491–507, 2001.

G. Nelemans, et al. "Limits on the X-ray and optical luminosity of the progenitor of the Type Ia supernova 2007sr." *MNRAS*, 388:487–494, 2008.

J.-U. Ness, et al. "A Chandra Low Energy Transmission Grating Spectrometer Observation of V4743 Sagittarii: A Supersoft X-Ray Source and a Violently Variable Light Curve." *ApJ*, 594:L127–L130, 2003.

M. T. B. Nielsen, et al. "Upper limits on bolometric luminosities of 10 Type Ia supernova progenitors from Chandra observations." *MNRAS*, 426:2668–2676, 2012.

M. T. B. Nielsen, et al. "Obscuration of supersoft X-ray sources by circumbinary material. A way to hide Type Ia supernova progenitors?" *A&A*, 549:A32, 2013.

M. T. B. C. Nielsen, et al. "On double-degenerate type Ia supernova progenitors as supersoft X-ray sources - A population synthesis analysis using SeBa." *A&A*, accepted.

K. Nomoto. "Accreting white dwarf models for type I supernovae. I - Presupernova evolution and triggering mechanisms." *ApJ*, 253:798–810, 1982.

K. Nomoto, et al. "Rapid Mass Accretion onto White Dwarfs and Formation of an Extended Envelope." *PASJ*, 31:287–298, 1979.

K. Nomoto, et al. "Thermal Stability of White Dwarfs Accreting Hydrogen-rich Matter and Progenitors of Type Ia Supernovae." *ApJ*, 663:1269–1276, 2007.

M. Orio. "FUV and X-ray grating spectra of novae and supersoft X-ray sources." *Advances in Space Research*, 38:1469–1474, 2006.

R. Pakmor, et al. "Sub-luminous type Ia supernovae from the mergers of equal-mass white dwarfs with mass ˜0.9M_{solar}." *Nature*, 463:61–64, 2010.

N. Panagia, et al. "A Search for Radio Emission from Type Ia Supernovae." *ApJ*, 646:369–377, 2006.

F. Patat, et al. "Detection of Circumstellar Material in a Normal Type Ia Supernova." *Science*, 317:924–, 2007.

S. Perlmutter, et al. "Measurements of Omega and Lambda from 42 High-Redshift Supernovae." *ApJ*, 517:565–586, 1999.

M. M. Phillips. "The absolute magnitudes of Type IA supernovae." *ApJ*, 413:L105–L108, 1993.

Planck Collaboration, et al. "Planck 2013 results. XVI. Cosmological parameters." *ArXiv e-prints*, 2013.

S. F. Portegies Zwart & F. Verbunt. "Population synthesis of high-mass binaries." *A&A*, 309:179–196, 1996.

T. Rauch. "A grid of synthetic ionizing spectra for very hot compact stars from NLTE model atmospheres." *A&A*, 403:709–714, 2003.

T. Rauch & K. Werner. "Non-LTE model atmospheres for supersoft X-ray sources." *Astronomische Nachrichten*, 331:146, 2010.

A. G. Riess, et al. "Observational Evidence from Supernovae for an Accelerating Universe and a Cosmological Constant." *AJ*, 116:1009–1038, 1998.

G. Roelofs, et al. "On the detection of the progenitor of the type Ia supernova 2007on." *MNRAS*, 391:290–296, 2008.

D. Rubin, et al. "Precision Measurement of The Most Distant Spectroscopically Confirmed Supernova Ia with the Hubble Space Telescope." *ApJ*, 763:35, 2013.

E. Scannapieco & L. Bildsten. "The Type Ia Supernova Rate." *ApJ*, 629:L85–L88, 2005.

B. E. Schaefer & A. C. Collazzi. "Novae with Long-lasting Supersoft Emission that Drive a High Accretion Rate." *AJ*, 139:1831–1843, 2010.

E. F. Schlafly & D. P. Finkbeiner. "Measuring Reddening with Sloan Digital Sky Survey Stellar Spectra and Recalibrating SFD." *ApJ*, 737:103, 2011.

F. Schweizer, et al. "a New Distance to the Antennae Galaxies (ngc 4038/39) Based on the Type ia Supernova 2007sr." *AJ*, 136:1482–1489, 2008.

B. J. Shappee & K. Z. Stanek. "A New Cepheid Distance to the Giant Spiral M101 Based on Image Subtraction of Hubble Space Telescope/Advanced Camera for Surveys Observations." *ApJ*, 733:124, 2011.

S. N. Shore, et al. "On the Interpretation of the Ultraviolet Spectra of Symbiotic Stars and Recurrent Novae. II. The 1985 Outburst of RS Ophiuchi." *ApJ*, 456:717, 1996.

A. D. Slyz, et al. "Towards simulating star formation in the interstellar medium." *MNRAS*, 356:737–752, 2005.

S. J. Smartt. "Progenitors of Core-Collapse Supernovae." *ARA&A*, 47:63–106, 2009.

J. Solf & H. Ulrich. "The structure of the R Aquarii nebula." *A&A*, 148:274–288, 1985.

S. Starrfield. "On the cause of the nova outburst." *MNRAS*, 152:307–322, 1971.

A. Sternberg, et al. "Circumstellar Material in Type Ia Supernovae via Sodium Absorption Features." *Science*, 333:856–, 2011.

M. Stritzinger, et al. "The Distance to NGC 1316 (Fornax A) from Observations of Four Type Ia Supernovae." *AJ*, 140:2036–2051, 2010.

B. Strömgren. "The Physical State of Interstellar Hydrogen." *ApJ*, 89:526, 1939.

D. Sugimoto, et al. "General theory for shell flash and nova explosion of accreting white dwarfs." In *IAU Colloq. 53: White Dwarfs and Variable Degenerate Stars*, editors H. M. van Horn & V. Weidemann, pages 280–284. 1979.

A. G. G. M. Tielens, et al. "The physics of grain-grain collisions and gas-grain sputtering in interstellar shocks." *ApJ*, 431:321–340, 1994.

S. Toonen, et al. "Supernova Type Ia progenitors from merging double white dwarfs. Using a new population synthesis model." *A&A*, 546:A70, 2012.

T. Totani, et al. "Delay Time Distribution Measurement of Type Ia Supernovae by the Subaru/XMM-Newton Deep Survey and Implications for the Progenitor." *PASJ*, 60:1327–, 2008.

J. Trümper, et al. "X-ray survey of the Large Magellanic Cloud by ROSAT." *Nature*, 349:579–583, 1991.

M. Turatto, et al. "The rate of (type IA) SNE in elliptical galaxies." *AJ*, 108:202–206, 1994.

A. Tutukov & L. Yungelson. "Evolution of massive common envelope binaries and mass loss." In *Mass Loss and Evolution of O-Type Stars*, editors P. S. Conti & C. W. H. De Loore, volume 83 of *IAU Symposium*, pages 401–406. 1979.

A. V. Tutukov & L. R. Yungelson. "Evolutionary Scenario for Close Binary Systems of Low and Moderate Masses." *Nauchnye Informatsii*, 49:3, 1981.

E. P. J. van den Heuvel, et al. "Accreting white dwarf models for CAL 83, CAL 87 and other ultrasoft X-ray sources in the LMC." *A&A*, 262:97–105, 1992.

M. H. van Kerkwijk, et al. "Sub-Chandrasekhar White Dwarf Mergers as the Progenitors of Type Ia Supernovae." *ApJ*, 722:L157–L161, 2010.

R. Voss & G. Nelemans. "Discovery of the progenitor of the type Ia supernova 2007on." *Nature*, 451:802–804, 2008.

R. Voss, et al. "Three X-ray transients in M ;31 observed with Swift." *A&A*, 489:707–711, 2008.

X. Wang, et al. "Optical and Near-Infrared Observations of the Highly Reddened, Rapidly Expanding Type Ia Supernova SN 2006X in M100." *ApJ*, 675:626–643, 2008.

A. H. Wapstra & N. B. Gove. "The 1971 Atomic Mass Evaluation." *Nuclear Data Tables*, 1:265, 1971.

R. F. Webbink. "Double white dwarfs as progenitors of R Coronae Borealis stars and Type I supernovae." *ApJ*, 277:355–360, 1984.

J. Whelan & I. Iben, Jr. "Binaries and Supernovae of Type I." *ApJ*, 186:1007–1014, 1973.

D. J. White, et al. "A list of galaxies for gravitational wave searches." *Classical and Quantum Gravity*, 28(8):085016, 2011.

J. Wilms, et al. "On the Absorption of X-Rays in the Interstellar Medium." *ApJ*, 542:914–924, 2000.

S.-C. Yoon, et al. "Remnant evolution after a carbon-oxygen white dwarf merger." *MNRAS*, 380:933–948, 2007.

L. R. Yungelson & M. Livio. "Supernova Rates: A Cosmic History." *ApJ*, 528:108–117, 2000.

T. Zhang, et al. "Optical Observations of the Rapidly Expanding Type Ia Supernova 2007gi." *PASP*, 122:1–11, 2010.

Summary

Type Ia supernovae are of import to galactic chemical and dynamic evolution, star formation, and as standardisable cosmic candles. However, despite decades of scientific investigation the nature of the progenitor systems giving rise to these stellar explosions remains mysterious. Two progenitor scenarios are usually considered: the single-degenerate, in which a white dwarf grows in mass by accreting hydrogen- and helium-rich material from a non-degenerate companion star (usually a giant), and the double-degenerate, in which a binary consisting of two degenerate white dwarfs merge. In both cases, the result is a single carbon-oxygen white dwarf with a mass at or exceeding the Chandrasekhar mass. Since the core temperature and density of such an object will be high enough to fuse carbon and oxygen to heavier elements, the Chandrasekhar mass white dwarf will experience thermonuclear runaway and explode as a supernova. However, it is unclear which of these scenarios is the correct one, or if the type Ia supernova rate comes about by a combination of the two progenitor channels.

In this PhD thesis, we have examined the topic of type Ia supernova progenitors, with a special emphasis on their X-ray properties. The common expectation is that single-degenerate progenitors will be persistent supersoft X-ray sources for several millions of years prior to the supernova explosions, as a result of the thermonuclear processing of hydrogen- and helium-rich material on the surface of the accretor. In contrast, double-degenerate progenitors are not generally expected to be X-ray sources, as they do not accrete significant amounts of material for an extended period of time before the merger. If the single-degenerate progenitor scenario is the dominant contributor to the type Ia supernova rate, a large number of supersoft X-ray sources must exist at any one time to account for the observed type Ia supernova rate.

In Chapter 2 and 4, we presented the results of a systematic search of the Chandra archive, with the aim of either directly observing the supersoft X-ray signature of a type Ia supernova progenitor immediately prior to the supernova explosion. Besides the ambiguous case of SN2007on, we have found no evidence for the presence of supersoft X-ray sources in the available pre-explosion observations of the positions of nearby supernovae. As the next best thing, we have therefore obtained stringent upper limits of the bolometric luminosities of the hypothetical sources. The absence of observable supersoft X-ray sources may be straight-forwardly explained by the progenitors simply not being supersoft X-ray sources. However, careful anal-

ysis shows that the upper limits on bolometric luminosities of the majority of the nearby type Ia supernova progenitors are higher than the luminosities of known compact binary and symbiotic supersoft sources in our own galaxy and the Magellanic Clouds. A statistical analysis of the entire sample favours the absence of sources, but only weakly so.

Furthermore, the number of observed supersoft X-ray sources are one to two orders of magnitude too small compared to what would be expected if the single-degenerate progenitor channel were the dominant one. This, combined with the absence of supersoft X-ray sources in pre-explosion observations of the positions of type Ia supernovae can mean either that the single-degenerate progenitor systems are not there, or they are there, but for some reason or another do not look like supersoft X-ray sources. In the latter case, this could be because they are in fact not supersoft X-ray sources at all (and therefore that our fundamental understanding of accreting white dwarfs is wrong), or because they are somehow hidden from observational view. To examine the latter option, we constructed a simple model for a single-degenerate progenitor system that has lost material into the local, circumbinary region. This analysis was presented in Chapter 3. The aim was to determine if it is possible to sufficiently obscure a supersoft X-ray source in such local material to render it undetectable to *Chandra* observations. Our analysis shows that it appears to be possible to fully obscure a supersoft X-ray source with relatively modest circumbinary mass-loss rates, at least under the somewhat simplistic assumptions of our model. This could explain the lack of observed supersoft X-ray sources and, incidentally, also the more general lack of observed symbiotic binaries that are not type Ia supernova progenitors.

In Chapter 5, we examined the claim that double-degenerate progenitor systems should be supersoft X-ray sources. We did this by analysing a large dataset from the SeBa binary population synthesis code. We found that even with unrealistically optimistic assumptions concerning accretion and retention rates, there is no reason to expect the existence of a significant population of double-degenerate progenitor systems that are supersoft X-ray sources. Also, since the accretion (if it takes place) and hence X-ray emission from such systems ceases long before the supernova explosion itself, it would be impossible to observationally associate a supernova with its corresponding double-degenerate supersoft X-ray source within the duration of a human lifetime. The conclusion is that the absence of supersoft X-ray sources is not a problem for the double-degenerate scenario. Whether it actually is a problem for the single-degenerate scenario is unclear, qua our analysis of obscured supersoft X-ray sources discussed in Chapter 3.

In the last chapter of this thesis, we examined the sample of type Ia supernovae within a distance of 50 Mpc, to determine if the local type Ia supernova rate agrees with that observed for intermediate and cosmological distances. We compared the observed number of type Ia and core-collapsee supernovae with theoretical presecriptions for the supernova rate at intermediate distances. We found that, when disregarding Poisson noise in the very nearby Universe, the local type Ia supernova rate agrees well with the theoretical two-component model. The majority of the local type Ia supernovae appear to originate from "prompt" progenitor systems. We found evidence for a larger-than-expected population of core-collapse supernovae within very short distances, in agreement with other recent studies. Finally, our study suggested that

even in the local Universe our current sample of observed supernovae of either type is likely to be incomplete.

Samenvatting

Type Ia supernova's zijn belangrijk voor galactische chemische en dynamische evolutie, stervorming, en als normaliseerbare "standaard-kaarsen". Ondanks decennia van wetenschappelijk onderzoek blijft de aard van de voorlopersystemen van deze sterexplosies een mysterie. Twee voorloper-scenario's worden meestal beschouwd: het 'enkel-gedegenereerde', waarin een witte dwerg groeit in massa door accretie van waterstof- en helium-rijk materiaal van een niet-gedegenereerde begeleidende ster (meestal een reus), en het 'dubbel-gedegeneerde', waarbij een dubbelstersysteem bestaande uit twee gedegenereerde witte dwergen samensmelt. In beide gevallen is het resultaat een enkele koolstof-zuurstof witte dwerg met een massa in de buurt of boven de Chandrasekhar massa. Omdat de kerntemperatuur en de dichtheid van een dergelijk object hoog genoeg is om koolstof en zuurstof te laten fuseren tot zwaardere elementen, zal de Chandrasekhar-massa witte dwerg exploderen als thermonucleaire supernova. Het is echter onduidelijk welke van deze scenario's correct is, ofwel of Ia supernovae ontstaat door een combinatie van beide scenario's.

In dit proefschrift hebben we het onderwerp van type Ia supernova voorlopers onderzocht, met een bijzondere nadruk op hun röntgen-eigenschappen. De algemene verwachting is dat enkel-gedegenereerde voorlopers superzachte röntgenbronnen zullen zijn gedurende enkele miljoenen jaren voor de explosies. Dit ten gevolg van de thermonucleaire fusie van waterstof- en helium-rijk materiaal op het oppervlak van de accreterende witte dwerg. Daarentegen worden dubbel-gedegenereerde voorlopers over het algemeen niet verwacht röntgenbronnen te zijn. Als het enkel-gedegenereerde voorloper scenario dominant is, zou er in ieder melkwegstelsel, op ieder moment een groot aantal superzachte röntgenbronnen bronnen moeten bestaan om het waargenomen aantal type Ia supernova te kunnen verklaren.

In hoofdstuk 2 en 4, hebben we de resultaten van een systematische zoektocht van het Chandra archief gepresenteerd, met als doel ofwel direct de superzachte röntgenbron te detecteren die later als supernova is ontploft, ofwel te laten zien dat er zeker geen zachte röntgenbron was voorafgaand aan de explosie. Behalve het dubbelzinnige geval van SN2007on, hebben we geen bewijs voor de aanwezigheid van een superzacht röntgenbronnen in de beschikbare pre-explosie waarnemingen van de posities van de nabijgelegen supernovae gevonden. Daarom hebben we strikte bovenlimieten bepaald van de bolometrische lichtkracht van de hypothetis-

che bronnen die we net niet hebben kunnen detecteren. De afwezigheid van waarneembare superzachte röntgenbronnen kan natuurlijk prima verklaard worden als de voorlopers simpelweg geen superzachte röntgenbronnen zijn. Echter, uit een zorgvuldige analyse blijkt dat de bovengrenzen aan bolometrische lichtkracht van de meerderheid van de nabijgelegen type Ia supernova voorlopers hoger zijn dan de helderheden van bekende compacte en symbiotische superzachte bronnen in onze eigen Melkweg en de Magellanse Wolken. Een statistische analyse van alle bovenlimieten samen geeft een kleine voorkeur voor de afwezigheid van bronnen, maar het is ook mogelijk dat we de bronnen er wel zijn, maar we ze net niet hebben gedetecteerd.

Een ander probleem met het enkel-gedegenereerde voorloperscenario is dat het aantal waargenomen superzachte röntgenbronnen in melkwegstelsels een factor tien tot honderd kleiner is dan wat zou worden verwacht als dit het dominante scenario zou zijn. Dit, gecombineerd met de afwezigheid van een superzacht röntgenbronnen in pre-explosie waarnemingen van de posities van het type Ia supernova kan zowel betekenen dat de enkel-gedegenereerde voorlopersystemen er niet zijn, ofwel dat ze er wel zijn, maar om de een of andere reden er niet uitzien als superzachte röntgenbronnen. In het laatste geval zou dit kunnen zijn omdat ze helemaal niet superzachte röntgenbronnen zijn (en dus dat ons fundamentele begrip van snel-accreterende witte dwergen verkeerd is), ofwel omdat ze op een of andere manier verborgen zijn. Om de laatste optie te onderzoeken, construeerden we een simpel model voor een enkel-gedegenereerd voorlopersysteem dat materiaal heeft verloren in de lokale, circumbinaire regio. Deze analyse werd gepresenteerd in hoofdstuk 3. Het doel was te bepalen of het mogelijk is om een superzachte röntgenbron in dergelijke lokaal materiaal voldoende verbergen dat ze niet meer detecteerbaar met Chandra zullen zijn. Onze analyse toont aan dat het inderdaad mogelijk lijkt om een superzachte röntgenbron volledig te verduisteren met relatief bescheiden circumbinair massa-verlies, althans onder de ietwat simplistische veronderstellingen van ons model. Dit zou het gebrek aan waargenomen superzachte röntgenbronnen en overigens ook de meer algemene gebrek aan waargenomen symbiotische dubbelsterren kunnen verklaren.

In hoofdstuk 5 hebben we ook de bewering onderzocht dat dubbel-gedegenereerde voorlopersystemen ook superzachte röntgenbronnen zouden zijn. We deden dit door het analyseren van een grote dataset van de SeBa dubbelster-populatie-synthese code. We vonden dat zelfs met onrealistisch optimistische veronderstellingen over de hoeveelheid massa die witte dwergen kunnen accreteren, er geen reden is om te verwachten dat dubbel-gedegenereerde voorloper-systemen een substantiële populatie van superzachte röntgenbronnen vormen. Omdat de massa-overdracht (indien deze plaatsvindt) en daardoor eventuele röntgenstraling uit dergelijke systemen plaatsvind lang voordat de dubbelster explodeert, zou het hoe dan ook onmogelijk zijn om een supernova observationeel associëren met het bijbehorende röntgenbron. De conclusie is dat het feit dat er heel weinig superzachte röntgenbronnen worden waargenomen geen probleem is voor het dubbel-gedegenereerde scenario. Of het eigenlijk een probleem is voor het enkel-gedegenereerde scenario is onduidelijk, gezien onze analyse van verduisterde superzachte röntgenbronnen besproken in hoofdstuk 3.

In het laatste hoofdstuk van dit proefschrift onderzochten we alle bekende type Ia supernovae binnen een afstand van 50 Mpc, om te bepalen of het lokale frequentie waarmee type Ia supernova's exploderen overeenkomt met wat is waargenomen op veel grotere afstanden

van de Zon. We vergeleken het waargenomen aantal type Ia supernovae en het aantal supernovae waarin een zware ster aan het eind van zijn leven ineenstort met gevonden frequenties op grotere afstanden. We vonden dat, wanneer we Poisson-ruis in de zeer nabije heelal verwaarlozen, het lokale aantal type Ia supernova goed overeen komt met de verwachtingen. De meerderheid van de lokale type Ia supernova blijken afkomstig te zijn van voorloper systemen die relatief snel (binnen een paar honderd miljoen jaar) na de vorming van de dubbelster uit interstellaire wolken exploderen. We vonden bewijs voor een groter-dan-verwacht aantal supernovae van zware sterren binnen zeer korte afstanden, in overeenkomst met andere recente studies. Ten slotte suggereerde onze studie dat zelfs in het lokale heelal onze huidige set van de waargenomen supernovae van beide type waarschijnlijk onvolledig is.

Acknowledgments

First and foremost, I would like to thank my PhD supervisor Prof. Dr. Gijs Nelemans for being a scientific inspiration, and for allowing me the freedom to work on my own terms. Thanks are also owed to my scientific collaborators: Rasmus Voss, Carsten Dominik and Silvia Toonen, and to my office mates, fellow PhD students, master students and postdocs at the Department of Astrophysics, Radboud University Nijmegen. A special thanks goes to the department secretaries (especially Cisca Custers and Daisy Maurits) who took exceedingly good care of me when I just arrived in the Netherlands.

I would also like to thank Ella Fonteyn, Jan Kuijpers, Bojan Weert, Eltjo Benedick, and the group of (mainly) expats who made my 3 years of living in Utrecht a lot of fun.

Lastly, I thank my parents for bringing me up to appreciate science, reason and humanism, to be skeptical of established authority and blind faith, and for encouraging me to find my own path.